UNIVERSITEIT VAN PRETORIA
UNIVERSITY OF PRETORIA
YUNIBESITHI YA PRETORIA

Analysis of trace amounts of oxygen, carbon monoxide and carbon dioxide in nitrogen using gas chromatography

by

Mellisa Janse van Rensburg

Submitted in partial fulfilment of the requirements for the degree of

Magister Scientiae

In the Faculty of Natural and Agricultural Sciences

University of Pretoria

Pretoria

Supervisor: Professor E R Rohwer

April 2007

Declaration

I declare that the thesis “Analysis of trace amounts of oxygen, carbon monoxide and carbon dioxide in nitrogen using gas chromatography” has not previously been submitted for a degree at this or any other university, and that it is my own work in design and execution and that all reference material that I have used or quoted have been indicated and acknowledged by means of complete references.

Mellisa Janse van Rensburg April 2007

ACKNOWLEDGEMENTS

For his kindness, patience and excellent suggestions during numerous drafts of this work, I would like to thank my supervisor, Professor Egmont Rohwer.

Thank you to my metrology group leader at CSIR NML, Angelique Botha, for the encouragement and support during the past few years, and the editing of the text.

Thanks to John Swinley of Scientific Supply Services cc and Piet de Coning (Sasol) for help with editing, fruitful discussions and technical assistance.

Thank you to the CSIR National Metrology Laboratory for allowing me to carry out this research and paying for my studies.

Thank you to my husband Derik, who has supported and loved me unconditionally. Thank you to my family, the Govenders and my extended family, the Janse van Rensburgs for your encouragement too.

My Father in heaven has answered all my prayers and I praise Him.

Lastly, this is dedicated to my late brother, Leonard Govender.

Abbreviations

GC	Gas Chromatography
BIPM	International Bureau for Weights and Measures
CCQM	Consultative Committee for Amount of Substance
DTI	Department of Trade and Industry
SI	International System of Units
GC-PDHID	gas chromatography-pulsed discharge helium ionisation detector
PDHID	pulsed discharge helium ionisation detector
GC-TCD-FID	gas chromatography - thermal conductivity detector - flame ionisation detector
FID	flame ionisation detector
TCD	thermal conductivity detector
FTIR	Fourier Transform Infrared Spectroscopy
BIP™	built-in purifier
CSIR NML	Council for Scientific and Industrial Research National Metrology Laboratory
Å	angstrom
MS 5Å	molecular sieve 5Å
NMI	National Metrology Institute
CRM	certified reference material
ppm	parts per million
ppb	parts per billion
$\mu mol \cdot mol^{-1}$	10^{-6} mole per mole
pp	pages
RGA	reduction gas analyser
DID	discharge ionisation detector
PLOT	porous layer open tubular
µℓ	microlitre
nℓ	nanolitre
ℓ	litre
cm	centimetre
m	metre
mm	millimetre
µm	micrometre
nm	nanometre

eV	electron volt
kg	kilogram
g	gram
mg	milligram
ng	nanogram
psi	pounds per square inch
kPa	kilopascal
$m\ell.min^{-1}$	millilitre per minute
$ng.\ell^{-1}$	nanogram per litre
$cm.sec^{-1}$	centimetre per second
$J.K^{-1}$	joule per Kelvin
ESDM	experimental standard deviation of the mean
LOD	limit of detection
LOQ	limit of quantification
LOD_{SN}	limit of detection (signal to noise ratio method)
LOD_{IUPAC}	limit of detection (IUPAC method)
LOQ_{IUPAC}	limit of quantification (IUPAC method)
$[O_2]$	concentration of O_2
$[CO_2]$	concentration of CO_2
[CO]	concentration of CO
$[N_2]$	concentration of N_2

Abstract

An in-house developed method is presented for the purity analysis of nitrogen (N_2) built-in purifier (BIP™) gas for the trace contaminant gases carbon dioxide (CO_2), oxygen (O_2) and carbon monoxide (CO), using gas chromatography with a pulsed discharge helium ionisation detector (GC-PDHID). Nitrogen BIP™ gas is used as a "matrix" gas or diluent gas for the gravimetric preparation of binary reference materials of CO, CO_2, sulphur dioxide (SO_2) and nitric oxide (NO) at the CSIR NML gas metrology laboratory. Purity analysis of nitrogen BIP™ is required to decrease the measurement uncertainty of the calculated gravimetric concentrations of the gaseous reference materials produced. The aim of the research was to find a method where amounts <0.25 x 10^{-6} mol·mol^{-1} of CO_2, O_2 and CO could be simultaneously analysed in high purity nitrogen within a short time, with minimum cost and on a routine basis.

Gas mixtures of trace amounts of CO_2, O_2 and CO in N_2 were separated and quantified using a parallel dual capillary column configuration with temperature and pressure programming and a pulsed discharge helium ionisation detector (PDHID). The detection limits were 9 x 10^{-9} mol·mol^{-1} for CO_2, 7 x 10^{-9} mol·mol^{-1} for O_2 and 37 x 10^{-9} mol·mol^{-1} for CO with repeatability precision of 1% for carbon dioxide, 1% for oxygen and 10% for carbon monoxide for a 0.2 x 10^{-6} mol·mol^{-1} standard. The detection limits obtained were lower than those reported previously by other investigators for similar methods and the validation for the method as set out in this investigation seems to be the first for trace amounts of CO_2, O_2 and CO in nitrogen.

The method was validated by comparison of the CO_2 and CO results with results obtained using a flame ionisation detector and methanisation. The technique of sequence reversal was used to improve the peak shape of CO but there was no improvement on the results obtained with temperature and pressure programming. Although no helium purging was used to reduce atmospheric contamination, it was shown that the main source of contamination from the air was through the sampling system which was reduced to a level of ± 20 x 10^{-9} mol·mol^{-1} oxygen simply by using a higher sample flow rate. It was also found that even when large amounts of CO_2 were adsorbed onto the molecular sieve column, this made no difference to the column performance at trace levels. The method has also been validated for the analysis of nitrogen in high purity oxygen and may also be used to analyse carbon dioxide and carbon monoxide in oxygen as well.

Contents Page

List of Figures

Addendum

List of Tables

Addendum

Chapter 1
Introduction

1.1. Project Background

The CSIR-National Metrology Laboratory (CSIR NML) is the custodian of the national measurement standards of South Africa, having the mandate from the Department of Trade and Industry (DTI) to provide traceability for national measurement standards. The gas metrology laboratory of the CSIR NML has established a facility for the gravimetric preparation of gas mixtures, which is a method that has been identified to be a potential primary method for chemical measurement by the CCQM (Consultative Committee for Amount of Substance), of the BIPM (Kaarls *et al*, 1997).

The gas metrology laboratory of the CSIR NML has completed the pilot projects for the preparation of binary mixtures of carbon monoxide (CO)-in-nitrogen as well as carbon dioxide (CO_2)-in-nitrogen. These gaseous reference materials as well as binary gas mixtures for sulphur dioxide (SO_2)-in-nitrogen will become commercially available in 2007. The laboratory has also started with the pilot project for the development of the national standard for binary gas mixtures of nitric oxide (NO)-in-nitrogen.

The gaseous reference materials are prepared gravimetrically, through a static process, which means that the mixtures are prepared and stored in containers from which the gas can be decanted. The gravimetric preparation of gas mixtures is recognised to be of the highest metrological quality. Measurement traceability for gravimetrically prepared gas mixtures is obtained through accurate weighing (traceable to the SI unit for mass, the kilogram), the purity assessment of the component gases and the balance gas, as well as the evaluation of the behaviour of the component gases in the cylinder.

A very important uncertainty contributor to the gravimetric concentration is the purity of the parent gases. To illustrate the importance of purity analysis we can take the example of preparing a mixture of a 1000 $\mu mol \cdot mol^{-1}$ CO-in-nitrogen. If the nitrogen is of 99.999% purity then the maximum impurity is 10 $\mu mol \cdot mol^{-1}$. If this impurity in the nitrogen is assumed to be only CO then the uncertainty

contribution from this impurity is a maximum of 1% of the required concentration. However, the target expanded uncertainty for the gravimetric concentration is limited to 0.5% relative, so the assumption of this maximum impurity is unacceptable and the CO impurity will need to be quantified with a higher level of accuracy.

The impurities that are analysed in the nitrogen gas are carbon dioxide at less than 0.25 x 10^{-6} mol·mol^{-1}; oxygen at less than 0.01 x 10^{-6} mol·mol^{-1} and carbon monoxide at less than 0.25 x 10^{-6} mol·mol^{-1}. The manufacturer of the high purity nitrogen gas used in the laboratory also confirmed that the argon level varied between 20 and 100 x 10^{-6} mol·mol^{-1} from batch to batch and was therefore not quantified as part of the purity certificate supplied with the cylinders.

At the CSIR NML, a Varian 3800 gas chromatograph (GC) with thermal conductivity detector (TCD) and a catalytic converter (methaniser) in series with a flame ionisation detector (FID) is currently used for the analysis of the CO and CO_2 impurities found in BIP™ nitrogen.

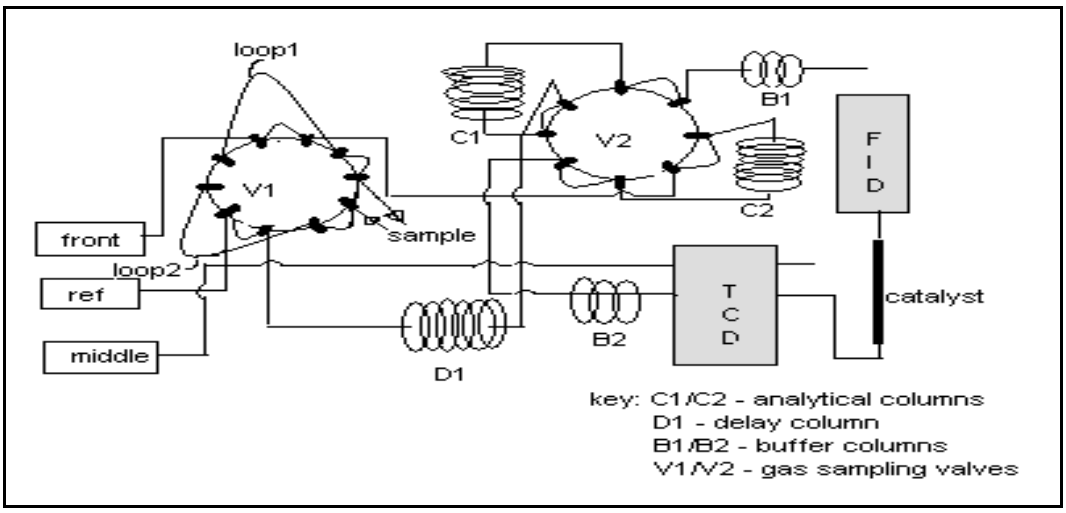

Figure 1: Schematic diagram of the GC-TCD-FID system.

The methaniser, situated just before the FID detector, consists of a Ni/Zr catalyst operating at 350°C to 400°C, which converts the carbon dioxide and carbon monoxide eluting from the column to methane in the presence of hydrogen and allows the detection of these gases on the FID.

A 2 mℓ sample loop; a 1.2 m, 3.2 mm internal diameter stainless steel column packed with molecular sieve 13X (45/60 mesh) is used to separate the permanent gases at 55 ºC isothermal and 172 kPa (25 psi) from nitrogen while a 1.8 m, 3.2 mm internal diameter stainless steel column packed with Hayesep N (80/100 mesh) was used to analyse CO_2 by a second injection when the molecular sieve column was being back-flushed to get rid of adsorbed CO_2.

One of the shortcomings of this system is that the separation of oxygen and argon is not possible at ambient temperature. The separation of oxygen and argon is crucial when the level of oxygen in the gas must be quantified.

Table 1

Levels of impurities expected in BIP^{TM} N_2 and detection limits of these impurities with GC-TCD-FID

Impurity in BIP^{TM}	Level of Impurity	Detection limit of GC-TCD-FID
O_2	<0.010 µmol·mol^{-1}	-
CO	<0.25 µmol·mol^{-1}	0.042 µmol·mol^{-1}
CO_2	<0.25 µmol·mol^{-1}	0.038 µmol·mol^{-1}
H_2	<1 µmol·mol^{-1}	Not determined
H_2O	<0.020 µmol·mol^{-1}	Not determined
C_nH_m (as CH_4)	<0.100 µmol·mol^{-1}	Not determined

A Varian CP 3800 GC with a pulsed discharge helium ionisation detector (PDHID) was previously used in conjunction with a 6-port injection valve and a ±3 metre Molecular sieve 5Å column (**Figure 2**) for the analysis of permanent gases.

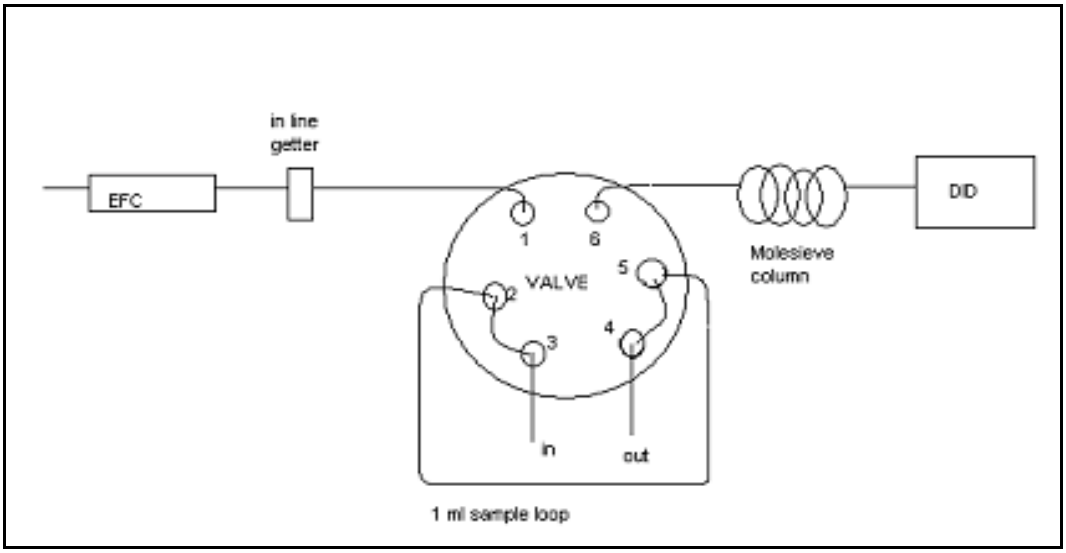

Figure 2: Schematic diagram of the GC-PDHID system

The PDHID detector system shown in **Figure 2** would be expected to provide lower detection limits than the GC-TCD-FID system shown in **Figure 1** since the PDHID is known to be more sensitive than the FID (Etiope, 1998), but a 1.2 m 13X packed molecular sieve column (80/100 mesh size) in the present configuration gave a detection limit of 0.7 µmol·mol^{-1} for CO because of the CO peak eluting on the tail of the large N_2 matrix peak.

CO_2; O_2 and CO can be detected using the PDHID (Wentworth *et al*, 1994) but due to its universal response to all gases except neon, chromatographic separation that allows quantification of all three gases in the presence of a large nitrogen matrix becomes crucial. Capillary columns, where only a small amount of sample (<250 µℓ) is injected compared to the amount for packed columns (1 mℓ to 2 mℓ), would be expected show less adverse effects due to the nitrogen matrix.

Although CO and CO_2 can be quantified using gas chromatography with flame ionisation detection and catalytic conversion of CO and CO_2 to CH_4 (ISO 8186, 1989) at levels less than 0.25 x 10^{-6} mol·mol^{-1} (Novelli, 1999; Kaminski et al, 2003), the simultaneous analysis of trace amounts of oxygen could not be achieved with existing methods in the gas metrology laboratory at CSIR NML. A method was sought where concentrations less than 0.25 x 10^{-6} mol·mol^{-1} of CO_2; O_2 and CO could be simultaneously analysed in high purity nitrogen within a short time, with minimum cost and on a routine basis.

1.2 Approach followed

Initial work using the PDHID detector for the analysis of CO in N_2 showed that the detection limit for CO was not adequate for the analysis of CO in BIP™ nitrogen.

A literature search was performed to obtain an overview of the methods used to analyse permanent gases by gas chromatography. A dual capillary column set, comprising a molecular sieve and a porous polymer column was identified as the most universal approach to analyse the permanent gas impurities found in nitrogen gas. A ten-port valve was purchased in addition to the existing six-port diaphragm valve to enable column switching as required. An eight-port valve would have sufficed for the application, but the decision was made to purchase a valve that could be used for other applications once the current project was completed.

A dual column set, marketed by Restek (Restek, 2005) was purchased and installed along with the ten-port valve, in the CP 3800 GC with the existing PDHID detector. A series of three-component gas mixtures of CO_2, CO and O_2 in BIP™ nitrogen were prepared gravimetrically at the gas metrology laboratory and used for the method development and validation.

The dual capillary column set was first installed with the ten-port valve in a sequence reversal configuration (see chapter 5). The dual capillary column set was then installed with the six-port valve to compare the results obtained with sequence reversal and the results obtained without sequence reversal.

For purposes of validating the reliability of the method, the results obtained were compared with the results obtained using the GC-TCD-FID method for CO_2 and CO in N_2. The results for O_2 in N_2 could not be similarly validated because no method is available to analyse O_2 in the sub-ppm range in our laboratory at present.

The project was started in 2003 with the evaluation of a packed column to analyse CO using the PDHID. The literature study, purchasing and installation of the columns, method development and method validation took place from 2004 to 2006. The final draft of the results and conclusions was completed in July 2006.

Chapter 2

Summary of chromatographic theory as applied to gas analysis

2.1 Introduction to the technique of gas chromatography

Chromatography is a science that permits the separation of complex mixtures. Russian botanist Mikhail Semyonovich Tswett (1872-1919) invented the first chromatography technique in 1901 during his research on chlorophyll. He used liquid-adsorption columns to separate plant pigments with a calcium carbonate stationary phase and a petroleum ether mobile phase. The chromatographic zones were distinguished by their natural colours and Tswett's name for the method was derived from the Greek word for colour, *chromatos* (Peters, Hayes, Hieftje, 1974, pp 523).The method was described on December 30, 1901 at the XI Congress of Naturalists and Doctors in St Petersburg. The first printed description was in 1903, in the Proceedings of the Warsaw Society of Naturalists, section of biology. He first used the term chromatography in print in 1906 in his two papers about chlorophyll in the German botanical journal, Berichte der Deutschen Botanischen Geselschaft (Wikipedia, 2004).

Gas chromatography includes the use of all chromatographic methods in which the mobile phase is a gas (Jeffrey and Kipping, 1964, pp 4). The concept of liquid-liquid partition chromatography was introduced by Martin and Synge in 1942 who had also put forward the combination of a gaseous mobile phase with a liquid stationary phase (Peters, Hayes, Hieftje, 1974, pp 523). It was only a decade later that James and Martin published papers on the theory, construction and operation of a gas chromatograph. The first commercial gas chromatographs (GCs) were sold by Burrell Corporation, the Perkin-Elmer Corporation and the Podbielnak Corporation (Hogan, 1997, pp 10).

All chromatographic separation processes consist of a gas, liquid or supercritical fluid in which the sample is transported, called the mobile phase. The sample, carried along by the mobile phase, is forced through an immiscible stationary phase that is fixed in a column or on a solid surface.

The separation is achieved by choosing the stationary and mobile phases so that the components of the complex mixture are distributed between these phases to varying degrees due to the physical and chemical differences between the components. The stationary phase strongly retains some components, which consequently spend less time in the mobile phase and therefore pass relatively slowly through the column. The weakly retained components spend more time in the mobile phase and therefore move relatively quickly through the column. It is these differences in retention by the stationary phase that result in separation of the components of a mixture into bands or zones as they are moved along the column by the mobile phase. (Skoog, 1998, pp 674)

Chromatographic methods may be categorised depending on the means by which the mobile and stationary phases are physically brought into contact. In planar chromatography, the stationary phase is supported on a flat plane through which the mobile phase moves by capillary action or gravity. When the stationary phase is held in a long, narrow tube through which the mobile phase is forced under pressure, the term column chromatography is used.

Column chromatography, where a solid stationary phase is used, may be classified further depending on the type of mobile phase used. Using the mobile phase as a criterion for classification, column chromatography may be divided into liquid chromatography, supercritical fluid chromatography and gas chromatography.

In chromatography, the time spent in the column by a component of the mixture being separated on a particular column, is called its retention time. The retention time of a particular compound on a particular column may be used to aid in the identification of that compound in a complex mixture. The amount of a compound is indicated by the intensity of the signal it produces when exiting the column. The graphical representation of the retention time and this signal intensity in two dimensions is called a chromatogram.

2.2. Distribution constants

A mixture of gases may be separated by a stationary phase fixed to the inner surface of a column with the mobile gas phase flowing through it if the equilibrium

constants for the reactions by which the gases distribute themselves between the mobile and stationary phases are sufficiently different to ensure that the gases elute from the column at different rates (Skoog, 1998).

Equation 1 shows the equilibrium constant, K which is calculated from the distribution of the analyte between the stationary and the mobile phases.

$$K = \frac{C_S}{C_M} \qquad (1)$$

K is also called the distribution constant, C_S is the concentration of the analyte in the stationary phase and C_M is the concentration of the analyte in the mobile phase. **Equation 1** is the equation for linear chromatography which is the type of chromatography used in gas analysis and ideally, K would be expected to be constant over a range of concentrations with a resultant chromatogram of symmetric Gaussian peaks with retention times independent of analyte concentration (Skoog, 1998).

2.3 Retention time

The time taken for a peak from injection until it reaches the detector is called the retention time t_R and the time taken for an unretained peak to reach the detector is called the dead time, t_M. The average linear rate of analyte migration along the column, $\bar{v}$ can be calculated from the column length, L and the retention time of the analyte, t_R as shown in **Equation 2**. Similarly, the average linear rate of movement of the molecules of the mobile phase ($\bar{u}$) can be calculated from the dead time (t_M) and the length of the column, L as shown in **Equation 3** (Skoog, 1998).

$$\bar{v} = \frac{L}{t_R} \qquad (2)$$

$$\bar{u} = \frac{L}{t_M} \qquad (3)$$

2.4 Obtaining the selectivity factor from a chromatogram

The selectivity factor (α) for two species A and B on a particular column can be defined by the distribution constants as shown in **Equation 4**, with K_B being the distribution constant for the more strongly held species, and K_A the distribution constant for the less strongly retained species.

$$\alpha = \frac{K_B}{K_A} \qquad (4)$$

Since K_B will always be greater than K_A by definition, the selectivity factor will always have a value greater than one. **Equation 5** shows how the capacity factor (the factor used to describe the migration rates of analytes in columns) for an analyte A, is defined in the case of gas liquid chromatography (Skoog, 1998).

$$k'_A = \frac{K_A V_S}{V_M} \qquad (5)$$

In **Equation 5**, V_S is the volume in the stationary phase and V_M is the volume in the mobile phase. With rearrangement of **Equation 5** and the combination of **Equations 3 and 4**, a relationship between the capacity factors and the selectivity factor for a column may be obtained as shown in **Equation 6** (Skoog, 1998).

$$\alpha = \frac{k'_B}{k'_A} \qquad (6)$$

The capacity factor may be expressed in terms of the retention times of the analyte and the dead time as shown in **Equation 7**.

$$k'_A = \frac{t_R - t_M}{t_M} \qquad (7)$$

Combining **Equations 6 and 7**, enables the calculation of the selectivity factor, α from a chromatogram for analytes A and B as shown in **Equation 8**. The selectivity factor is useful for assessing the potential resolving power of a column for a pair of analytes (Skoog, 1998).

$$\alpha = \frac{(t_R)_B - t_M}{(t_R)_A - t_M} \qquad (8)$$

2.5 Column performance

2.5.1 Plate theory

The progress of an analyte carried along by the mobile phase through a packed column is envisioned as a stepwise transfer, via the mobile phase, through chambers or zones of the column. Each zone contains an amount of mobile phase and of stationary phase. These zones, called “theoretical plates”, are of a length that enables the complete equilibration of the analyte between the stationary and the mobile phases. The length of these theoretical plates in the column are designated as “height equivalent to the theoretical plate” (H.E.T.P.) or the “plate height” (Skoog, 1998).

A sample is added to the column and enters the first theoretical plate. A fraction remains in the mobile phase while a fraction enters the stationary phase. After equilibration is complete, a small volume of mobile phase is added to the column and the amount of sample in the mobile phase is transferred to the second plate (Peters, Hayes, Hieftje, 1974). The number of theoretical plates (N) can be calculated by dividing the column length (L) by the plate height (H) as shown in **Equation 9**.

$$N = \frac{L}{H} \qquad (9)$$

From **Equation 9**, it is clear that the longer the column and the smaller the plate height, the larger the number of theoretical plates. More theoretical plates mean more equilibria per column length and therefore a more efficient column.

Plate theory makes the assumption that the partition coefficient, K (from **Equation 1**), is always constant. The theory also assumes that the equilibration is rapid compared to the movement of the mobile phase, but diffusion is never instantaneous, particularly at high mobile phase flow rates and material may be transferred to the next theoretical plate before equilibration is complete. When this

occurs, it will cause a reduction in the value of N and or the column efficiency as shown in **Equation 9** (Peters, Hayes, Hieftje, 1974 pp 527.

The plate theory assumes that the spreading of the chromatographic zone by longitudinal diffusion from one theoretical plate to another does not occur whereas the effects of longitudinal diffusion are particularly evident at low mobile phase flows. The assumption that the column consists of discrete volume elements and that the mobile is added in discrete increments, when it is in fact added continuously, also adds to the shortcomings of the plate theory. Variables such as the mobile phase velocity and the phase dimensions are also excluded from the plate theory (Peters, Hayes, Hieftje, 1974 pp 527). **Figure 3** is a schematic representation of the stepwise progress of a band of analyte carried along the column by the mobile phase, achieving equilibrium along the way in each of these theoretical plates (Littlewood, 1962, pp 120).

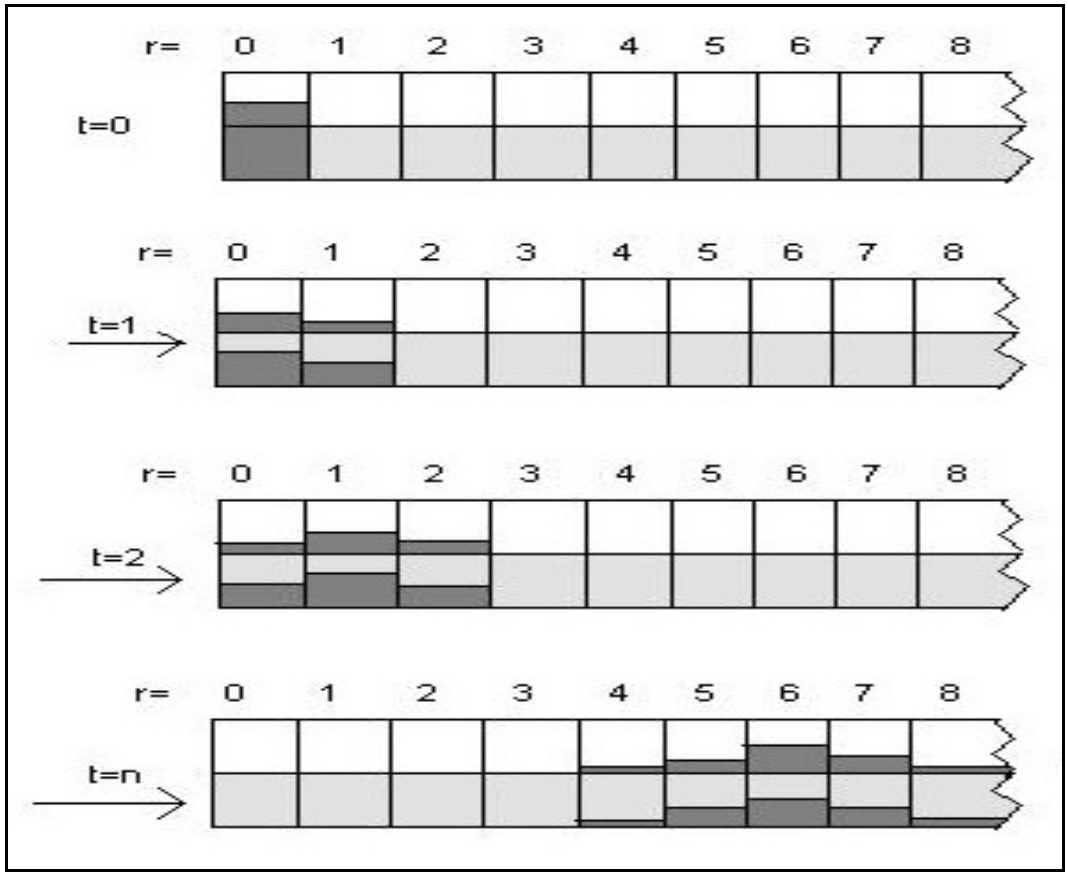

Figure 3: Schematic representation of Plate Theory (Littlewood, 1962, pp120)

2.5.2 Rate theory and the Van Deemter equation

Rate theory can better explain the phenomenon of band broadening of chromatographic peaks because it takes into account the finite time necessary for the analyte to equilibrate between the stationary and mobile phases in the column based on the rates of diffusion in the mobile and stationary phases. As opposed to Plate Theory, it does not require the hypothetical incremental transfer of mobile phase analyte molecules into subsequent physical chambers or zones. Plate theory incorrectly assumes that this equilibration is infinitely fast, but with the constant motion of the mobile phase, equilibrium is actually never reached (Skoog, 1998, pp 682).

The Van Deemter equation was experimentally derived for packed columns by Van Deemter, Zuiderweg and Klinkenberg in 1956 (Littlewood, 1962, pp 168) and was adapted for capillary columns by Golay (Sandra, 1989). Giddings modified this equation further for gas adsorption chromatography (Giddings, 1962). Since there is no liquid phase present, one of the terms of the equation derived by Golay was replaced by a mass transfer term for the kinetics of adsorption and desorption. **Equation 10** shows how the plate height for open tubular adsorption columns is expressed while **Equations 11 and 12** show how the *f* terms in **Equation 10** are calculated.

$$H = \left[\frac{B}{\mu_0} + C_g\mu_0\right] f_1 + C_k\mu_0 f_2 \qquad (10)$$

$$f_1 = \frac{9\left(p^4-1\right)\left(p^2-1\right)}{8\left(p^3-1\right)^2} \qquad (11)$$

$$f_2 = \frac{3\left(p^2-1\right)}{2\left(p^3-1\right)} \qquad (12)$$

H is the plate height; the term, $B = 2D_g$, is the longitudinal gaseous diffusion term where D_g is the gaseous coefficient; μ_o is the linear gas velocity at the column outlet; C_g is the term of resistance to mass transfer in the gas phase and

C_k is the term of resistance to mass transfer for adsorption and desorption kinetics. In **Equation 10,** the terms f_1 and f_2 correct for the effect of the pressure gradient on column efficiency and *p* is the ratio of the column inlet to the column outlet pressure (De Nijs *et al*, 1983).

Figure 4 shows the theoretical Van Deemter curves for a capillary column for the three most common carrier gases where plate height, H is plotted against carrier gas velocity, μ. The minimum plate height for optimum column efficiency will be found at the optimum value for μ (μ_{opt}). In practice, a carrier gas velocity slightly higher than μ_{opt} is used to shorten analysis times.

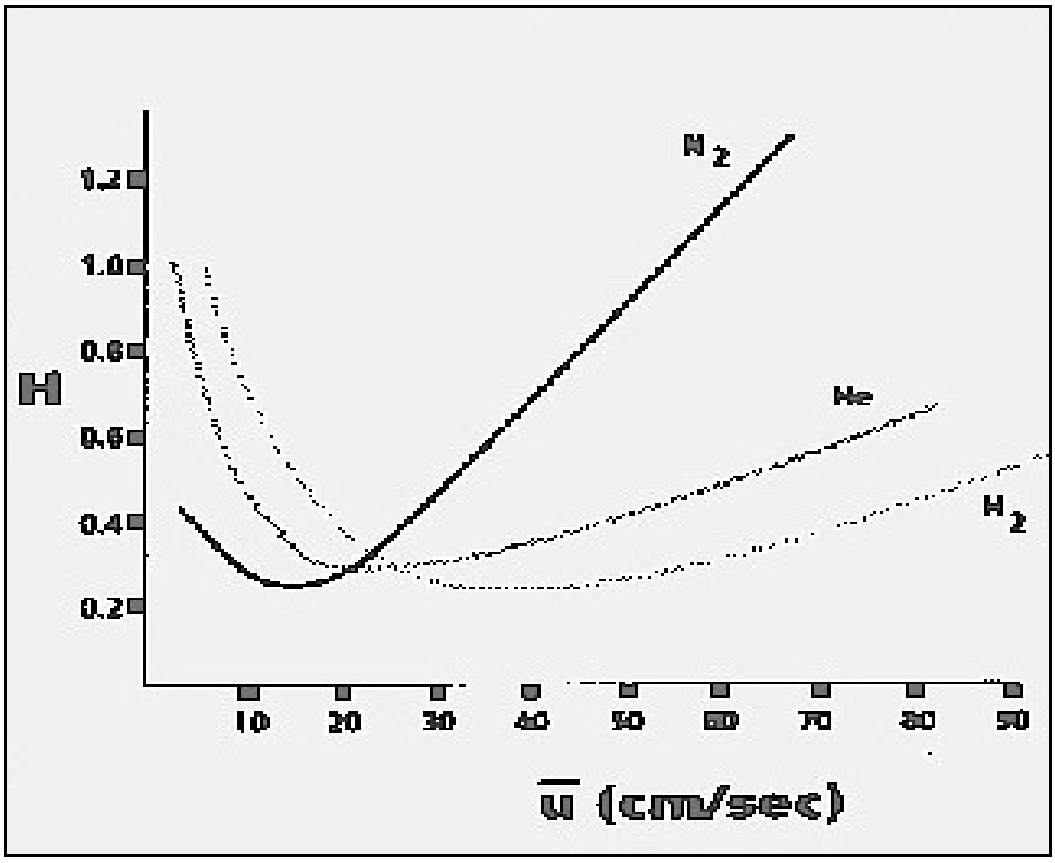

Figure 4: Van Deemter curves for N_2, He and H_2 carrier gases (Agilent, 2004).

The first term in the Van Deemter equation ($\frac{Bf_1}{u_0}$) is called the longitudinal diffusion term; the second term ($C_B\mu_0 f_1$) is called the resistance to mass transfer in the mobile phase term and the third term ($C_k\mu_0 f_2$) is called the resistance to mass transfer in the stationary phase term (Skoog, 1998).

The longitudinal diffusion term ($\frac{Bf_1}{u_0}$) determines how much band broadening takes place as the solutes diffuse out of a concentrated zone as they move along the column. This term is directly proportional to the diffusion coefficient D_g (since $B = 2D_g$) and is inversely proportional to the mobile phase velocity u_0. For gaseous mobile phases, D_g is proportional to temperature and thus the longitudinal diffusion term can be decreased by operating the column at low temperature (Skoog, 1998, page 685-686) and increasing the mobile phase velocity.

The second term in the Van Deemter equation is called the resistance to mass transfer in the mobile phase ($C_g u_0 f_1$) and is one of the terms that account for the time taken for equilibrium to be reached in the column. The analyte molecules take a finite time to move from the mobile phase to the stationary phase and this time lag results in non-equilibrium conditions along the column with subsequent band broadening. The mass transfer term is increased when the carrier gas flow is increased, contributing to greater plate heights and reduced column efficiency.

The third term in the Van Deemter equation for PLOT columns is called the resistance to mass transfer in the stationary phase ($C_k u_0 f_2$) and incorporates the constant C_k that accounts for the kinetics of adsorption and desorption of the gas on the stationary phase. The value of C_k is very important with regard to column efficiency (Giddings, 1964), as can be seen when choosing stationary phases for a particular application. The third term is also increased by increased carrier gas flow, making the value for H greater and decreasing column efficiency.

In reality, all the mechanisms described by the terms of the Van Deemter equation act together and the effects of each one cannot be isolated. To visualize their effect, one can imagine a solute zone carried along by a moving gas stream. The solute will spread out as it moves along, the sharp boundaries becoming blurred as time passes. An infinitely thin zone will eventually take on a Gaussian distribution. Slow equilibration and flow patterns within the column will also result in spreading to a Gaussian profile (Peters, Hayes, Hieftje, 1974 pp 528).

2.5.3 Resolution

The resolution R_S provides a quantitative measure of the separation achieved between two analytes (Skoog, 1998, pp688). The goal of optimizing column efficiency is to completely resolve the analyte peaks from each other in the minimum time with minimum peak broadening.

The Gaussian peak is a product of a statistical theoretical treatment of the solutes' transit through a chromatography system. A normal Gaussian distribution curve can be characterized by the fraction of its total area that lies within certain distances from its midpoint. These distances are expressed in terms of the curve's standard deviation (σ), which is the distance between the apex of the peak and its midpoint and the inflection points. A distance of ± 2σ from the midpoint of a peak with the base width (w_b) accounts for more than 99,96% of the area (Hinshaw, 2004). Resolution can be written in terms of retention time and average standard deviation (σ_{av}), as shown in **Equation 13,** where Δt is the difference in retention time of two peaks in the chromatogram.

$$R_S = \frac{\Delta t}{4\sigma_{av}} \qquad (13)$$

The peak width is usually measured at half peak height because it is the easiest to measure manually. The relationship between the peak width at half height (w_h) and the curve's standard deviation (σ), is given by **Equation 14** (Hinshaw, 2004).

$$w_h = 2{,}354\sigma \qquad (14)$$

The peak width at the base of the peak (w_b) is related to the peak width at half height (w_h) by **Equation 15** (Hinshaw, 2004).

$$w_b = 4\sigma = 1{,}699 w_h \qquad (15)$$

From this relationship, **Equation 13** can be rewritten and the resolution calculated from a chromatogram as shown in **Equation 16**, where W_A refers to the peak width at half height of analyte A; W_B refers to the peak width at half height of

analyte B; $(t_R)_A$ refers to the retention time of analyte A and $(t_R)_B$ refers to the retention time of analyte B (Hinshaw, 2004).

$$R_S = 1{,}177 \times \frac{[(t_R)_B - (t_R)_A]}{W_A + W_B} \qquad (16)$$

Baseline resolution of two peaks is obtained when R_S has a value of 1,5. When R_S has a value of 1, peak A contains about 4% of peak B and vice versa. Resolution may also be written in terms of theoretical plates, the capacity factor (k') and the selectivity factor (α) as shown in **Equation 17** (Skoog, 1998).

$$R_S = \frac{\sqrt{N}}{4}\left(\frac{\alpha - 1}{\alpha}\right)\left(\frac{k_B'}{1 + k_B'}\right) \qquad (17)$$

From **Equation 17**, it may be seen that resolution is maximized when all three terms of the equation are maximized. Increasing the value of N, however, by lengthening the column may not be the answer since it leads to longer retention times and broader eluting peaks. Also, from **Equation 17**, the value of R_S has a square root dependence on the value of N, and the column would therefore have to be quadrupled in length in order to double the resolution. From **Equation 9**, the value of N is also increased by decreasing the theoretical plate height. The capacity factor (k') may be optimized by changing the column temperature and the selectivity factor (α) may be maximized by appropriate choice of stationary phase and to a lesser extent, column temperature (Skoog, 1998).

The number of theoretical plates (N) in a column may be calculated from a chromatogram by using the retention time of a peak (t_R) and the peak width at half height (w_h) as shown in **Equation 18**. Columns of greater theoretical plate numbers will broaden the solute band less than columns with fewer theoretical plates (Hinshaw, 2004).

$$N = \left(\frac{t_R}{\sigma}\right)^2 = 16 \times \left(\frac{t_R}{w_b}\right)^2 = 5{,}545 \times \left(\frac{t_R}{w_h}\right)^2 \qquad (18)$$

Chapter 3

Summary of the literature study on the analysis of permanent gases by gas chromatography

It is expedient to give an overview of the work that has been done in the field of gas analysis in order to put into perspective the work done in the present study.

3.1 Gas analysis by gas chromatography

Gas analysis by gas chromatography is almost exclusively done using gas solid chromatography, also known as adsorption chromatography, which comprises all gas chromatographic methods in which the stationary phase is a solid material with surface-active properties (Jeffrey and Kipping, 1964, pp 4,5). Ramsey (as cited by Hogan, 1997, pp 9, 10) is credited as being the first person to attempt the separation of gases using an activated charcoal column in 1905 (Wikipedia, 2004).

By 1964, only a small number of solid stationary phases were being used to achieve the chromatographic separation of gases namely; charcoal, silica gel (SiO_2), alumina (Al_2O_3) and molecular sieves (Jeffrey and Kipping, 1964, pp 27).

Silica gel and alumina are polar columns, have a high affinity for water and must be activated at high temperature to get rid of adsorbed moisture.The first methods of preparation of silica gel columns greatly affected their separation characteristics and the chromatograms were difficult to reproduce. Early charcoal columns also differed according to the method of preparation of the column packing and required high temperatures to produce acceptable peak shapes, with the concomittant disadvantage of reduction in the packing absorptivity and therefore the deterioration in the separation characteristics. Alumina has been traditionally used for the separation of the hydrocarbon gases, specifically the separation of unsaturated hydrocarbons from saturated hydrocarbons (Hogan, 1997, pp 55). Of the four stationary phases first used, the molecular sieves (or zeolites) proved to be the most useful and enduring for the analysis of the permanent gases.

The first naturally occurring zeolite, stilbite, was identified by Baron Axel Frederik Crönsted in 1756 (Sherman, 1999) and since then, 50 naturally occurring zeolites have been described. The term “molecular sieve” was coined when it was found that the adsorption characteristics of the zeolite, chabazite, could be attributed to tiny pores (<5 Å in diameter) that obstructed large molecules, allowing only smaller ones to enter. In 1953, Linde Type A zeolite became the first synthetic zeolite to be commercialised as an adsorbent to remove oxygen impurity from argon at a Union Carbide plant. Since then, many synthetic zeolites (aluminosilicates of sodium, potassium or calcium) have been manufactured. The most commonly used synthetic zeolites used for gas chromatography are type 5 Å, calcium alumino-silicate, with an effective pore diameter of 5 Å, and type 13X, sodium alumino-silicate, with an effective pore diameter of 10 Å (Zhenghua Ji *et al*, 1999). Synthetic zeolites have the advantage of high purity and uniformity over the naturally occurring zeolites (Sherman, 1999).

Glass columns were first used to house the stationary phases, but these had the disadvantage of inflexibility and once packed, were impossible to coil. Metal tubing has been successfully used for making packed columns due to the ease of coiling and coupling the metal columns to the fittings of the gas chromatograph (Jeffrey and Kipping, 1964, pp 23 to 27).

The first gas samples intended for chromatographic analyses were injected into packed columns by using gas-tight syringes, where the hypodermic needle of the syringe was inserted through a rubber septum into the carrier gas stream. This method cannot be considered accurate where the carrier gas stream is above atmospheric pressure and it achieved only approximate results. Fixed volume pipettes, four way and six way taps were the predecessors of the first multiport sample valves that were developed to replace gas-tight syringes in the quest for quantitative gas analysis (Jeffrey and Kipping 1964, pp 8 to 22)

The detectors housed in the first commercial GCs in 1955 were thermal conductivity detectors (TCD), the concept of which (the cooling of a hot wire in a gas) was first patented by the Siemens and Halske company in 1913 for the determination of methane in air. The gas density balance was based on the principle that a gas sample would distribute itself in a vertical passage according to the density of its components. This vertical passage was connected in two other ways containing or joined by a flow-sensitive device. The distribution of the gases

in the mixture as sensed by these flow-sensitive devices formed the basis of chromatographic response (Jeffrey and Kipping, 1964, pp 48 to 51).

The reduction gas analyser (RGA) in which heated mercuric oxide is reduced to mercury, was being marketed in 1954 for the analysis of trace amounts of carbon monoxide and hydrogen in gas samples. In 1958, the flame ionisation detector (FID) made its appearance for the analysis of carbon-hydrogen containing compounds in an air-hydrogen flame. Also in 1958, the predecessor of the helium ionisation detector (HID), the argon ionisation detector, proved to be several orders of magnitude more sensitive than the TCD (Hogan, 1997, pp 9 to 11).

A detector widely used today for trace gas analysis is the pulsed discharge helium ionisation detector (PDHID) which was developed in 1992 by Wentworth *et al* and proved to be universally sensitive to permanent gases at trace levels (Wentworth, Vasnin, Stearns and Meyer, 1992). The TCD detector is still used, although it has been superseded by the micro-machined TCD, which comprises a sample injection chamber of a few microlitres in volume and dead volumes of less than 2 nℓ and therefore leads to a much higher sensitivity than the traditional TCD (Etiope, 1997).

The separation of fixed gases today is still achieved by means of gas solid chromatography. The molecular sieves or zeolites are still the stationary phase of choice for the separation of the permanent gases H_2, 0_2, Ar, N_2, CO and CH_4. Packed columns are still used, but are being supplanted for many applications by porous layer open tubular (PLOT) columns that were developed by De Zeeuw *et al* (1983). The same solid supports that were used in packed columns have been integrated onto the walls of wide bore capillary columns, leaving the centre of the PLOT column open. Where longer packed columns had the disadvantage of the high pressure drop across the column, PLOT columns have combined the separating power of the longer column (most PLOT columns are 30 metres long), lower pressure drop, lower flow requirements and faster run times. Both molecular sieves and porous polymers are available as PLOT columns. Charcoal PLOT columns have been used to separate permanent gases and light hydrocarbons in less that eight minutes under isothermal conditions by Hao and Lee (1995).

The development of the carbon molecular sieves Carbosieve and Carboxen (Supelco, 2005) has led to the separation of the permanent gases and C1 to C3

hydrocarbons on a single Carboxen column under temperature programming. Newer, more standardised grades of silica gels like Spherosil and Porosil (Supelco, 2005) are used in some applications as precolumns due to their strong retention of CO_2 and water (Hogan, 1997, pp 43 to 79).

Porous polymers have been developed for use as stationary phases in gas solid chromatography and have the advantage that their selectivity may be modified by changing the chemical composition of the polymer. Alpha and beta cyclodextrin, chemically bonded to porous layer fused silica open tubular columns has been used as a stationary phase to separate C_1 to C_6 hydrocarbons and permanent gases (Reid and Armstrong, 1994). HayeSep polymers, Porapak and Chromosorb (Supelco, 2005) are examples of porous polymers that are in wide use for gas analysis today. Porous polymers do not adsorb CO_2 and water as strongly as silica gel and can therefore be used to analyse these two compounds with shorter run times and better peak shapes. It is worthwhile to note that the use of porous polymers is complementary to the use of the molecular sieves in gas analysis (Hogan, 1997, pp 43 to 79).

Repeatable and accurate injections of gas samples are achieved by means of gas sampling valves. These are available in 4, 6, 8 and 10-port configurations that are actuated either electrically or with pressurised air. Gas sampling valves may be of the diaphragm variety or rotor valves. In order to ensure the integrity of the gas sample, the valves are sometimes housed in helium-purged housings that exclude leaks from the atmosphere. All injections are made using fixed volume metal sample loops.

3.2 Detection of the permanent gases

3.2.1 The pulsed discharge helium ionisation detector (PDHID)

The pulsed discharge helium ionisation detector (PDHID) was developed in 1992 by Wentworth *et al* and was described as having the source of ionisation and excitation as a high voltage pulsed-discharge that replaced the radioactive source most commonly used in the conventional helium ionisation detector (HID).

The high voltage pulsed discharge for the PDHID was developed when it was found that a helium ionisation detector operated in a fixed-frequency, pulsed

mode, led to a reduction in noise and background current from that obtained in a direct current mode (Ramsey and Todd, 1987). The discharge in the PDHID occurs between two platinum electrodes spaced about 2 mm apart. The platinum electrode is a small piece of wire tapered to a sharp point and the discharge between these sharp points has a fine thread-like appearance. The diameter of the discharge region is very small, and measures <3 mm.

All insulators and electrodes are very finely polished and held tightly together to minimise the diffusion of air into the detector. A 3 mm quartz window enables light emitted from the detector to be observed and may be useful when the PDHID is used in connection with a monochromator that enables observation of the analyte spectrum. The quartz window may be used to ascertain whether the discharge is from pure helium because the colour observed from the intense helium emission at 576 nm is a peach colour whereas the presence of nitrogen from the air gives the discharge a blue tint (Vasnin *et al*, 1992).

Since the frequency of the discharge is low and the intervals between the discharges are long, the platinum electrodes are allowed to cool between pulses. The stability of the discharge is important since the analyte signal is observed as an increase in ionisation above that of the helium carrier gas.

Ionisation in the PDHID is said to occur by two means i.e. by direct ionisation of the analyte AB by the electrons accelerated by the high voltage direct current pulse and secondly, by the ionisation following the reaction of the analyte with the relatively long-lived helium metastables. These processes may be represented as in **Equations 19 to 22** (Wentworth *et al*, 1992).

$$e^{-}(V) + He \rightarrow He^{+} + 2e^{-} \qquad (19)$$

$$e^{-}(V) + He \rightarrow He^{**} \rightarrow He^{*}(2^{3}S) + hv \qquad (20)$$

$$e^{-}(V) + AB \rightarrow AB^{+} + 2e^{-} \qquad (21)$$

$$He^{*}(2^{3}S) + AB \rightarrow AB^{+} + e^{-} + He \qquad (22)$$

The helium metastable state (denoted as He^* in **Equation 22**) is 19,7 eV above the ground state compared to the neon ionisation potential of 21,5 eV. The process that occurs in **Equation 21** is the direct ionisation of the analyte in the discharge region and this has been proven to be sufficient to ionise even neon (Lasa *et al*, 2004). Wentworth *et al* (1992) also hypothesised that the excitation of helium probably does not occur directly to the metastable state (He^* in **Equation 22**), but through a higher energy state (He^{**} in **Equation 20**) which decays to He^* with the emission of a photon.

Forsyth (2004) gave an alternative explanation of the process of ionisation as being the process where the diatomic helium undergoes transition to the dissociative $2He$ ground state resulting in a photon emission, as shown in **Equation 23 and 24**.

$$He_2(A^{1}\Sigma_u) \rightarrow 2He(1^1S_0) + h\upsilon \qquad (23)$$

$$AB + h\upsilon \rightarrow AB^+ + e^- \qquad (24)$$

This transition is known as Hopfield emission, which occurs at very short wavelengths (60 to 100 nm) with energies ranging from 13,5 eV to 17,5 eV and provides enough energy to ionise all elements and compounds with the exception of neon (**Equation 24**).

A schematic diagram of the D4 PDHID (VICI-Valco, 2004) model used in this investigation is shown in **Figure 5**. The detector is divided into two zones i.e. the discharge zone and the reaction zone. As the flow of excited helium passes through the discharge zone into the reaction zone, the analytes exit the GC capillary column directly into the reaction zone near the repelling bias electrode, flowing counter to the flow of the helium discharge gas. The separation of the discharge zone from the ionisation or reaction zone along with the counter helium gas flow configuration ensures that only pure helium passes through the discharge region, minimising the possibility of contamination of the discharge electrodes (Forsyth, 2004).

The GC column eluents are universally photoionised by Hopfield emission with the resulting electrons producing a measured electric current. The electrons are

focussed toward the collector electrode by the bias electrodes (Forsyth, 2004). The collection of electrons at the collecting electrode comprises the detector response. This signal is sent to the electrometer of the GC and processed by software into a signal against a background signal of helium carrier gas.

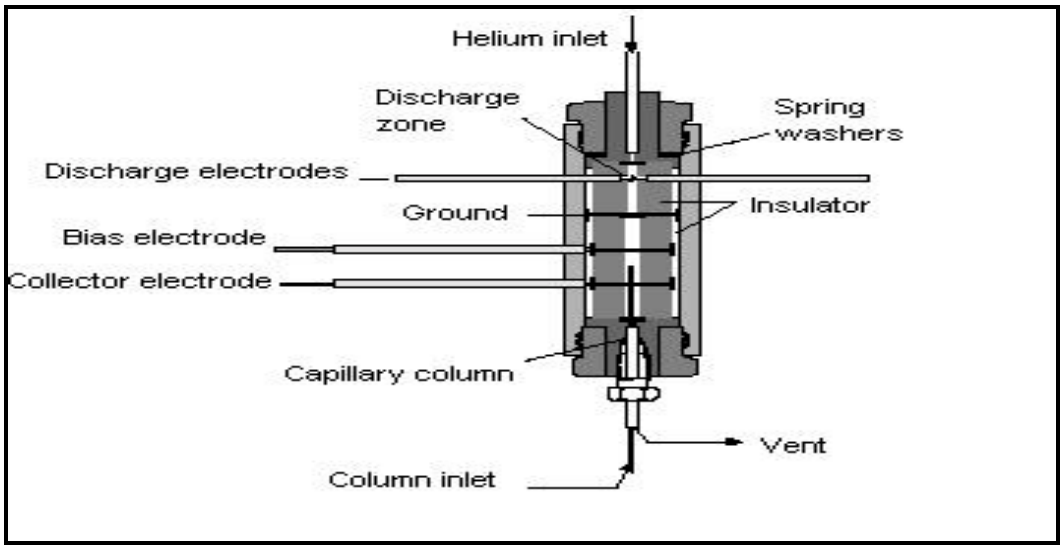

Figure 5: Schematic diagram of a D4 model PDHID detector (VICI-Valco, 2004)

Wentworth *et al* (1994) have proved that neon can be detected by the PDHID if the analyte were allowed to pass directly through the discharge region, where neon is detected as a result of direct ionisation. The PDHID has been shown to have a detection limit of 0,5 ng for neon where the analyte was introduced directly into the discharge region and the helium discharge gas was doped with 33 $\mu mol \cdot mol^{-1}$ neon to achieve acceptable linearity for the method (Lasa *et al*, 2004).

It has been suggested that the sensitivity of the PDHID for permanent gases may be increased by a factor of 5 to 10 by the direct ionisation that results when the analytes are allowed to pass directly through the discharge region (Wentworth et al, 1994).

Wentworth *et al* (1994) have isolated four parameters that affect the sensitivity and the linearity of the response with concentration of the PDHID. These factors are: the power transmitted to the primary coil of the pulsed high voltage transformer (which in turn affects the voltage and current of the discharge); the frequency or interval of the pulsed discharge; the potential applied to repel the electrons to the collecting electrode and fourthly, the helium flow rate through the discharge

region. Pertaining to the D4 PDHID used in this investigation, only the last of these, the helium flow rate through the discharge region, was variable.

The helium that passes through the discharge region has two purposes i.e. it keeps the discharge region clean so that the excited helium species can be generated and it serves as a make-up gas so that the residence time of the analyte in the detector is reduced. The residence time of the analyte in the detector should be as short as 10 to 20 % of the peak width in order to maintain chromatographic integrity. Sharper peaks require a higher helium discharge gas flow rate.

As the discharge gas flow decreases, the eluting analyte is less diluted and the response increases, but reaches a constant value at lower flow rates where the higher air back-diffusion and lower detector pressure contribute to a decreased detector response. For a detector with a 3 mm internal diameter, a helium discharge flow of 10 $m\ell \cdot min^{-1}$ has been shown to be sufficient to maintain chromatographic integrity (Wentworth *et al*, 1994).

The PDHID requires a very pure source of helium gas and Wentworth *et al* (1992) recommended grade 6 helium (99.9999% pure) which was additionally purified by passing it through a VICI helium purifier (Valco Instruments Company, Inc., Houston, Texas, USA). The helium purifier uses a non- volatile alloy at high temperature to remove all impurities except inert gases and nitrogen. There is still the possibility that impurities can enter the gas stream from leaks as well as from the tubing connecting the purifier to the detector.

3.2.2 The flame ionisation detector (FID)

The FID is the simplest of all the ionisation detectors, yet one of the most universally used. All ionisation detectors are based on the conduction of electricity by gases, which under normal circumstances do not conduct electricity, but can do so when an energy source is used to ionise the gas in the presence of an electric field. The energy source used to ionise the gas in an FID is an air-hydrogen flame. The flame ionisation detector does not respond to most permanent gases or water (Jeffrey and Kipping, 1964, pp 70). Flame ionisation detectors are simply two electrometer plates between which a hydrogen flame burns. The flame has non-zero conductivity due to ions and free electrons in the flame. The introduction of

analytes into the flame changes this conductivity by altering the concentration of conducting species. The electrometer is capable of sensing very small changes in conductivity and therefore very small quantities of analyte (Carlin, 2004). **Figure 6** is a schematic diagram of a FID.

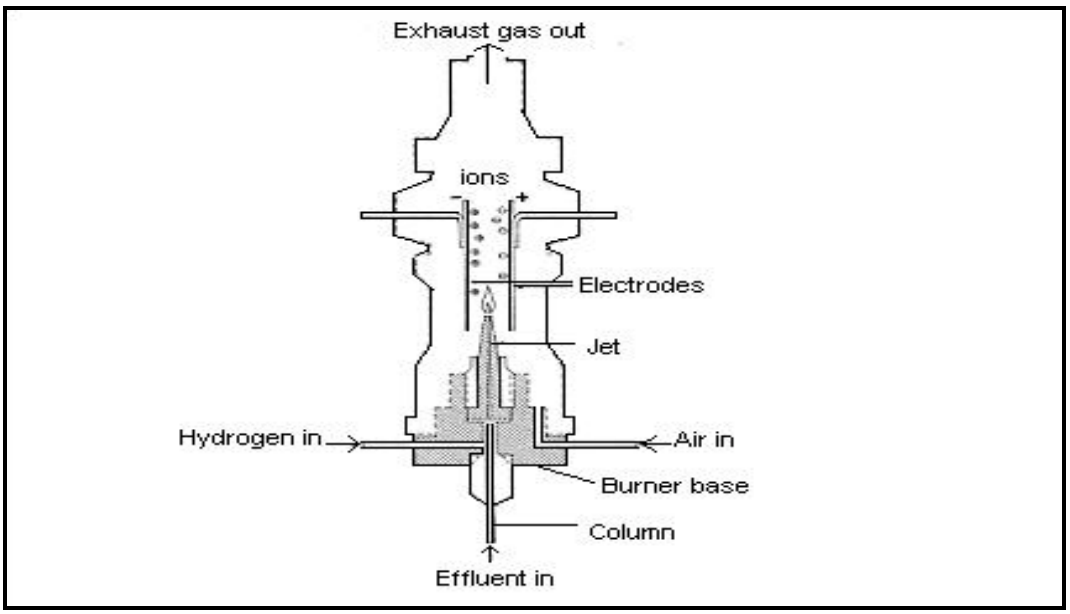

Figure 6: Schematic diagram of an FID (Carlin, 2004)

The FID is favoured in gas chromatography because of its high sensitivity, quantitative proportional output and linearity up to seven orders of magnitude. The FID is considered as a carbon counting device because its response to hydrocarbons is proportional to the rate of introduction of carbon into the flame. The FID is not, however, sensitive to all carbon containing compounds, having no response for CO, CO_2 and CH_2O. Even though the FID was invented more than half a century ago, the mechanism by which the FID ionizes the sample molecules is not fully understood (Dojahn *et al*, 2001).

The weak response towards the permanent gases namely CO, CO_2, CH_2O, O_2, Ar and N_2 may be explained by considering the mechanism by which the FID is thought to ionise the sample. The ionisation is thought to be the result of the formation of an excited species CHO* during the oxidation process and the flame ionisation the result of the following chemical ionisation step shown in **Equation 25**.

$$CHO^* \rightarrow CHO^+ + e^- \qquad (25)$$

Generally, the FID response is proportional to the number of carbon atoms in the molecule. The presence of heteroatoms in the molecule can be expected to decrease the FID response since they add mass to the molecule but do not undergo ionisation in the flame (Wentworth *et al*, 1998).

Holme and Madsen (1996) have shown, however, that all hydrocarbons are converted to methane in the cooler inner cone region of the flame in a quantitative manner prior to the combustion process in the outer portion of the flame. They claim that this quantitative formation of methane prior to combustion explains the equal response per carbon atom observed for the hydrocarbons. Since carbon atoms bonded to O or N atoms do not undergo this quantitative conversion to methane, they do not give a response proportional to the number of carbon atoms, therefore accounting for the poor response of the FID to CO and CO_2. Oxygen and nitrogen cannot undergo conversion to methane or combustion and are therefore practically invisible to the FID.

The fact that N_2 is practically invisible to the FID becomes useful when analysing for impurities present in this gas. Methanisation of CO and CO_2 prior to detection by the FID using a catalyst (nickel, ruthenium, zirconium or platinum) in the presence of hydrogen, allows the conversion of these gases to CH_4 and H_2O. The CH_4 is then detected by the FID with sufficient sensitivity for trace analysis (Etiope, 1999). The methanisation reaction occurs at temperatures of 300 °C to 400 °C and the catalysts used are robust, however significant problems can arise in the presence of low levels of chlorinated compounds and oxygen (Hogan, 1997, pp 72-73). When there are no significant interferences, CH_4, CO and CO_2 may be detected at sub-ppm level by the FID and identified by virtue of their respective retention times upon elution from a suitable separation system and subsequent conversion to methane by the methaniser. **Equations 26 and 27** show how CO and CO_2 are converted to methane by the methaniser.

$$CO + 3H_2 \rightarrow CH_4 + H_2O \qquad (26)$$

$$CO_2 + 4H_2 \rightarrow CH_4 + 2H_2O \qquad (27)$$

The nickel catalyst used in the present system, has been known to have a finite lifetime, especially when operated at high temperatures in the conversion of CO_2 to CH_4. In this case, the converter efficiency may decrease and the catalyst may need to be replaced. A mixture of methane in nitrogen of similar concentration to the highest carbon monoxide standard used can be used to measure the conversion efficiency of the catalyst. The methane mixture is sampled and the peak area for methane compared with the peak area for carbon monoxide (converted to methane by the converter), the ratio of the peak areas being a measure of the converter efficiency (ISO 8186, 1989).

3.3 Separation of the permanent gases

3.3.1 Separation media

By 1964, molecular sieves were being used to separate O_2 and N_2 (Jeffrey and Kipping, 1964, pp 29 to 33) and these are still the stationary phase of choice for separation of these gases. The separation was achieved in a few minutes with a column temperature of 100 ºC and a molecular sieve 5 Å column of a metre or longer. The nomenclature of 4 Å (pore diameter 0.4 nm), 5 Å (pore diameter 0.5 nm), 10X (pore diameter 1.0 nm) and 13X (pore diameter 1.3 nm) are an indication of the pore size and crystal structure (A or X designation) of the zeolite. The separation of O_2 and N_2 was found to be poorer on charcoal, alumina and silica gel columns.

Molecular sieves adsorb water very strongly at ambient temperatures and the accumulation of water has been shown to deteriorate the separating power of the column over time (Grob, as cited in Hogan, 1997, pp 54). Carbon dioxide has been found to be almost irreversibly adsorbed onto molecular sieves at ambient temperatures, but Graven (Graven, as cited in Jeffrey and Kipping, 1964) succeeded in analysing a mixture of O_2, N_2, CO, C_2H_6, N_2O and CO_2 in the order given by using a 2 foot (0.6 m) column of molecular sieve 5 Å with temperature programming. At ambient temperature however, the retention of carbon dioxide on molecular sieve columns has been said to deteriorate the separation characteristics of the column over time (Hogan, 1997 pp 53-54). Other investigators, having injected large quantities of CO_2 into packed molecular sieve columns, have shown that CO_2 does not significantly change the retention characteristics of the molecular sieve column, but elutes slowly as an insignificant

rise in the baseline upon temperature programming when present in small amounts (Thompson, 1977, pp 10).

Argon has been found to have similar retention characteristics to oxygen in all the adsorbents, but was resolved from oxygen using a 10-metre packed column of molecular sieve 5 Å (that had been preheated in an oven at 400 ºC), with hydrogen gas as a carrier at room temperature (Vizard and Wynn, 1959, as cited in Littlewood, 1962, pp 375). A 1.8 metre packed molecular sieve column was also used to resolve argon and oxygen at -72 ºC (Lord and Horn, 1960, as cited in Littlewood, 1962, pp 375). Resolution of argon from oxygen at ambient temperature must therefore be carried out with a long packed column (with long retention time and broader peaks), or with a shorter packed column at sub-ambient temperatures. If there are other permanent gases present (e.g. CO and CH_4), they will elute with much longer retention times and greater peak broadening than oxygen and argon, which are not ideal circumstances for routine analysis.

CO has been separated easily from the air gases at ambient temperature using a molecular sieve column greater than one metre in length. Novelli (1999) described common analytical systems for CO analysis as comprising of a silica gel or alumina pre-column followed by an analytical column comprised of a molecular sieve. The purpose of the pre-column was to capture CO_2, non-methane hydrocarbons and water that are backflushed to prevent contamination and subsequent deterioration of the analytical column performance.

Laurens *et al* (2000, 2001) have analysed trace impurities (H_2, O_2, N_2, CO, CO_2) in corrosive gases by using a backflush system with one of the analytical columns being a molecular sieve 13X column. The detector used was a pulsed discharge helium ionisation detector (PDHID) and the detection limits reported were around 10 $ng \cdot L^{-1}$. A silica gel pre-column with a molecular sieve 5 Å analytical column in a backflush configuration with a PDHID detector was also used by Stevens and Bellows (2004) to analyse trace impurities in beverage grade CO_2.

The ISO-8186 (1989) standard method for the determination of CO in air by gas chromatography employs a GC-FID methaniser system with a backflush configuration, and a molecular sieve 5 Å recommended as the analytical column. Kaminski *et al* (2003) also used a short molecular sieve 5 Å column and a

Porapak Q in a backflushing configuration and GC-FID with a methaniser to analyse CO, CH_4 and CO_2 in refinery gases and air.

The OSHA standard method for CO in workplace atmospheres (Method number ID-210, 1991) uses a molecular sieve 5 Å column in series with another column with no backflushing stipulated, although it is stated that CO_2 does not interfere due to it being adsorbed onto the column. The detector used in the OSHA method is a discharge ionisation detector (DID).

As stated earlier, molecular sieve columns are now available in porous layer open tubular (PLOT) configuration. Vanssay *et al* (1994) stated in their literature search to find suitable columns for the study of permanent gases for the NASA Cassini-Huygens probe study of Titan's atmosphere, that the molecular sieve 5 Å PLOT column provided very good results for the separation of permanent gases. NASA has since rejected the PLOT columns in favour of micro-packed Carboxen columns (Navale *et al*, 1999) because the PLOT columns were considered too fragile for space applications. Column manufacturers (Restek catalogue, 2005), however, claim that their PLOT columns have been bonded to immobilise the stationary phase even under conditions of continual valve cycling.

Porous polymers do have separating characteristics for permanent gases, but do not provide the required resolution for the purity analysis of permanent gases. However, they can be made to resolve O_2 and N_2 if a PLOT column is run under sub-ambient temperature conditions (Restek catalogue, 2005 pp 649). A relatively long (>8 metre) packed Hayesep Q or Hayesep A column (Chemlab) can give baseline separation of O_2 and N_2 at 30°C provided that the concentrations are less than 10^{-5} $mol.mol^{-1}$ (de Coning, 2005). Porous polymer columns are useful for their ability to elute CO_2, which does not elute from molecular sieve columns under ambient temperature.

Restek (Restek catalogue, 2005, pp 649) have developed a technique for gas analysis by combining two PLOT columns using a Presstight® fitting to join them together. The gas stream from the injector is split into two, entering both columns simultaneously and exiting the columns to be joined into one stream before entering the detector. This technique has been shown to work for permanent gases in helium with a TCD detector but for impurities in nitrogen, the peak from the matrix gas could be very large, making it difficult to detect impurities at trace

levels. The advantage of this technique though, is that CO_2, O_2 and CO could be separated in one run with only two columns and fewer valves. **Figure 7** shows the Restek dual column system, the chromatographic conditions used and the peaks obtained for permanent gas analysis (Restek catalogue, 2005, pp 649). In the Restek application, the concentrations used are large (5 % of each component in helium) and no detection limits or precision is quoted.

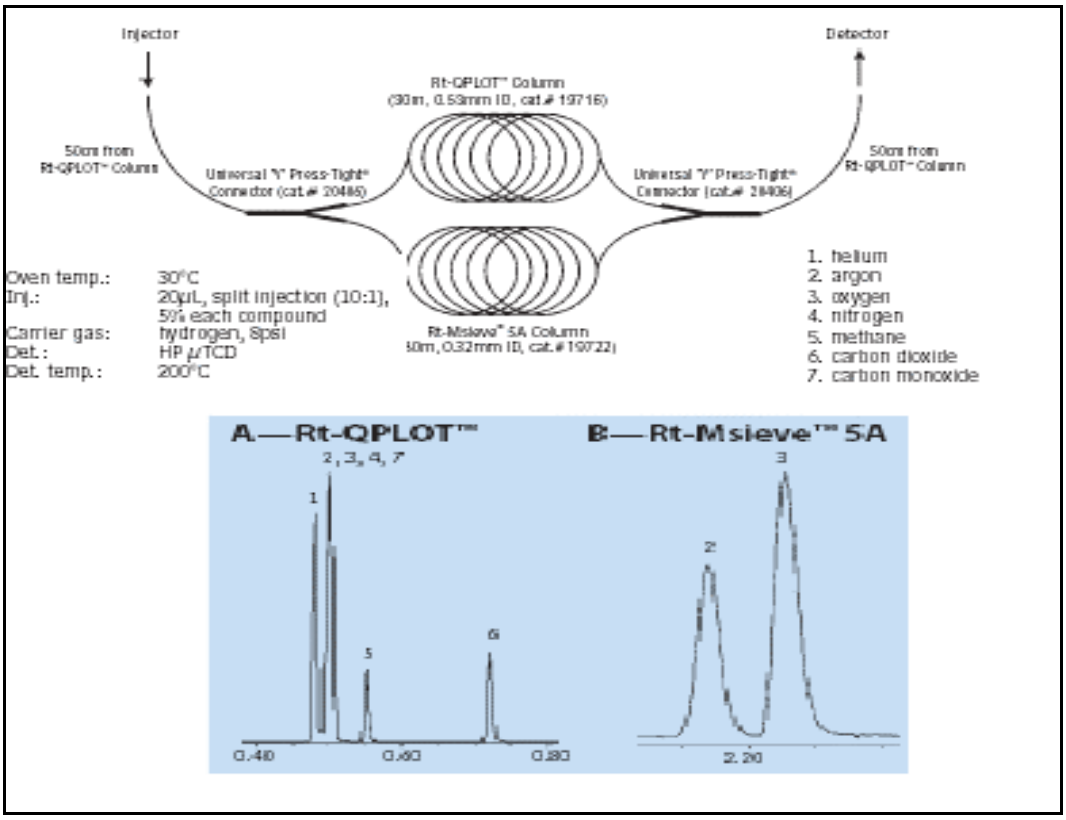

Figure 7: Dual column system from Restek (Restek catalogue, 2005, pp 649).

Wurm *et al* (2003) also used a dual column configuration to analyse low levels of oxygen, carbon monoxide and carbon dioxide in polyolefin feed streams with a Model D1 PDHID as the detector. The columns used in parallel were an HP Molesieve column (15 m; 0,53 mm internal diameter; 50 µm coating) and a Varian/Chrompack PPQ (30 m; 0,53 mm internal diameter; 20 µm coating). They analysed O_2, CO_2 and CO in nitrogen, but could not achieve satisfactory chromatograms due to the large nitrogen matrix and the large amount of argon that partially co-eluted with the oxygen peak. Consequently, they switched to using standards of O_2, CO_2 and CO in helium and cited detection limits for the method (calculated using a 10 ppm mixture of O_2, CO_2 and CO) as being between 50 and 250 ppb, with precision being ±4.2% for O_2; ±7.8% for CO_2 and ±2.0% for CO. The

calculation of detection limits and precision was based on a single concentration standard (10 ppm CO_2, O_2 and CO in helium) which is not in accordance with international requirements for method validation (Eurachem Guide, 1998).

3.3.2 Multidimensional techniques

Multidimensional techniques are used to achieve complete separation of permanent gases and generally refer to the use of two distinctly different adsorbents within a single separation. The most common is the series bypass technique (see **Figure 8**) where, for example, the gases H_2, Ar, O_2, N_2, CO, and CH_4 are passed through a porous polymer onto a molecular sieve column for determination (valve position A in **Figure 8**). The gas stream is then directed through the porous polymer (valve position B in **Figure 8**) and a restrictor to the detector where CO_2 and the other light hydrocarbons are analysed, thereby bypassing the molecular sieve column. The bypass technique is used when there are some components that may cause deterioration of column performance. In this case, the carbon dioxide will adsorb onto the molecular sieve column at ambient temperature (Thompson, 1977, pp 37).

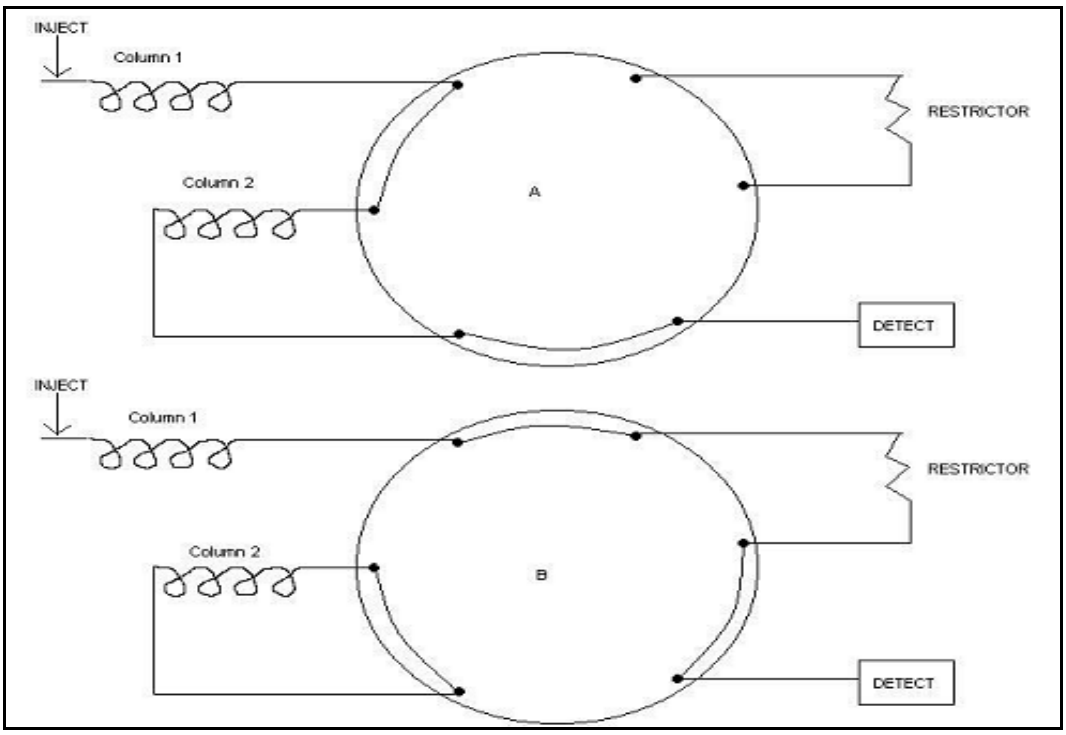

Figure 8: Valve configuration for the series bypass technique

Another technique is the 'heartcut' or 'foreflush', where one component of a chromatogram is sent to vent away from the detector. This may be necessary to reduce the effects of a matrix on the chromatogram. When the nitrogen matrix is removed by the 'heartcutting'-technique, the detection of a small adjacent peak is easier (Hogan, 1996, pp 62). **Figure 9** illustrates the valve configuration for the 'heartcut'-technique using a 10-port valve.

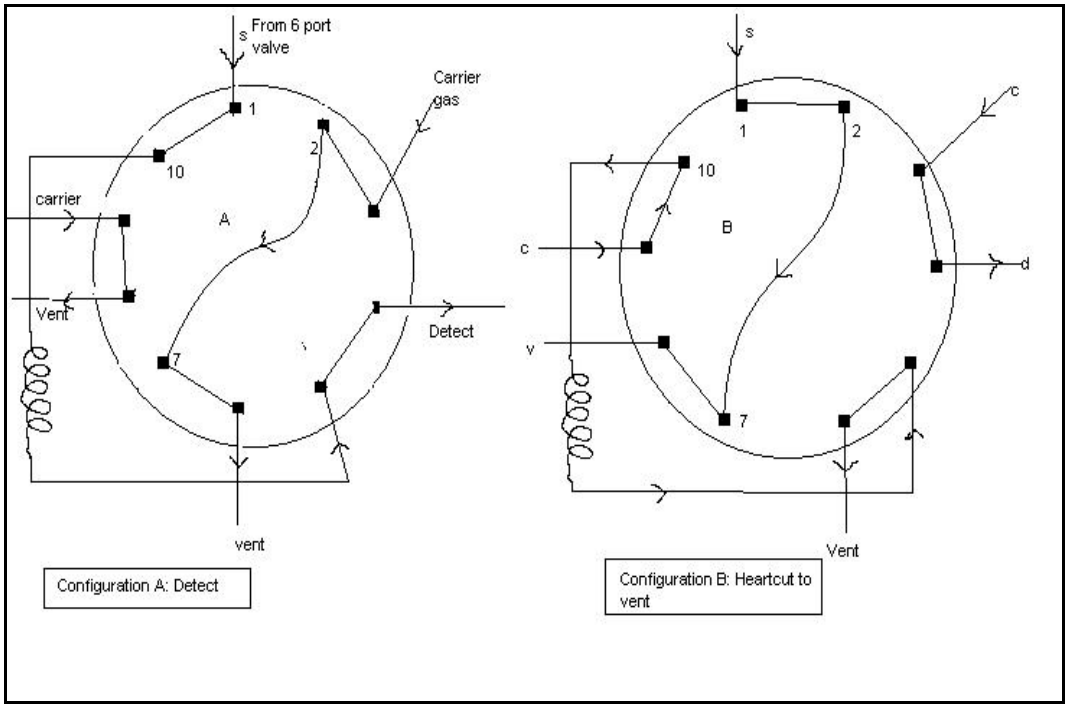

Figure 9: Valve configuration for heartcut to vent

A technique that may not strictly be considered multidimensional is the backflush technique which is used to get rid of undesirable components that have longer retention times on a particular column. The backflush technique is often used to get rid of CO_2 and heavier hydrocarbons from a pre-column before they reach and adsorb onto a molecular sieve column. **Figure 10** shows a valve configuration for a porous polymer column and a molecular sieve column with a 6-port valve. After the required gases reach the molecular sieve (valve position A in **Figure 10**), the valve is switched and the flow through the porous polymer reversed (valve position B in **Figure 10**) so that the heavier components are vented away from the molecular sieve column (Hogan, 1996, pp 61, 62).

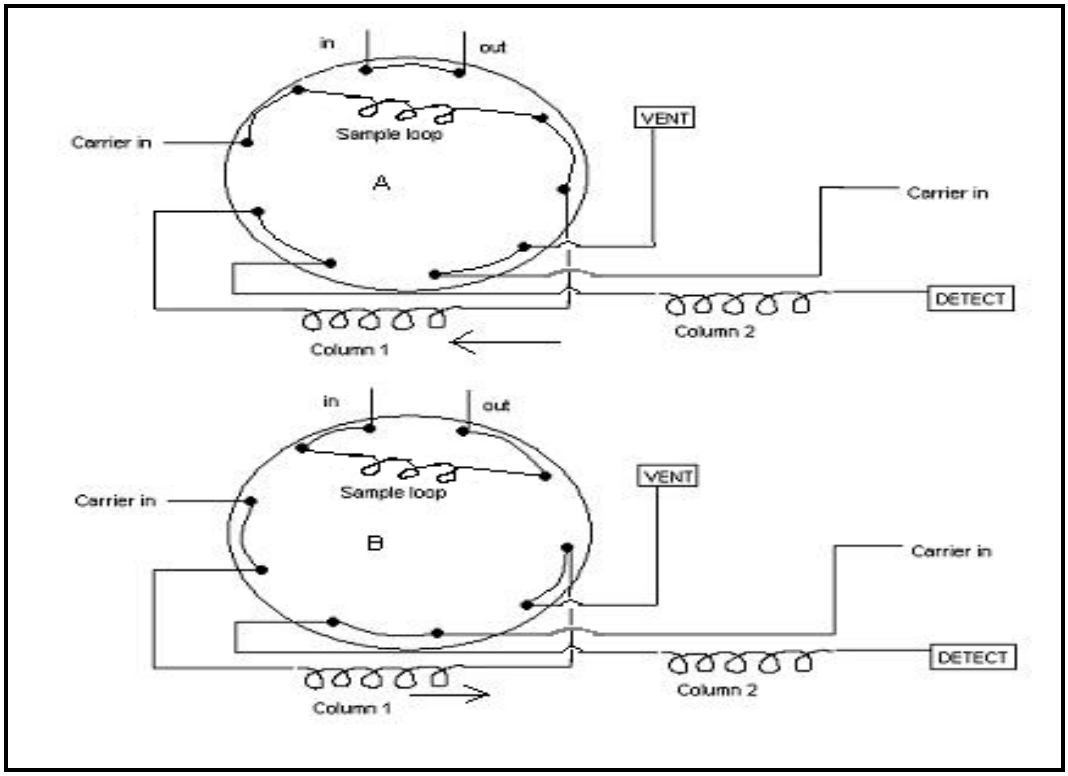

Figure 10: Valve configuration for the backflush technique

The use of two columns in parallel is also a multidimensional separation technique. The columns may be teed together at both ends so that the sample is split between the columns and the column effluent recombined before entering the detector. The split ratio between the columns need not be 1:1 as long as the split is consistent for the samples and the calibration standards. Samples of widely different compositions, however, may split inconsistently between parallel columns that are teed at the sample entry side (Thompson, 1977, pp 35). The manipulation of column lengths, temperatures and other parameters can aid in varying the order of elution of the separated components from two columns connected in parallel.

3.4 Other considerations concerning the analysis of permanent gases

In two publications concerning the analysis of impurities in permanent gases (Laurens *et al*, 2000, 2001); the practical aspects of achieving reliable results were discussed. Since the atmosphere consists of 78.1% nitrogen; 20.9% oxygen; 0.9% argon and 0.035% carbon dioxide by volume (Wikipedia, 2004), the chances of leaks into the gas chromatographic system from the atmosphere interfering with the analysis of trace amounts of these gases are very high.

Laurens *et al* (2000) used pre-cleaned stainless steel tubing throughout the system (PTFE tubing allows influx of air into the system) with gold plated ferrules for integrity where connections had to be made. They avoided possible leaks from pressure regulators by making use of fixed restrictors in the connecting tubing to regulate gas flow. The gas lines were deactivated by flushing with the matrix gas a few times and evacuating between flushing. The rotary gas sampling valves were also located in housings purged with helium to prevent leaks.

In a later publication, Laurens *et al*, 2001 used a PDHID to analyse for atmospheric impurities in tungsten hexafluoride. They found that the PDHID showed some flow sensitivity and they placed fixed restrictors on the supply and vent lines to ensure that the flow through all the columns used were balanced since needle valves were not leak proof. They also found that unless the pressure regulator was purged thoroughly when connected to the cylinder, the air in the regulator could mix with the contents of the cylinder, changing the concentration.

Wurm *et al* (2003) also stressed that air contamination was a problem in their analysis of trace amounts of O_2, CO_2 and CO in polyolefin feed streams and managed to reduce the amount of air contamination by careful sampling. They had also found that when their standards were made up with nitrogen as the diluent or balance gas, there was a large amount of argon also present.

3.5 Conclusions from the literature study

The PDHID is a good choice for a “universal” detector for the analysis of permanent gases. It can detect O_2, Ar, N_2, CH_4, CO, CO_2 in the 10^{-9} mol·mol^{-1} (parts per billion) concentration range, however the responses are not equal for equal amounts of different gases and individual responses for all contaminants must be determined. The operation of the PDHID is simple and cost efficient once a helium purifier is installed in the carrier gas line to provide the system with high purity helium carrier gas.

Molecular sieve 5Å columns are the best choice for the chromatographic separation of permanent gases. Molecular sieve 5Å PLOT columns are the best choice for the separation of O_2 and Ar, which is necessary for the quantification of

the oxygen impurity in nitrogen. A porous polymer PLOT column may be used to separate CO_2 from the other permanent gases.

The Restek dual column system, combining a molecular sieve 5Å PLOT column in parallel with a RT QPLOT porous polymer column can be used as a convenient multidimensional technique to obtain a complete analysis in one injection of the permanent gas impurities in nitrogen viz. O_2, Ar, N_2, CH_4, CO, CO_2. Although the application has been demonstrated by Restek for high concentrations of CO_2, O_2 and CO in helium, the analysis of trace amounts of these gases in nitrogen has not been demonstrated or validated (Restek, 2005).

Wurm *et al* (2003) have shown that the trace analysis of CO_2, O_2 and CO in helium is possible but they did not follow the internationally accepted procedures to validate the method (Eurachem, 1998). Therefore, there is scope to validate the dual capillary column configuration coupled with a PDHID D4 model detector as applied to the trace analysis of CO_2, O_2 and CO in nitrogen.

Since the CO peak elutes some time after the nitrogen peak from a longer Molecular Sieve 5Å column with poor peak shape, the technique of sequence reversal could help to improve the shape of the CO peak and thus the detection limit for CO. Temperature and pressure programming could also be used to elute the CO peak with a better peak shape in a shorter time.

In order to protect against leaks from the atmosphere, stainless steel tubing should be used throughout the system, with gold plated ferrules used for connections. Fixed restrictors, rather than mechanical flow controllers, should be used at the vent and supply lines to balance flows (Laurens *et al*, 2000).

Chapter 4

Summary of the methods used for the preparation of the calibration standards and the method validation process

4.1 Preparation of standard gas mixtures

4.1.1 Gravimetric preparation of gas mixtures

The gravimetric preparation of gas mixtures is recognised to be of the highest metrological quality and has been identified to be a potential primary method for chemical measurement because the calculated concentration is directly traceable to the SI unit for mass, the kilogram (Alink *et al*, 2000).

Depending on the component gases of the mixture, the gas cylinder to be used needs to be pre-treated to ensure that there will be no adsorption effects or side reactions taking place on the inner surface of the cylinder. The gas metrology laboratory has purchased aluminium cylinders of 5 ℓ water capacity, both for their ease of handling and the suitability to the capacity of the 10 kg mass comparator balance, which is used for the accurate weighing of the mixtures.

Aluminium is not as inert to the air pollution gases as stainless steel, and treatment of the inner surface of the cylinders was required. The CSIR NML opted for the use of a fluorination process of the inner surface of the cylinder done by a local company Fluoropack (Pty) Ltd, Gauteng.

Apart from the passivation of the inner surface of the cylinders, the preparation of the cylinders just before filling is also an important step. The process that will be followed by the CSIR NML is to clean the cylinders three times with the balance gas before filling. After the third cleaning cycle the cylinder is evacuated to a high vacuum in the order of 10^{-5} Pa, after which the evacuated cylinder is marked as clean and ready for filling.

The weighing process consists of first weighing the evacuated (empty) cylinder on the high accuracy mass comparator balance (Mettler Toledo PR 10003; capacity 10 kg; readability; 1 mg). The Borda - also called substitution - method of

weighing (Alink *et al*, 2000) is used, where the cylinder is weighed against a reference cylinder for several times on a balance called a mass comparator balance. The mass difference between the cylinders is compensated for by adding or removing mass pieces thereby allowing accurate weighing within a small window (at the CSIR NML, this window of accuracy is 1 g).

The uncertainty sources that are considered during the weighing process are the uncertainty in the masses of the mass pieces, the linearity and repeatability of the balance and buoyancy effects. The temperature, atmospheric pressure and humidity of the weighing chamber are measured during the weighing process to calculate the air density, which is used to correct for the buoyancy effects. Other possible uncertainty contributions; such as residual gas in the cylinder before filling (the cylinder is evacuated to below 10^{-5} Pa); thermal effects (cylinders are allowed to equilibrate to room temperature before weighing) and reactions between the mixture components (non-reactive components are chosen) or the mixture components and the cylinder wall (the cylinder walls are deactivated by fluorination) are reduced to an insignificant level or eliminated during the preparation procedure.

The weighed empty cylinder is then connected to the filling station and filled with the calculated amount of the first gas component of the mixture. The filling station consists of a turbomolecular vacuum pump, a rotary vane forepump, electropolished stainless steel tubing, a pressure indicator and a needle valve to control flow and open/close diaphragm valves. The vacuum pumps are used to pump the filling station down to 10^{-10} Pa before filling the tubing with gas.

To make sure that the correct amount of gas is added to the cylinder, it is placed on a target balance (Mettler Toledo SB12001; capacity 12 kg; readability 0.1 g) and the pressure in the transfer system is monitored while the gas is added. After filling, the cylinder is weighed on the accurate mass comparator balance again to accurately determine the amount of the first component added and to recalculate the mass of the second component or balance gas that must be added to obtain the final mixture at the required gravimetric concentration.

Once the addition of all the component gases have been completed the cylinder is filled with the balance gas to the target mass and then the cylinder is left to stand for a few hours to reach thermal equilibrium before it is weighed accurately on the

mass comparator balance for the final time and the gravimetric concentration is calculated. To homogenise the gas mixture, the cylinder is rolled for at least 12 hours.

Primary reference materials imported from the Nederlands Meetinstituut Van Swinden Laboratory (NMi-VSL) are used for the verification of the gravimetric concentrations of gas mixtures made at the CSIR NML. In future, the laboratory will prepare two sets of calibration series for each of the different component mixtures to compare against each other with only selected cylinders from other NMIs included as blind samples in the analysis sequence for verification of the accuracy of the calibration (Botha, 2004).

In the laboratory primary reference materials are subjected to short term stability testing over a minimum period of three weeks before being made available to customers. The primary standard mixtures will remain in the laboratory for stability testing over a longer period of time to enhance the characterisation of the mixtures and for longer term shelf-life investigations. The stability testing data will also be used to evaluate the efficiency of the fluorination process for the passivation of the inner surface of the cylinders. The stability will be included as an uncertainty component in the combined standard uncertainty of the mixture (Botha, 2004).

4.1.2 Preparation of a calibration series of gases

To prepare a series of standards, the high purity CO_2; O_2 and CO gases were added to an evacuated cylinder and the mixture diluted to the required concentration with BIP™ nitrogen. A series of dilutions were then made from the original mixture using the same BIP™ nitrogen cylinder to make up the mixtures. The flow diagram in **Figure 11** shows how a 1% mixture of O_2; CO and CO_2 in BIP™ nitrogen was diluted using the same BIP™ cylinder to make up seven calibration standards. **Figure 11** is the flow diagram for the gravimetrically prepared three component series i.e. O_2; CO and CO_2 in BIP™ nitrogen. The 0.2 ppm and the 2 ppm standards were prepared later from the 100 ppm standard when the 5 ppm and 10 ppm standards were depleted by the method development and the method validation for the sequence reversal experiments.

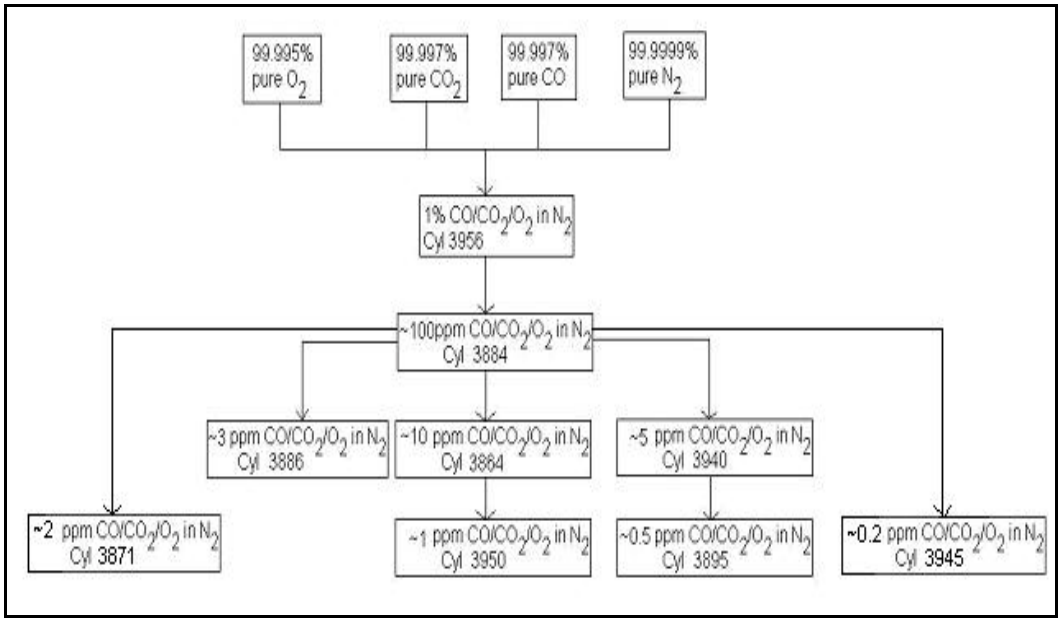

Figure 11: Dilution flow diagram of calibration series for the preparation of O_2: CO and CO_2 in BIP™ nitrogen. Nominal concentrations are in ppm (parts per million) which is equivalent to µmol·mol^{-1}.

4.2 Calibration method

The five lowest concentration calibration standards for each series were used to set up the calibration curve, using the BIP™ nitrogen cylinder that was used in the dilution as the 'blank'.

The standard addition method (Miller and Miller, 2000, pp126) was used to quantify the required impurity in BIP™ nitrogen. The B_LEAST software package (Bremser, version 1.1, 1997) was used to draw up the linear regression line with the five calibration standards and the value of the impurity in the BIP™ nitrogen was calculated from this calibration line by the software, as the intersection of the calibration curve with the x-intercept. If there was no signal for the analyte in the blank, the level of analyte in the blank was then taken as below the limit of detection. B_LEAST was written according to the ISO 6143 standard for gas analysis (ISO 6143, 2001).

For adequate linearity, a goodness-of-fit measure (T), defined as the maximum value of the weighted differences between the coordinates of measured and adjusted calibration points, of T≤2 was considered acceptable (ISO 6143, 2001).

4.3 Method validation process

The Eurachem Guide for the Fitness for Purpose of Analytical Methods (Eurachem, 1998) describes method validation as "being the process of defining an analytical requirement and confirming that the method under consideration has performance capabilities consistent with what the application requires". Method validation enables chemists to show that a method is "fit for purpose".

An analytical result is fit for the purpose for which it was intended when it has been shown to be sufficiently reliable so that any decision based on it can be taken with confidence. The method must therefore be validated and the uncertainty of the result established at a given level of confidence. The method under discussion was validated using the guidelines given in the Eurachem guide according to the criteria discussed below (Eurachem, 1998).

4.3.1. Repeatability

The repeatability of a measurement method is the agreement between the results of successive measurements of the same measurand carried out under the same conditions of measurement (Eurachem/Citac Guide, 2000). Accuracy expresses the closeness of a result to the true value, and is normally studied as two components i.e. trueness and precision. Repeatability is an expression of the lowest measure of precision (best precision) of a method. Repeatability will give an idea of the sort of variability to be expected when a method is performed by a single analyst on one piece of equipment over a short timescale, for example when a sample is analysed in duplicate (Eurachem, 1998).

To examine the repeatability of the method, the average and standard deviation of a set of ten measurements (for each concentration level) made on the same day and under the same conditions, was determined.

The coefficient of variation (International Vocabulary of basic and general terms in Metrology (VIM), 1993) is an estimate of the standard deviation of a population from a sample of n results divided by the mean of that sample, and is frequently stated as a percentage ($\%CV$). The lower the $\%CV$, the more precise the method. **Equations 28 and 29** show how the standard deviation (s) and the

percentage coefficient of variation ($\%CV$) are calculated. From **Equation 28**, x_i is the measurement made, $\bar{x}$ is the average of all the measurements and n is the total number of measurements made.

$$s = \sqrt{\frac{\sum_{i=n}^{n}\left(x_i - \bar{x}\right)^2}{n-1}} \qquad (28)$$

$$\%CV = \left(\frac{s}{\bar{x}}\right) \times 100\% \qquad (29)$$

4.3.2 Reproducibility

Reproducibility is the closeness of the agreement between the results of measurements of the same measurand carried out under changed conditions of measurement (Eurachem/Citac Guide, 2000). Reproducibility is the largest measure of precision (worst precision) normally encountered in a measurement method. Changed conditions could mean changing the temperature at which the analysis is done, having different analysts perform the analysis or performing the analysis of the same sample in different laboratories using different instruments.

An intermediate measure of reproducibility was identified for the purpose of intra-laboratory method validation where it was decided to test the reproducibility by performing the analysis of the same sample on different days. The pressure regulators that were used to reduce the cylinder pressures were also removed and connected at random to different cylinders and the sequence of analysis of the samples was changed randomly to introduce as much variation as possible (Eurachem, 1998).

The reproducibility limit, R, is defined as the value less than or equal to which the absolute difference between two test results obtained under reproducibility conditions may be within a probability of 95%. R is calculated from **Equation 30** where t_∞ is the Student's two tailed value for $v = \infty$ for a given confidence level (for a confidence level of 95% t_∞ has a value of 1.96) and σ_R is the standard deviation measured under reproducibility conditions. If the reproducibility limit is

more than the absolute difference between the two results, the difference is insignificant and the reproducibility precision is considered acceptable (Eurachem, 1998).

$$R = t_{\infty} \times \sqrt{2} \times \sigma_R \qquad (30)$$

4.3.3 Limit of detection

The limit of detection of a method is the lowest level of analyte that produces a response detectable above the noise level of the system; typically three times the noise level (Currie, 1999, pp 105-126). The IUPAC definition focuses on the variability in blanks, requiring twenty or more blank determinations and the use of a statistical multiplier (t value) where t is a one-tailed statistic multiplier with $n-1$ degrees of freedom and an implicit 0.13% risk level for a false detect. **Equation 31** shows how the IUPAC detection limit (LOD_{IUPAC}) is calculated, with S_b being the standard deviation of the blank and m the slope or sensitivity of the calibration curve. The uncertainty of the LOD is calculated using the confidence interval of the standard deviation (which is asymmetric because the upper limit can theoretically be infinite and the lower limit must be greater than zero) (Huber, 2003). For 10 determinations of the lowest concentration standard (in the case where the blank has zero standard deviation or in other words, no signal for the peak of interest), the lower confidence limit of the LOD is obtained by multiplying the LOD by 0,688 and the upper confidence limit is obtained by multiplying the LOD by 1,826 at a confidence level of 95% (Huber, 2003).

$$LOD_{IUPAC} = t(S_b / m) \qquad (31)$$

The limit of detection may also be quantified by the signal to noise ratio method using peak height or peak area (Hogan 1997, pp 165-167) and **Equation 32** shows how this detection limit (LOD_{SN}) is calculated, with C being the concentration of the lowest standard, k being the multiplier by which the signal must exceed the noise level, S the signal level (the peak height in millivolts) and N , the quantified noise level. The noise level, N , can be quantified by the chromatography software as a value in microvolts (mV) before the start of each run or quantified from a specified part of the chromatogram using the integration

software. **Figure 12** shows how the LOD is calculated by the signal to noise ratio method.

$$LOD_{SN} = \frac{kC}{S/N} \qquad (32)$$

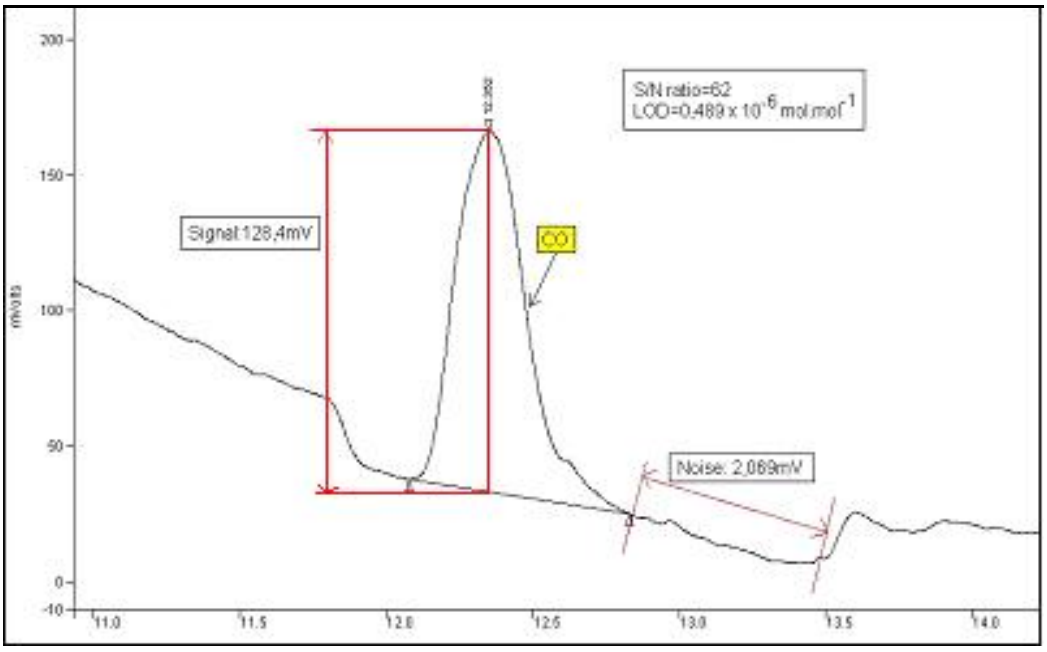

Figure 12: Illustration of LOD calculation by the signal to noise ratio method.

Other methods of limit of detection calculation include the Hubaux-Vos approach (which involves the calculation of upper and lower confidence limits of the calibration curve) and the root mean square error method or RMSE (which involves the generation of a calibration curve and the calculation of the root mean square error) (Corley, 2003).

It was decided to use the IUPAC method for the calculation of the limit of detection because it afforded a simple way of determining the uncertainty as well (Huber, 2003). No references for the calculation of uncertainty were found for the other methods. The uncertainty of the LOD was considered crucial when performing purity analysis because the analyte of interest is often not detected in high purity gases and a reliable estimate of the LOD and its uncertainty is then required.

4.3.4 Limit of quantification

The limit of quantification is normally defined as the lowest level of analyte that can be quantified with an acceptable level of repeatability, precision and trueness. The limit of quantification can be 5, 6 or 10 standard deviations of the blank or lowest concentration standard if the blank has no signal for the peak of interest. **Equation 33** defines the limit of quantification (LOQ_{IUPAC}) with 10 standard deviations of the blank.

$$LOQ_{IUPAC} = 10 \times \frac{S_b}{m} \qquad (33)$$

4.3.5 Selectivity or specificity

It is necessary to establish that the signal produced at the measurement stage which has been attributed to the analyte, is only due to the analyte and not from the presence of something chemically or physically similar arising as a coincidence (Eurachem, 1998, pp 14). In the case of a chromatographic method, the method must be designed so that the peaks of the different analytes are adequately separated to be free from interferences.

4.3.6 Accuracy or Bias

The bias of a measurement method is due to the systematic error inherent in the method and may be described as the degree to which the method yields results that are consistently different from the sample's true value (Eurachem/Citac Guide, 2000). The bias is an expression of the trueness of a method which in turn is one of the two components reflecting the accuracy of a method (Eurachem, 1998). Bias is studied through the use of reference materials or spiking studies. It may be expressed as analytical recovery (value observed divided by value expected).

In this case, the true value of the amount of a specific impurity in BIP™ nitrogen is not known and the analytical recovery cannot be calculated. It is possible, however, to analyse a certified reference material (CRM) using the measurement method to have an indication of the bias. Ideally, a CRM that is within the concentration range of the calibration curve, and whose value can be predicted by

the calibration curve would indicate the bias since the predicted value can be compared with the certified value.

The bias of a method can also be studied through comparison of the results obtained with the test method to a previously validated method.

4.3.7 Linearity

A linearity study verifies that the standards are in a concentration range where the analyte response is proportional to concentration. The number of low concentration standards was restricted to five or less because the dilution series had to be made from the same BIP™ nitrogen cylinder and the amount of gas available in one cylinder is limited. For adequate linearity, a goodness-of-fit measure (T) of T≤2, was considered acceptable (ISO 6143, 2001). Linearity is also expressed by the correlation coefficient (r^2). If there is any doubt of the linearity, a t-test should be performed to test for significant non-linearity. The data should also be physically plotted on a graph for visual examination of linearity. Microsoft Excel XP software was used to plot the calibration data.

4.3.8 Influence of pressure, temperature and other possible sources of error

The method can be susceptible to pressure changes in the columns and in the atmosphere, which would in turn change the retention time of the peaks. The columns must therefore always be kept at the pressures specified in the analytical method in order to avoid interferences with the analyte peaks. Temperature is also only variable within one or two degrees from the column temperature specified in the method to ensure that the resolution between peaks is adequate to prevent interference.

The temperature of the laboratory should be controlled by an air conditioning system that ensures that the temperature and humidity stay within defined limits so that the gas chromatographs have no difficulty in maintaining low temperatures.

The column performances must be investigated and suitable intervals of column conditioning specified so that the performance of the column remains consistent and predictable.

4.3.9 Measurement uncertainty and the uncertainty budget

Uncertainty is formally defined as the parameter, associated with the result of the measurement that characterises the dispersion of values that can be reasonably attributed to the measurand (Eurachem/Citac Guide, 2000). Uncertainty is a 'single figure expression of the accuracy' of a method (Eurachem, 1998).

Traceability is the property of the result of a measurement or the value of a standard whereby it can be related to stated references, usually national or international standards, through an unbroken chain of comparisons all having stated uncertainties (VIM, 1993).

4.3.9.1 Gravimetric preparation uncertainty

The gravimetrically prepared standards have associated uncertainties that were calculated using the weighing data. The total uncertainty is calculated by taking into consideration the weighing uncertainty and the effect of the environment in the weighing room. The degrees of freedom for the calculation of the gravimetric concentration and uncertainty is ∞, and multiplying the result for the uncertainty by a coverage factor of 2 ensures a level of confidence of 95,45% in the result (GUM, 1994).

The uncertainty that is used to construct the calibration curve is the standard uncertainty (the value before multiplication by the coverage factor). The concentrations are calculated using the weighing formulae and include the uncertainty from the gravimetric preparation of the standard as well as the uncertainty of the pre-mixture that was used to prepare the standard by dilution. **Table 2** shows the values of the uncertainties associated with the gravimetric preparation of the standards for the three component series.

Table 2: Uncertainties associated with the gravimetric preparation of the standards for the three component series

Cylinder Number	Component	Actual concentration (μmol·mol^{-1})	Weighing Uncertainty (μmol·mol^{-1})	Standard Uncertainty (μmol·mol^{-1})
3956	CO	8993.637	10.797	5.399
	CO_2	13107.675	5.136	2.568
	O_2	12679.580	8.121	4.060
3884	CO	94.963	0.205	0.103
	CO_2	138.377	0.258	0.129
	O_2	133.842	0.254	0.127
3864	CO	9.151	0.027	0.014
	CO_2	13.837	0.050	0.025
	O_2	13.370	0.026	0.014
3940	CO	4.770	0.022	0.011
	CO_2	6.926	0.046	0.023
	O_2	6.685	0.014	0.007
3886	CO	3.150	0.020	0.010
	CO_2	4.566	0.046	0.023
	O_2	4.402	0.010	0.005
3950	CO	0.979	0.018	0.009
	CO_2	1.401	0.043	0.021
	O_2	1.340	0.006	0.003
3895	CO	0.506	0.018	0.009
	CO_2	0.712	0.042	0.021
	O_2	0.673	0.005	0.003

4.3.9.2 Uncertainty due to repeatability error

There is associated uncertainty with the peak evaluation originating in sample injection error and the error caused by the integration process. The uncertainty is evaluated by calculating the standard deviation of 10 consecutive runs done on each calibration standard. The degrees of freedom for each measurement are 9 ($n = 10$). Although the 10 consecutive runs were performed under repeatability conditions the experimental standard deviation of the mean (ESDM) could not be

used for the evaluation of the standard uncertainty, because the consecutive runs were not strictly independent measurements (GUM, 1993).

The concentration of the calibration standards; the standard uncertainty of the calibration standards; the average signal measured from 10 consecutive readings and the standard uncertainty of the signal were then used to draw up the calibration curve using the B_LEAST regression software. The uncertainties of the slope and the intercept from the regression calculation therefore reflect the repeatability uncertainty (GUM, 1993).

4.3.9.3 Uncertainty due to intermediate reproducibility error

There is also an uncertainty associated with the runs performed on different days because of changes in the column performance due to the accumulation of moisture; the variation in the order that the samples were injected and the different regulators used for different days. This uncertainty is evaluated by comparing the results from the calibration curves for three different days, in the form of the standard deviation.

4.3.9.4 Uncertainty due to the assumption of linearity

The uncertainty arising from the assumption of a linear relationship between x and y is not normally large enough to require an additional estimate (ISO 6143, 2001). Linearity can be quantitatively expressed by the correlation coefficient (r^2) and a r^2-value as close to one as possible is desirable for acceptable linearity. The B_LEAST software also calculates the residuals as a “goodness of fit” value, where a ‘goodness of fit’-value less than 2 signifies that the uncertainty arising from the assumption of linearity is negligible.

4.3.9.5 Summary and classification of uncertainty contributions

The uncertainty due to the assumption of linearity may be ignored in the uncertainty calculations if it has been shown to be negligible. The repeatability uncertainty is taken as the results from the calibration curve for each day. The intermediate reproducibility is taken as the standard deviation of the results from three different days.

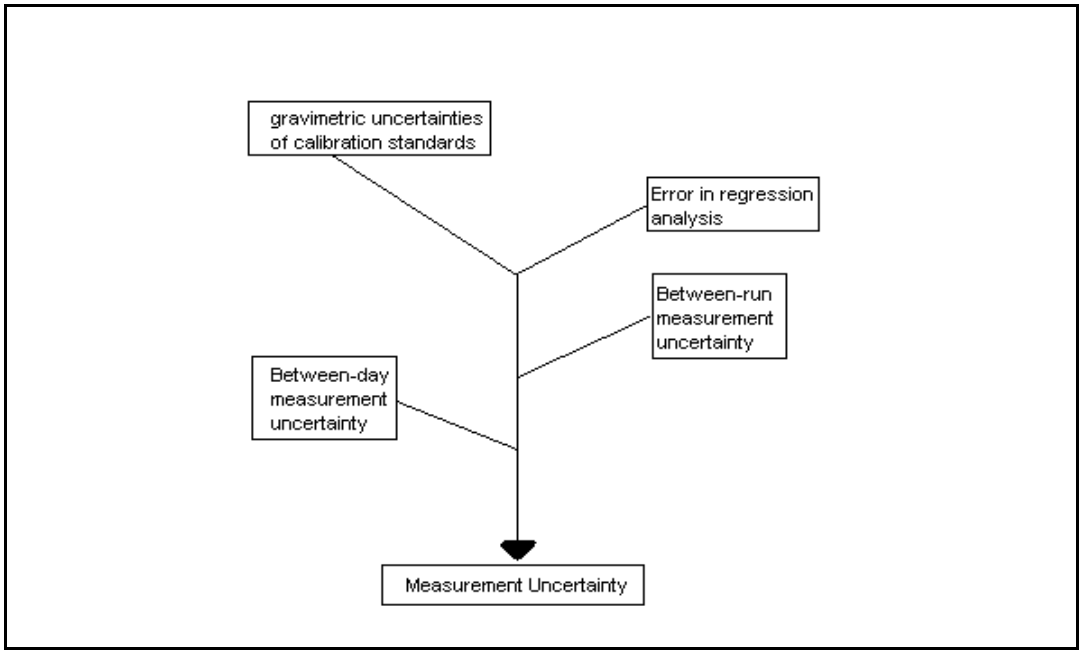

Figure 13: Schematic representation or "cause and effect diagram" of the uncertainty contributors in the measurement method.

4.3.9.6 Calculation of combined uncertainty, effective degrees of freedom and the expanded uncertainty

The combined uncertainty is found by combination of the individual uncertainties multiplied by their respective sensitivities. The sensitivities are calculated by taking partial derivatives of the equation used to calculate the final result. When uncertainties with the same unit are being combined (as in this case), the sensitivities are equal to 1. The verification uncertainties from three different days are combined as in **Equation 34**, where the sensitivities are all equal to 1 since uncertainties in the same units are being combined.

$$u_{VERIFICATION}(x) = \sqrt{\frac{(u_{DAY1})^2 + (u_{DAY2})^2 + (u_{DAY3})^2}{3}} \qquad (34)$$

The combined standard verification uncertainty and the intermediate reproducibility uncertainty (standard deviation of the result for three different days) are then combined as shown in **Equation 35**. The sensitivities are equal to 1 for the individual uncertainties since they are all in the same unit (x 10^{-6} mol.mol^{-1} or ppb).

$$u_c(x) = \sqrt{(u_{VERIFIC})^2 + (u_{REPRODUCIBILITY})^2} \qquad (35)$$

The effective degrees of freedom (v_{eff}) can be evaluated by the Welch-Satterthwaite formula (GUM, 1993) as shown in **Equation 36**, where $u_c(y)$ is the combined standard uncertainty, $u_i(y)$ is the standard uncertainty for each contributor and v_i the degrees of freedom associated with each uncertainty contributor.

$$v_{eff} = \frac{u_c{}^4(y)}{\sum_{i=1}^{N} \frac{u_i{}^4(y)}{v_i}} \qquad (36)$$

The CSIR NML has chosen a confidence level of 95.45% for all measurements made. From *t*-distribution tables, the appropriate value of k (the factor by which the uncertainty is multiplied to ensure a 95.45% degree of certainty in the final result) for v_{eff} is chosen and the standard uncertainty converted to an expanded uncertainty (GUM, 1993) for a 95.45% level of confidence. If any of the uncertainty contributors have infinite degrees of freedom, then v_{eff} from **Equation 36** evaluates to infinity and the appropriate value of k , at a 95,45% level of confidence, from *t*-distribution tables is 2.

Chapter 5

Method Development

5.1 Experimental design, setup and installation

5.1.1 Experimental design

5.1.1.1 Results obtained using a packed column

Initially, the analysis of CO in nitrogen was attempted using a molecular sieve 13X column (dimensions 2 metres in length, 3 mm internal diameter, 80/100 mesh packing size) with the PDHID D4 detector and helium as a carrier gas. By injection of 1 mℓ of sample using a 6-port valve, a detection limit of 0.7 x 10^{-6} mol.mol^{-1} was calculated using the signal to noise ratio method for CO in nitrogen (Janse van Rensburg, NML-03-0154, 2003). Since the amount of CO expected in BIP™ nitrogen was <0.25 x 10^{-6} mol.mol^{-1}, this detection limit for CO was not acceptable. Neither CO_2, nor O_2 could be analysed using the same column.

5.1.1.2 Valve configuration for sequence reversal with dual capillary columns

Using the dual capillary column set from Restek (see **Figure 7**), the first system, configured so that sequence reversal was made possible, is shown in **Figure 14**. A 10-port valve with a T-piece was used. The sequence reversal technique was used to improve the peak shape of the late-eluting CO peak so that a lower detection limit might be achieved.

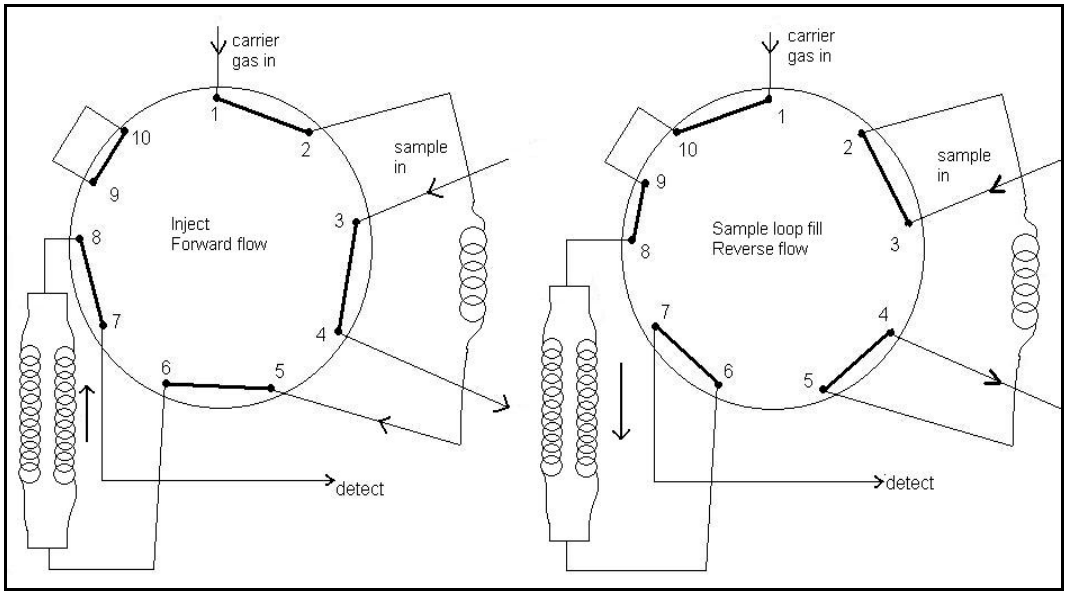

Figure 14: Schematic diagrams of the column configurations enabling sequence reversal using a 10-port valve.

5.1.1.3 Valve configuration for 6-port injection onto dual capillary columns (no sequence reversal)

The 6-port valve was configured as shown in **Figure 15**. The two schematic diagrams in **Figure 15** show the columns in the sample-flush configuration (A); the inject/detect position (B).

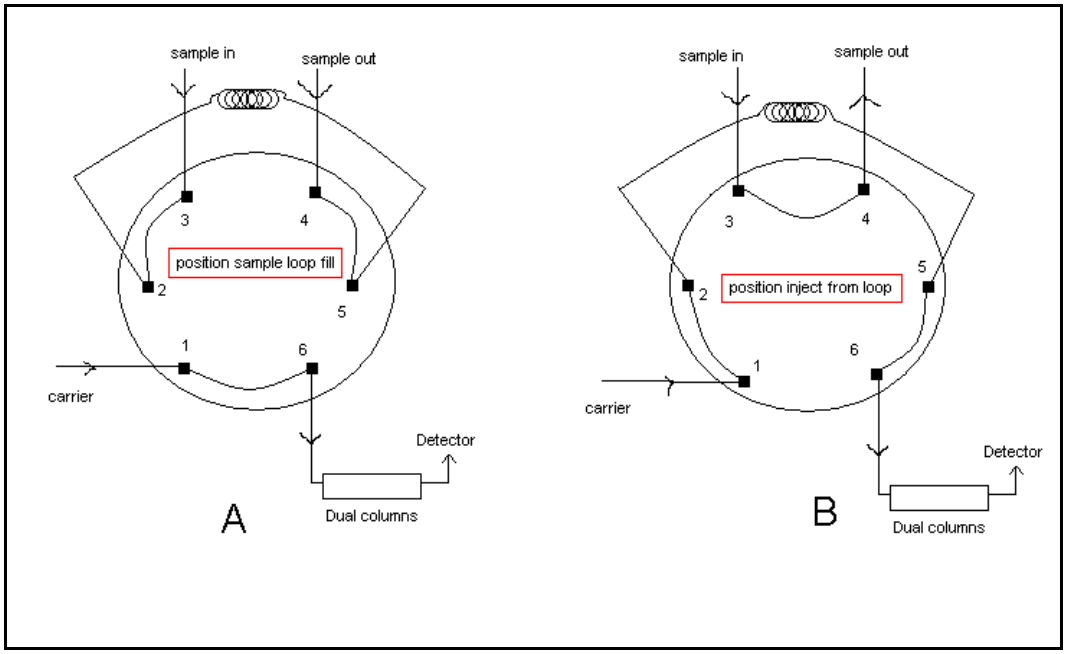

Figure 15: Schematic diagrams of the valve configuration enabling injection and detection using a 6-port valve.

With this design, a sample stream is injected and split between the RT-MS5A and RT-QPLOT columns and is recombined before detection. No sequence reversal is possible with this experimental design.

5.1.2 Experimental setup

A Varian CP 3800 gas chromatograph (Varian Inc, Palo Alto, California, USA) with a model D4-I-VA38-R PDHID detector (VICI AG International, Schenkon, Switzerland) was used for the analysis of trace impurities in nitrogen. The dual column set, comprising an RT-QPLOT (Divinylbenzene PLOT column) with dimensions 30 m x 0.53 mm internal diameter and a RT-Molesieve 5A (Molecular Sieve 5A PLOT column) with dimensions 30 m x 0.53 mm internal diameter, was obtained from Chromspec, Gauteng (Restek Catalogue, 2004/5, page 78). Stainless steel Valco Tee connectors (Product ZT1M, VICI-Valco Cheminert Catalogue, 2005) were obtained from Scientific Supply Services cc, Gauteng for the purpose of connecting the columns in parallel. Two 50 cm sections of the RT-QPLOT column were cut off with a ceramic wafer (making sure that the cuts were square by checking them under a light microscope) and attached to the Valco Tee connectors to connect the dual column system to the valves and the detector. These short column lengths were not expected to make any difference to the retention times or cause peak broadening.

Removable fused silica adapters (FSR) were used to adapt the column diameter to the 1/16 inch nut fittings that connected the column to the valves and to the detector inlet (Product FS1R.8-5; FS1L.8-5, VICI-Valco Cheminert Catalogue, 2005). Gold plated ferrules (Product ZF1GP-10, VICI-Valco Cheminert Catalogue, 2005) were used for the connections of the 1/16 inch nuts because they provided a better seal than stainless steel ferrules. These products were obtained from Scientific Supply Services cc, Gauteng.

An ET4C10UWE 10-port VICI-Valco micro-electric valve was purchased from Scientific Supply Services cc, Gauteng for the purpose of sequence reversal. An ET4C6UWE micro-electric 6-port VICI-Valco diaphragm was purchased from the same supplier for the purpose of sample injection.

Pre-cut, cleaned lengths of stainless steel tubing (1/16 inch diameter) were purchased from Scientific Supply Services *cc*, Gauteng, once the other hardware

had been installed and the minimum lengths for the connecting tubing established. A custom made crimper tool was purchased from the same supplier for the purpose of installing fixed restrictors where necessary at the vents to prevent back-diffusion of air into the system. A flow meter (Agilent 220-1171E ADM 2000 Flow meter), helium leak detector (GL Sciences LD-229 Helium leak detector) and an Imperial Tubing cutter for 1/16 inch tubing (3001-31701) were also purchased from Scientific Supply Services cc, Gauteng for the purpose of method development.

5.1.3 Installation of the components

Figure 16 is a schematic diagram of the experimental setup of the dual column in sequence reversal configuration with the 10-port valve in the Varian CP 3800 GC and the 16-port Stream Selection Valve (SSV) sampling system.

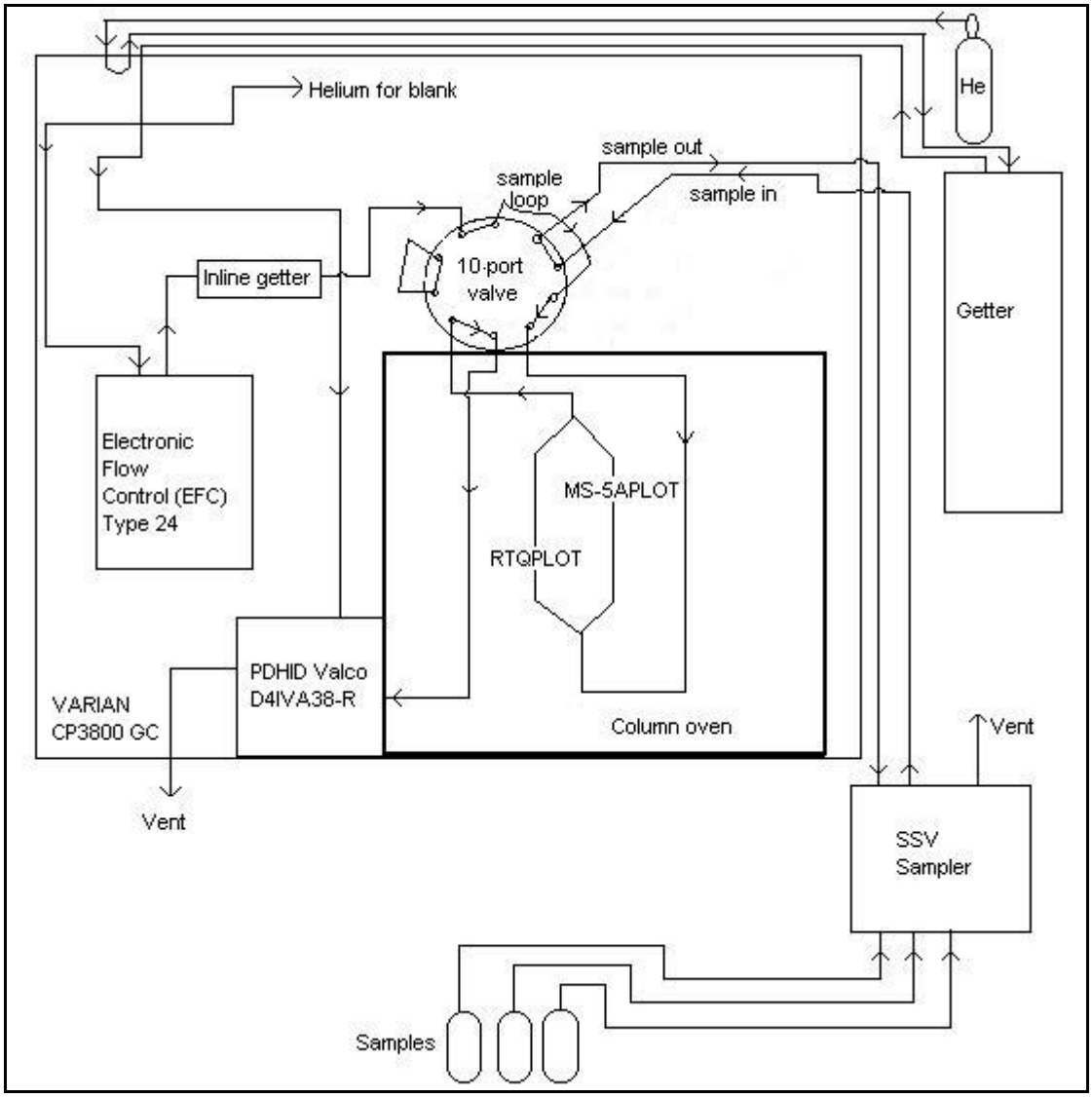

Figure 16: Experimental setup of dual column system with 10-port valve to enable sequence reversal, with a Varian CP 3800 GC and a 16-port SSV sampler.

Figure 17 is a schematic diagram of the experimental setup of the dual column with the 6-port valve, the Varian CP 3800 GC and the 16-port Stream Selection Valve (SSV) sampling system.

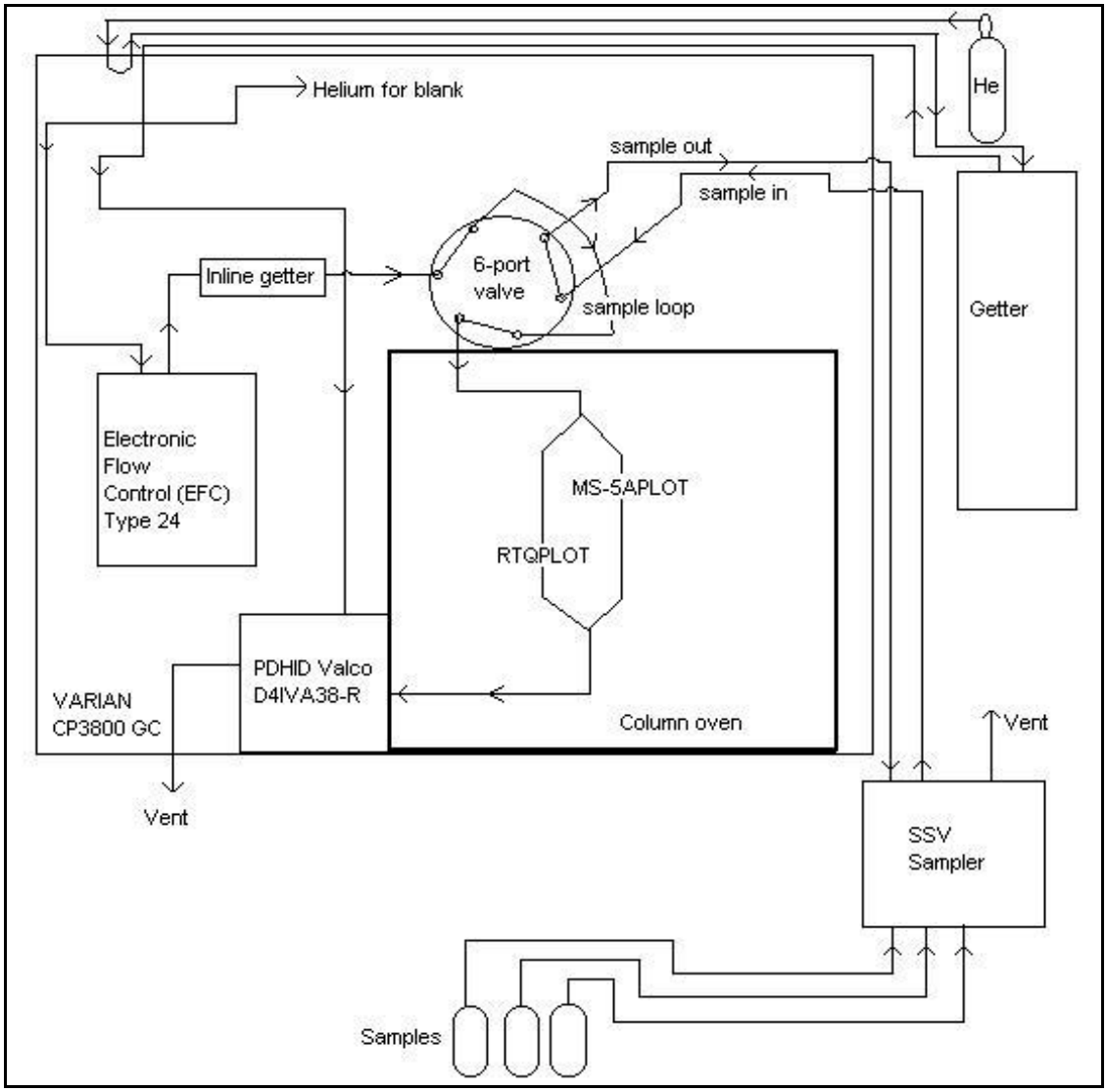

Figure 17: Experimental setup of dual column system with a 6-port valve, Varian CP 3800 GC and a 16-port SSV sampler.

Sample loops were made by cutting pieces of electro-polished stainless steel 1/16 inch tubing to the required lengths and attaching the relevant nuts and ferrules to allow connection to valves.

The GC was configured so that the detector discharge flow (see section 3.2.1) could only be set by choosing the helium 5.0 pressure through the getter. The line going from the Valco cross splitter to the discharge region of the detector had a fixed restrictor to regulate the flow so that a pressure of 550 kPa (80 psi) on the regulator gave a discharge flow of 35 mℓ·min^{-1} and the helium blank line from the cross splitter had a built-in restrictor that ensured a flow of 20 mℓ·min^{-1}. The line for the carrier gas passed through the electronic flow control (EFC) of the gas

chromatograph and an additional in-line helium purifier before reaching the 6-port valve.

The connecting lines from the 5 ℓ sample cylinders were kept as short as possible to save on the amount of sample used to flush the sampling lines. Electro-polished stainless steel was used for the lines, because FEP (fluorinated ethylene propylene) tubing has some permeability to air (Saint-Gobain Performance Plastics, 2005) which cannot be tolerated in the sampling lines.

5.1.4 Initial experimental conditions

Some of the experimental conditions used by RestekCorp (Restek Catalogue, 2005) for the dual column system in the analysis of permanent gases in helium (**Figure 7**), with a HP-μ-TCD detector were used initially (detector temperature; column temperature). The other initial conditions were derived from those in **Figure 7** with consideration for the 0.53 mm internal diameter columns used in this experiment (the original Restek application used a 0.32 mm internal diameter molesieve 5Å column). These experimental conditions are listed in **Table 3**.

Table 3: Initial experimental parameters for the GC-PDHID method

Criterion	**Setting**
Sample loop size	250 μℓ
Column Temperature	30 ºC isothermal
Carrier gas	Purified Helium
Carrier gas pressure	103.4 kPa (15psi)
Combined carrier gas flow	28.5 mℓ·min^{-1} (measured at outlet of dual capillary columns)
Detector temperature	100 ºC
Total Run time	20 minutes

The discharge flow for the PDHID was initially set at 550 kPa at the helium inlet, giving a discharge flow of 35 mℓ·min^{-1} and a helium blank flow of 20 mℓ·min^{-1}. The column was inserted directly into the detector using a fused silica adapter and liner instead of the knurled nut and capillary column adapter recommended by VICI Valco (Pulsed Discharge Detector Model D-4-I-VA38-R Instruction Manual, 2002). The length of the column insert was recommended as being 11,4 cm from the base of the capillary column nut to the tip of the column when a capillary column

nut and capillary column adapter is used. It was decided to test the effect of varying this parameter slightly to ascertain the effect on the peak areas since a fused silica adapter and liner was being used.

5.2 Characterisation of the columns

The retention times of the peaks were expected to be different from the Restek application because the column diameter used in the present application was larger than the diameter shown in the application (**Figure 7**). For method validation purposes (selectivity or specificity), the columns had to be separated and each component run individually at the same inlet pressure in order to identify the relevant peaks eluting from the columns. The peaks eluting from the dual column system could then be identified unambiguously. The RT-MS5Å column was connected and tested with standards each containing only one of the analytes. The peaks were identified and the retention times noted.

Figure 18 shows the chromatogram obtained when the BIP™ nitrogen was injected on the RT-MS5Å column while **Figure 19** shows the chromatogram obtained from the RT-MS5Å column for a mixture of oxygen in BIP™ nitrogen. **Figure 20** shows the chromatogram obtained from the RT-MS5Å column for a mixture of 10 $\mu mol \cdot mol^{-1}$ carbon monoxide in BIP™ nitrogen. Argon and oxygen are present in all the samples. Argon is present from the BIP™ nitrogen, and according to the manufacturer, may be present in quantities from 20 to 100 $\mu mol \cdot mol^{-1}$ differing from batch to batch. Oxygen is present due to leaks from the atmosphere into the system.

The RT-MS5Å column was removed and the RT-QPLOT column was connected. A BIP™ nitrogen cylinder was run in order to ascertain the position of the nitrogen peak (**Figure 21**).

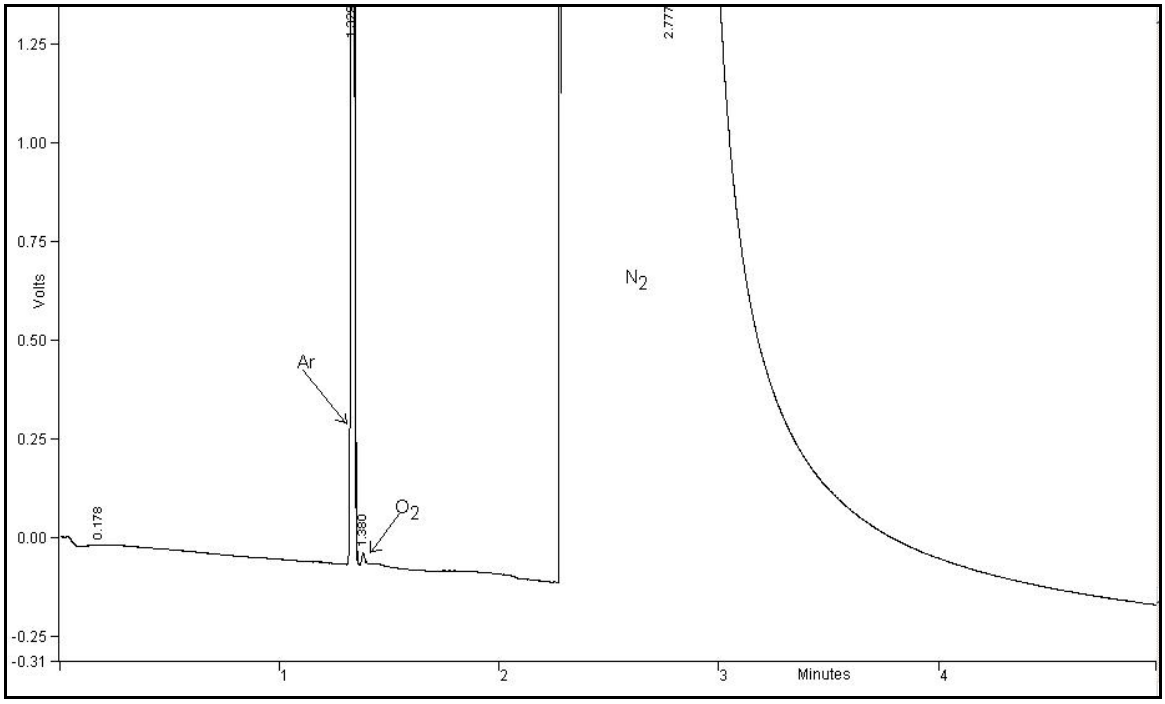

Figure 18: Chromatogram of BIP™ nitrogen on the RT-MS5Å column.

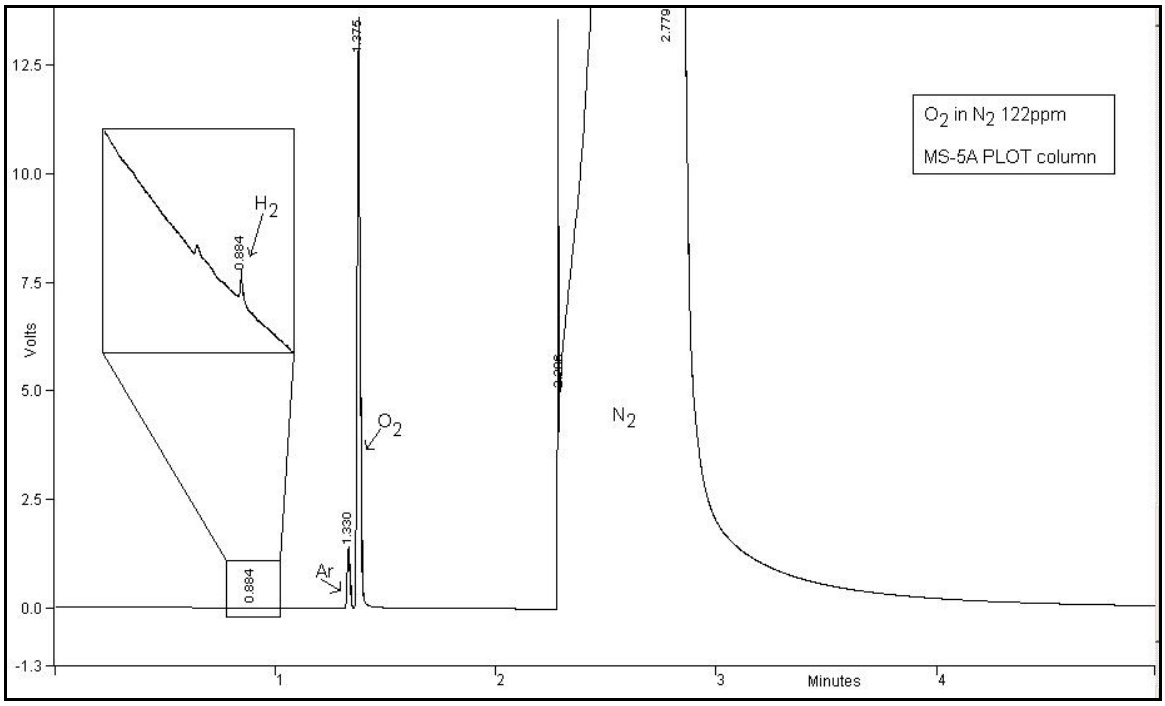

Figure 19: Chromatogram of 122 µmol·mol^{-1} O_2 in BIP™ nitrogen on the RT-MS5Å column. Note the small hydrogen peak (insert).

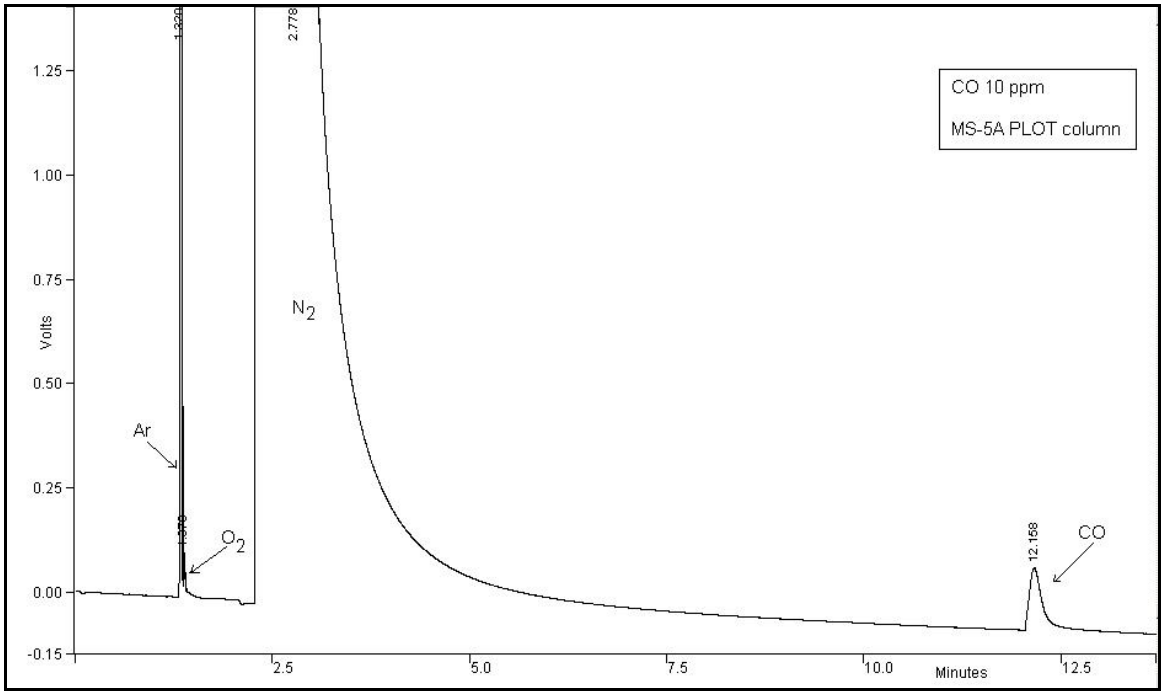

Figure 20: Chromatogram of 10 µmol·mol^{-1} CO in BIP Nitrogen on the RT-MS5Å column.

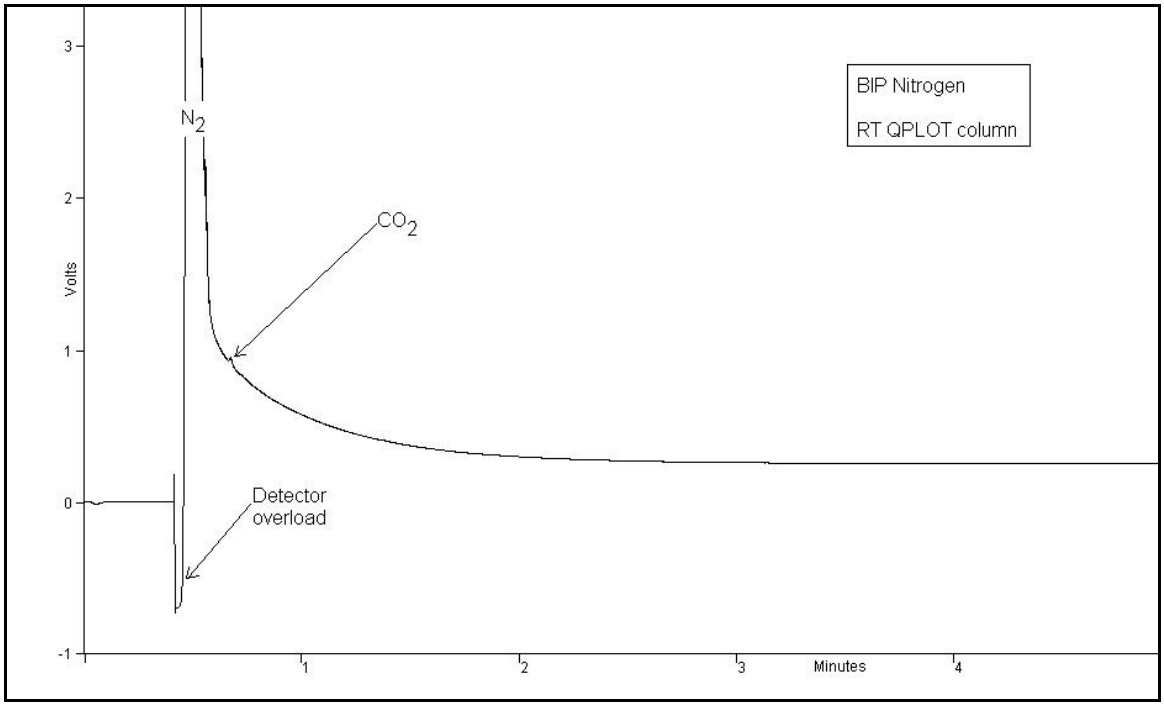

Figure 21: Chromatogram of BIP™ nitrogen on RT-QPLOT column showing a very small peak for CO_2 (amount less than 0.05 µmol·mol^{-1})

A 13 µmol·mol^{-1} mixture of CO_2 in BIP™ Nitrogen was run to verify the retention time of the CO_2 peak (**Figure 22)**.

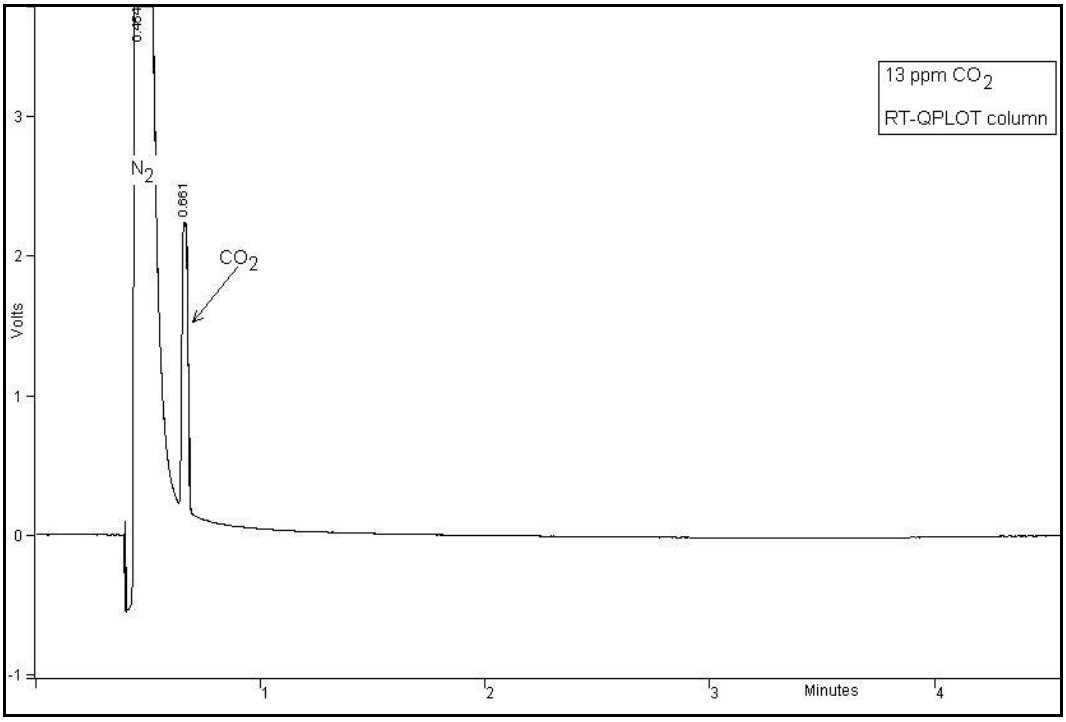

Figure 22: Chromatogram of 13 µmol·mol^{-1} CO_2 in BIP™ nitrogen on RT-QPLOT column.

The RT-MS5Å and the RT-QPLOT columns were connected in parallel and the components run individually to establish their retention times (**Figures 23 to 25**). In **Figures 26 and 27**, temperature and pressure programming were used to improve the peak shape of the CO peak.

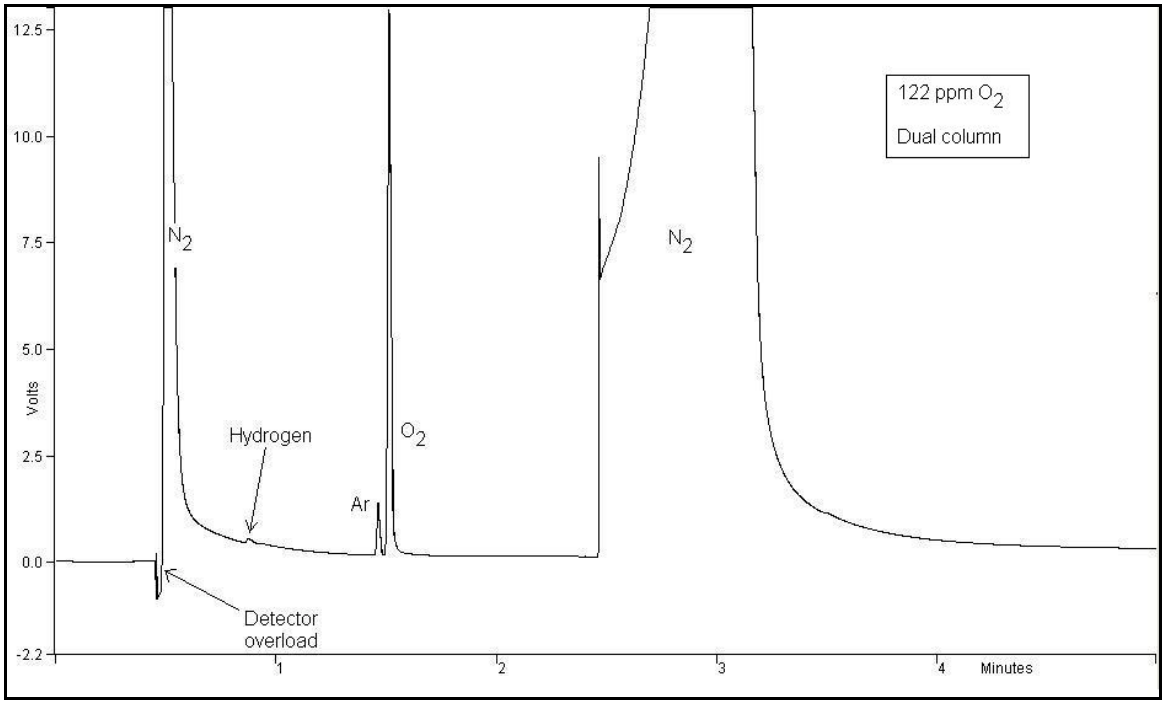

Figure 23: Chromatogram of 122 µmol·mol^{-1} O_2 in BIP nitrogen on the dual column system.

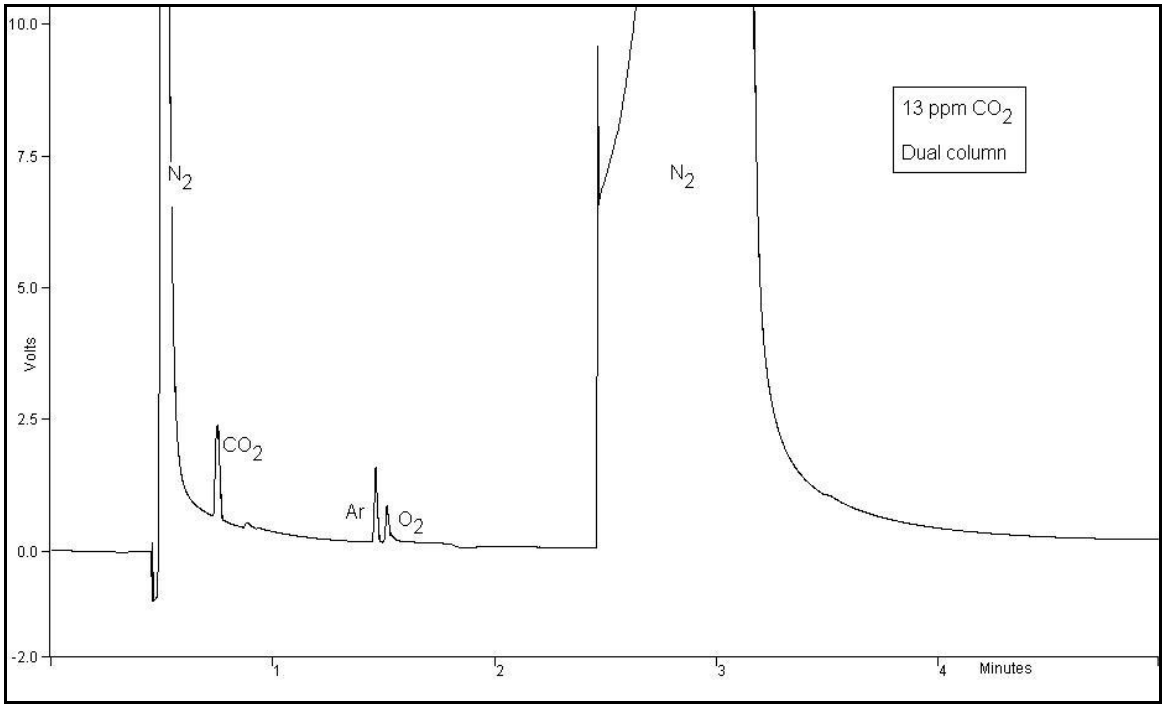

Figure 24: Chromatogram of 13 µmol·mol^{-1} CO_2 standard on the dual column system.

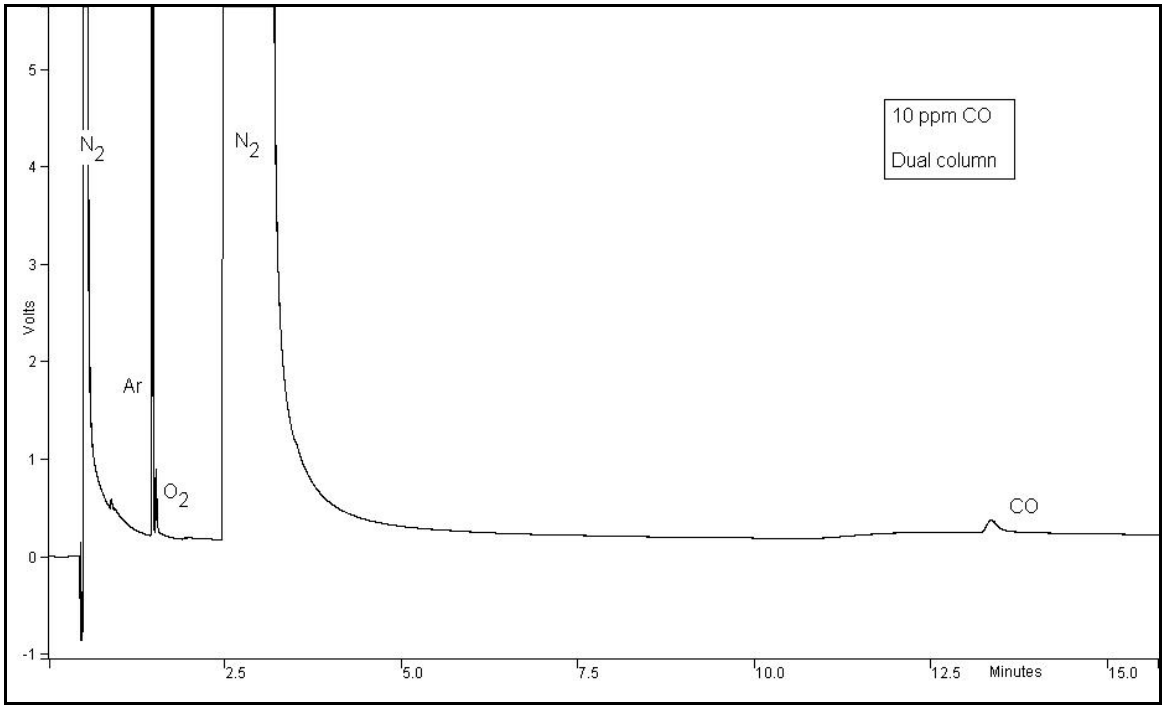

Figure 25: Chromatogram of the 10 µmol·mol^{-1} CO standard on the dual column system.

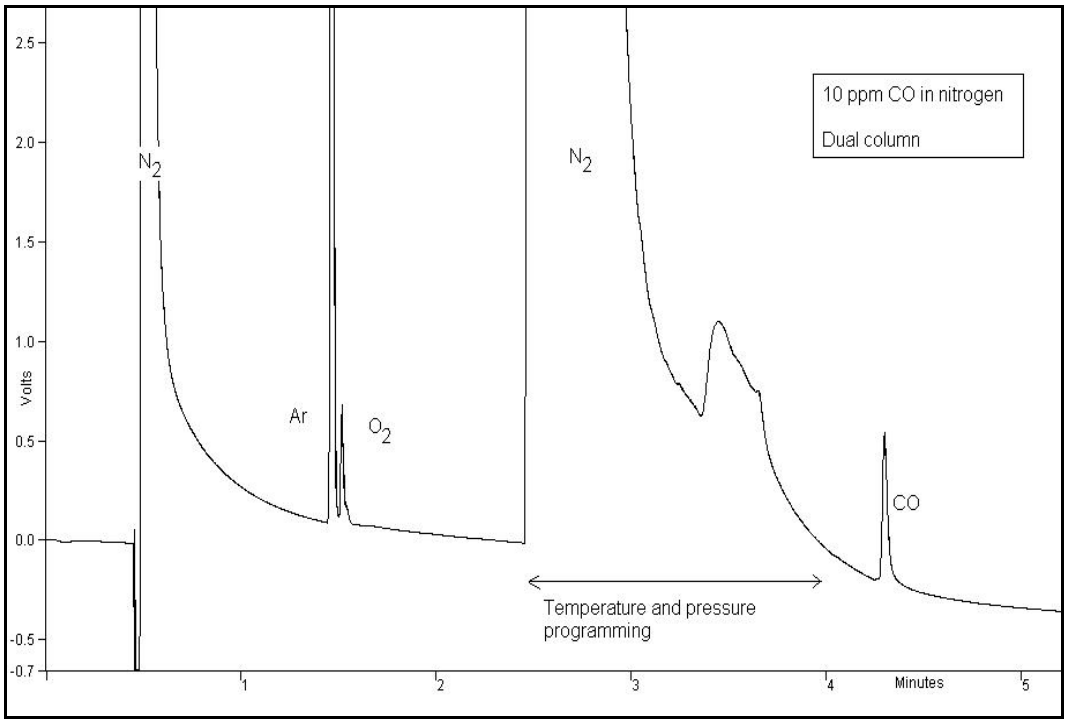

Figure 26: Chromatogram of the 10 µmol·mol^{-1} CO standard on the dual column system with temperature and pressure programming to improve CO peak shape.

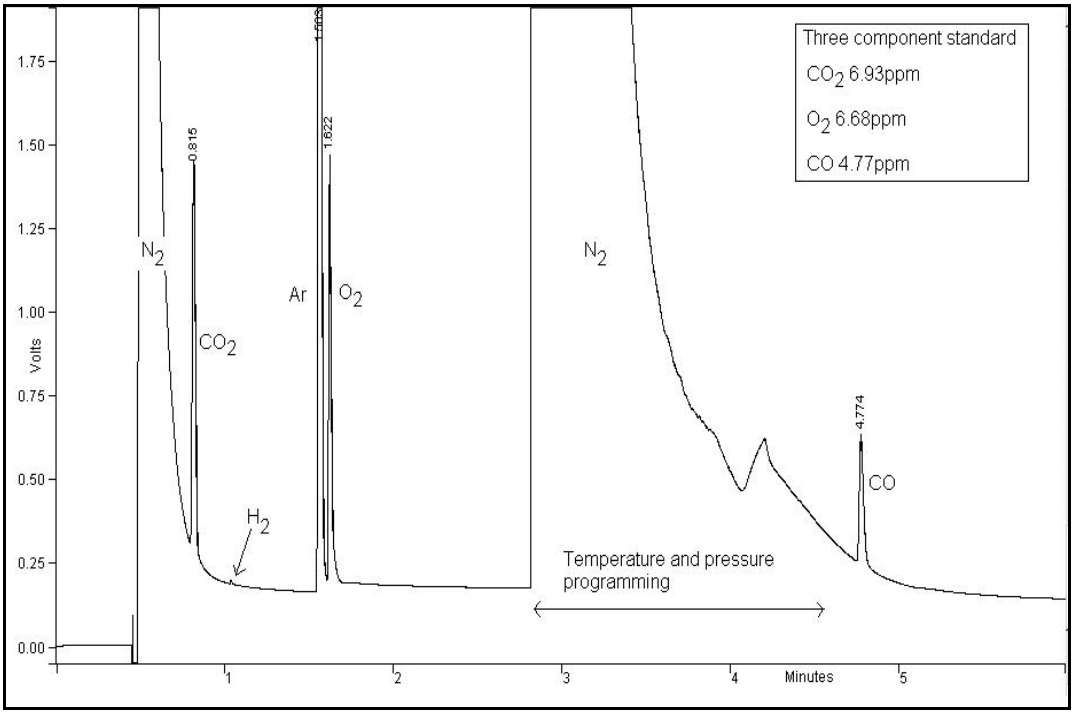

Figure 27: Chromatogram of the ~5 µmol·mol^{-1} three component standard on the dual column system with temperature and pressure programming to improve CO peak shape.

Since the peak shape for CO was not ideal, a sequence reversal technique was attempted in order to improve it. **Figure 28** shows the chromatogram obtained for the ~1 x 10^{-6} mol·mol^{-1} standard using the same temperature and pressure programming as for **Figure 27**, with sequence reversal. The results obtained with the sequence reversal technique are compared with the results obtained without sequence reversal in Chapter 6. From **Figure 28**, there is a small sharp nitrogen peak just before the CO peak, where the residual nitrogen in the column has overtaken the CO peak when the column flow was reversed.

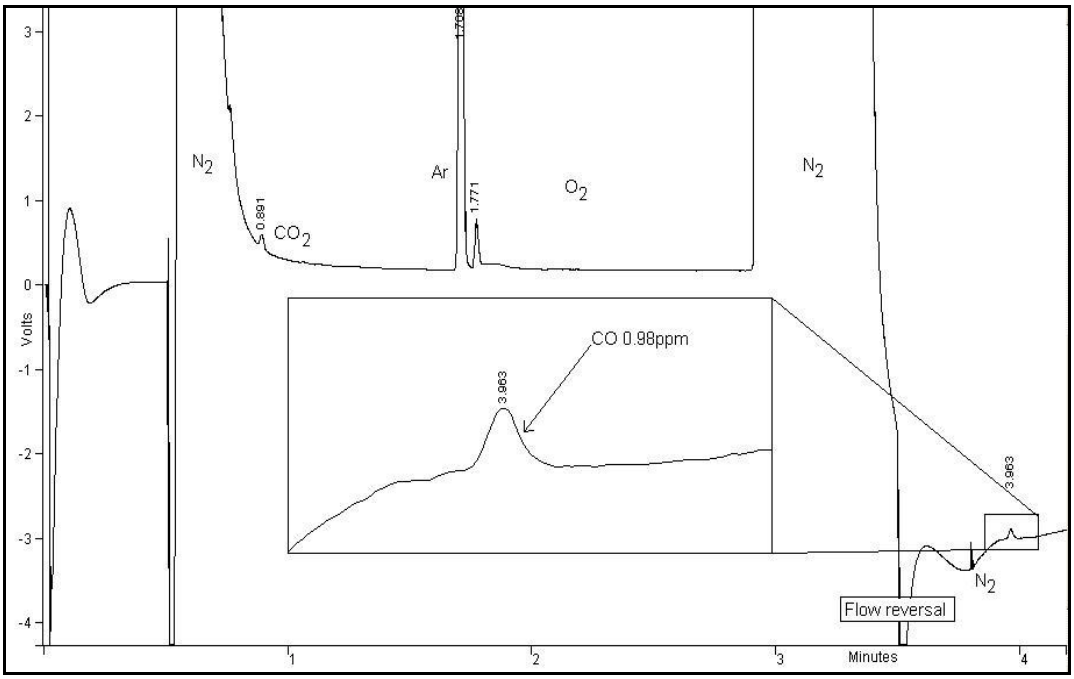

Figure 28: Chromatogram of ~1 x 10^{-6} mol·mol^{-1} standard with an enlarged section showing the improved peak shape for CO

5.3 Optimisation of the experimental parameters

The columns were optimised in the dual column configuration and not individually. The resolution between oxygen and argon was used as a criterion to gauge optimal performance and the separation between carbon dioxide and the air peak from the RTQPLOT column was considered acceptable when this was achieved.

5.3.1 Optimisation of the helium inlet pressure

Hogan (1997, pp 114) has recommended a discharge flow of 10 to 20 mℓ·min^{-1} for the discharge ionisation detector (DID). Since the discharge flow on the present system could only be changed by varying the helium 5.0 inlet pressure to the helium purifier, various inlet pressures were tested. **Figure 29** shows the results of this optimization experiment on the CO_2 peak. Unless otherwise stated, the ~5 µmol·mol^{-1} standard was used for all the optimisation experiments (where [O_2] was 6.685 µmol·mol^{-1}; [CO_2] was 6.926 µmol·mol^{-1} and [CO] was 4.770 µmol·mol^{-1})

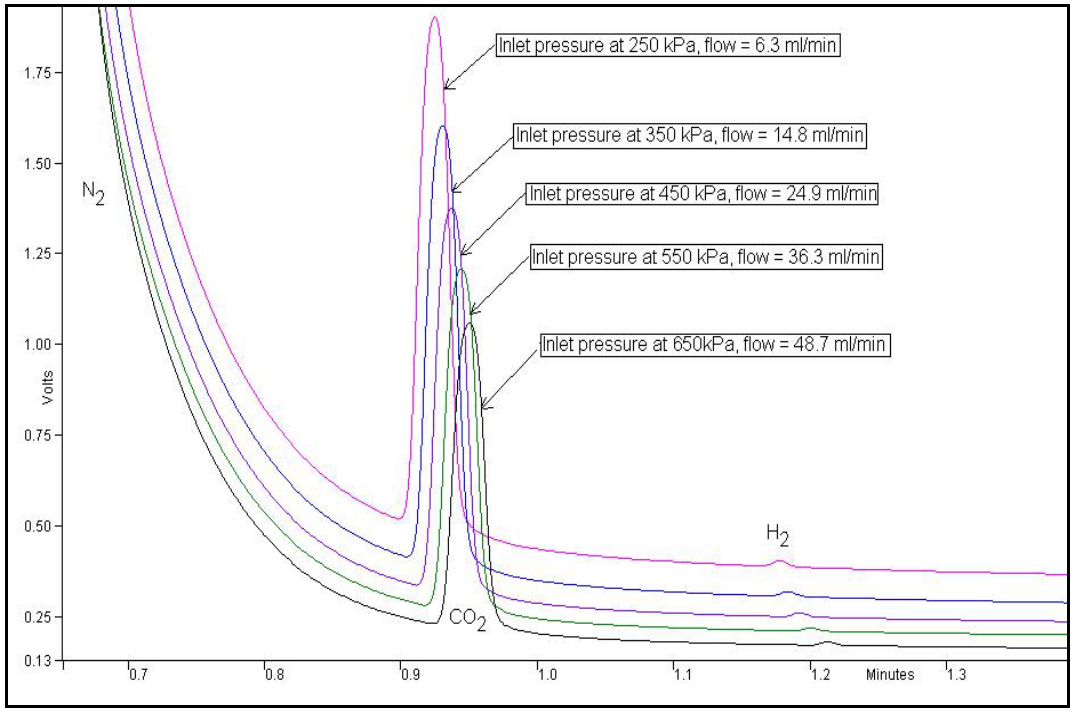

Figure 29: Chromatograms showing the effect of variation of the helium inlet pressure on the position of the CO_2 peak.

Although helium 5.0 inlet pressure of 250 kPa (6.3 mℓ·min^{-1}) gave the highest peak area (**Figure 29**), the discharge flow at this pressure is too low, and the detector is affected by back-diffusion of air as is seen by the increase in the background signal. A helium inlet pressure of 450kPa (24.9 mℓ·min^{-1}) was chosen as a compromise between the advantageous effect of the increase in peak area and the disadvantageous effect of back diffusion from the atmosphere into the detector.

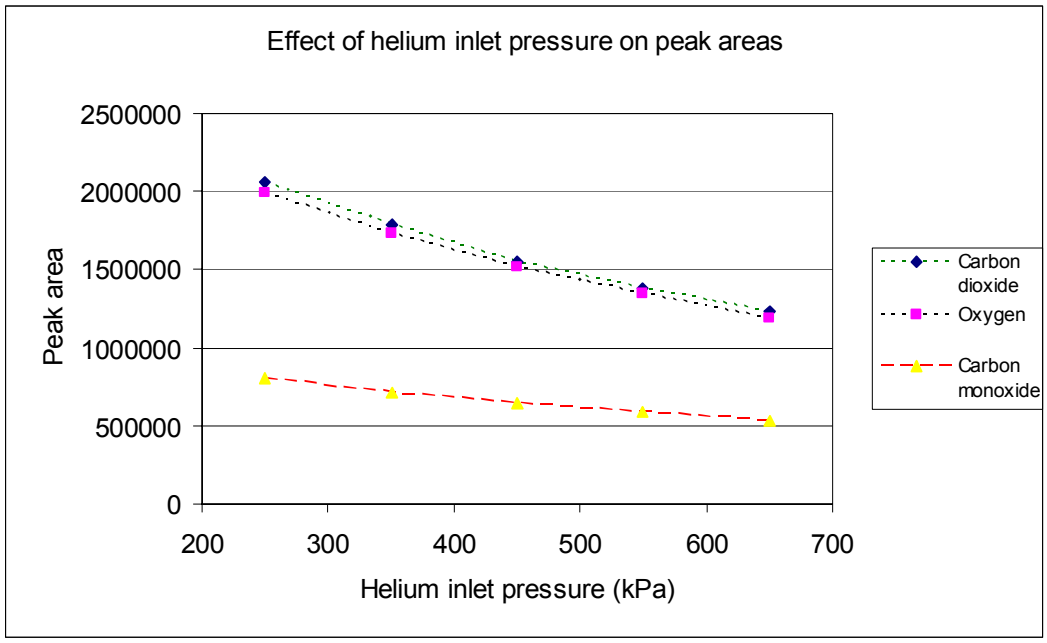

Figure 30: Plot of helium inlet pressure against peak areas of CO_2; O_2 and CO.

The fact that the retention times of the peaks changed slightly indicated that the flow through the dual column system was being changed by the helium discharge flow. It is hypothesised that the greater helium discharge flow created a slight positive head pressure at the column outlet, making the retention times of the gases eluting from the column longer (**Figure 30**).

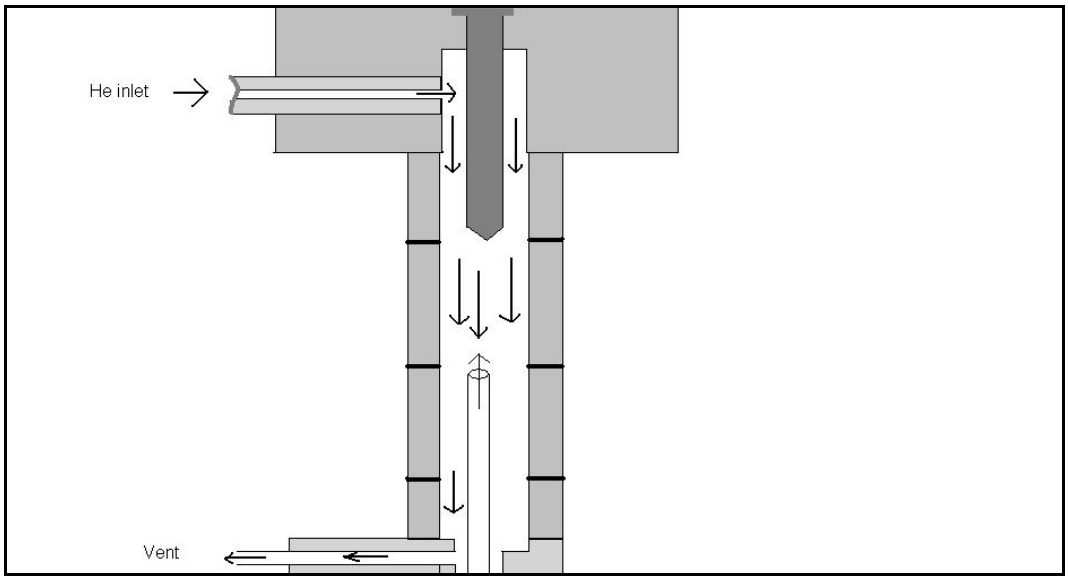

Figure 31: Effect of the helium discharge gas pressure on the column flow in the PDHID

5.3.2 Optimisation of the PDHID temperature

The PDHID recommended operating temperature is 100 ºC (Hogan, 1997, pp 121; Laurens *et al*, 2001), which was chosen to minimise moisture effects. It was decided to test the effect of detector temperature on the peak areas in order to choose an optimum detector operating temperature, with all other conditions being the same (**Figure 32**).

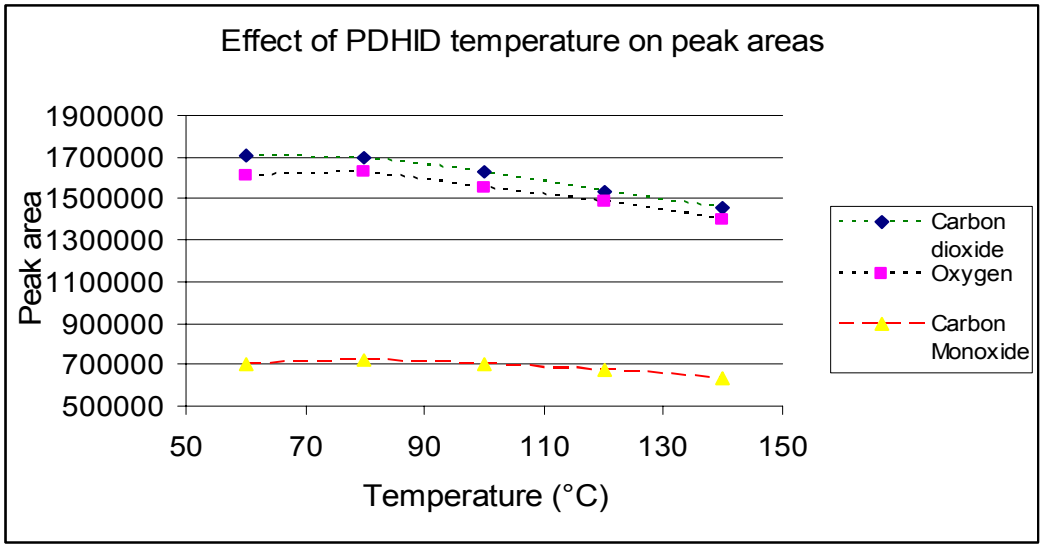

Figure 32: Plot of peak areas of CO_2; O_2 and CO against PDHID temperature (ºC).

It can be seen from **Figure 32** that the peak area is slightly higher at temperatures below 100ºC. However, temperatures lower than 100ºC may encourage the presence of water in the detector from the atmosphere and it was therefore decided to use a detector temperature of 100ºC to keep the results free from interference from moisture in the air.

5.3.3 Optimisation of the column temperature

The column temperature was varied slightly to show the effect on peak resolution between the critical O_2/Ar pair (**Figure 33**).

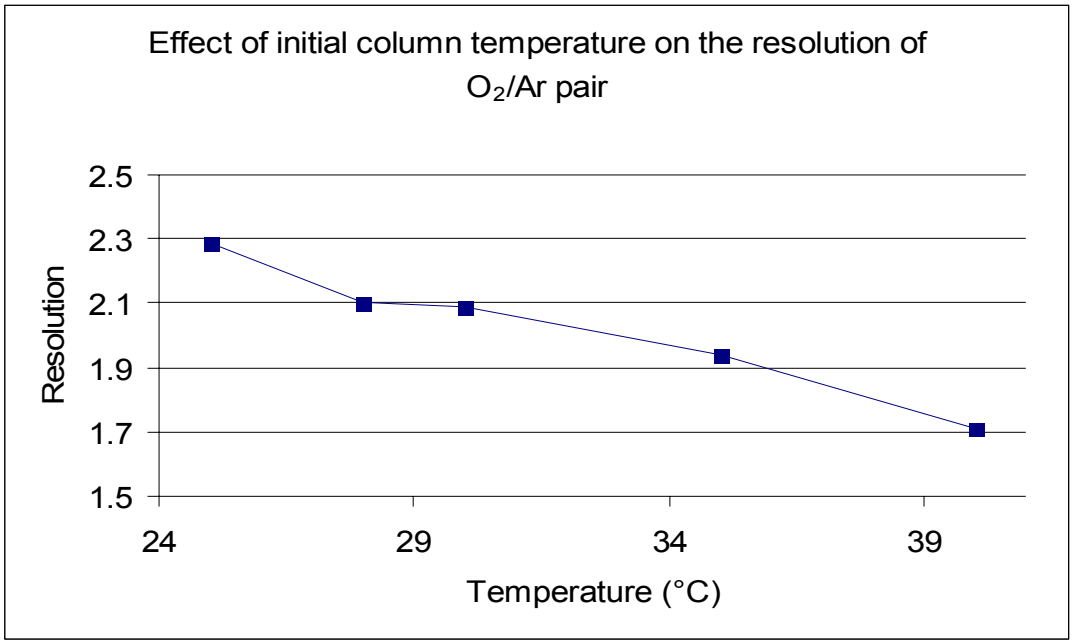

Figure 33: Optimisation of the column temperature showing the effect of varying the temperature on the resolution of the O_2/Ar.

Baseline resolution is obtained when the resolution is 1.5 (Sandra, 1989) for peaks of equal size. The Ar/O_2 resolution slowly decreased as the column oven temperature was increased with resolution at 25 °C being 2.29 and the resolution at 40 °C being 1.71. The GC column oven reaches 25 °C easily in winter but is not easily obtained in summer. The peak resolution at 2.09 with a column oven temperature of 30 °C was still adequate and this temperature is easily maintained in summer. Therefore, initial column oven temperatures can be varied between 25 and 30 °C with little effect on the method.

5.3.4 Optimisation of carrier gas pressure

Figure 34 shows the effects of varying the column pressure on the O_2/Ar peak pair.

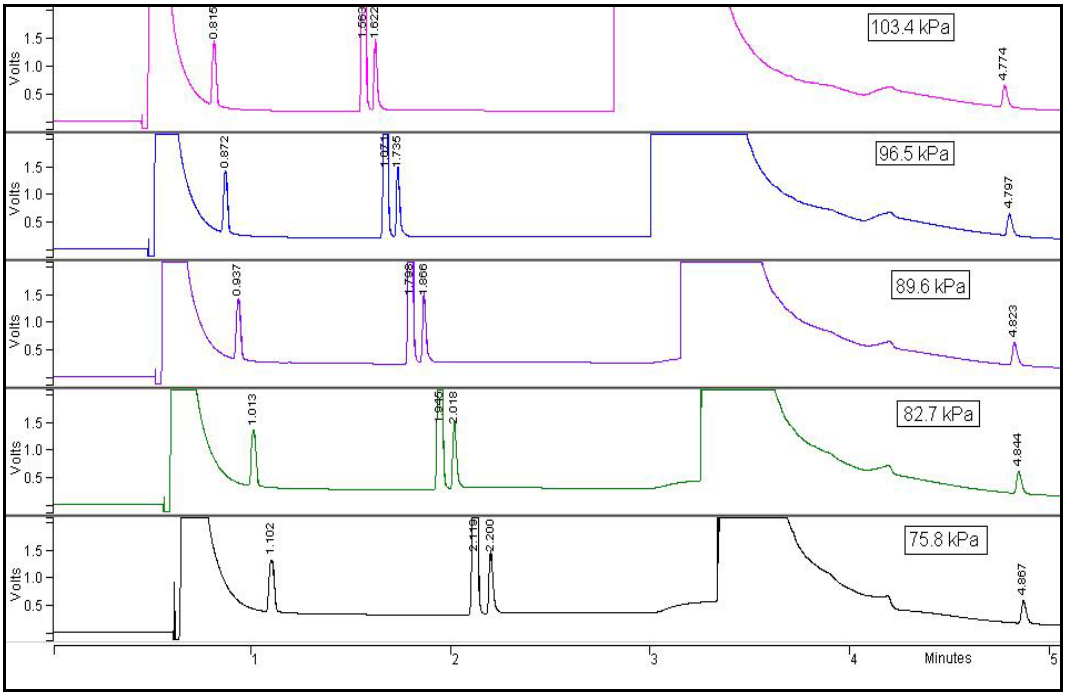

Figure 34: Chromatograms showing the effect of varying column pressure on the peak retention times and resolution of the O_2/Ar peak pair.

The resolution of the O_2/Ar pair decreased slightly from 2.38 to 2.19 as the pressure was increased from 75.8 kPa (11 psi) to 103.4 kPa (15 psi). A column pressure of 89.63 kPa gave the best compromise between good resolution and peak shape for the CO_2/N_2 separation and adequate resolution for the O_2/Ar pair.

5.3.5 Optimisation of the sample inlet pressure

The sample inlet pressure was varied to ascertain if this had any effect on the chromatography. The sample inlet pressure was changed by controlling the regulator on the sample cylinder, and the flow of sample was restricted by a 3 metre length of 1mm internal diameter stainless steel tubing as it exited the vent on the SSV sampler to prevent back diffusion of air to the sampling apparatus (**Figure 35**).

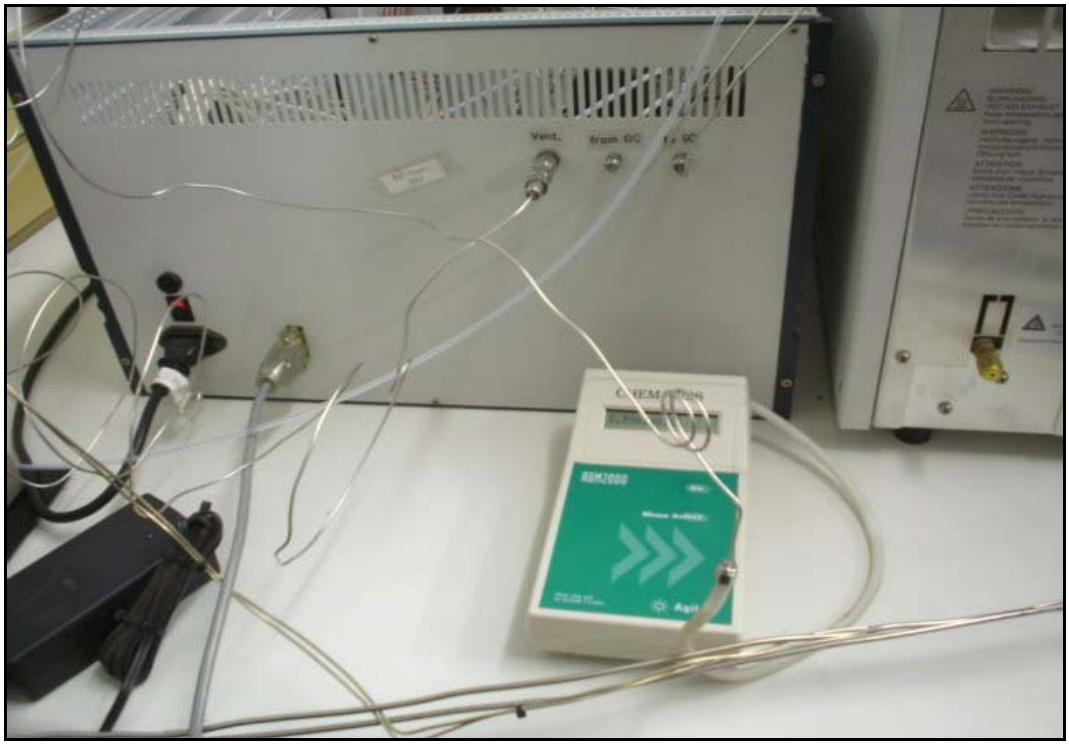

Figure 35: Photograph showing the measurement of the sample flow from the vent restrictor (a ±2 metre long, 1 mm internal diameter stainless steel tube) on the back of the SSV sampler using an Agilent 2000 flow meter (M. Janse van Rensburg, 2005)

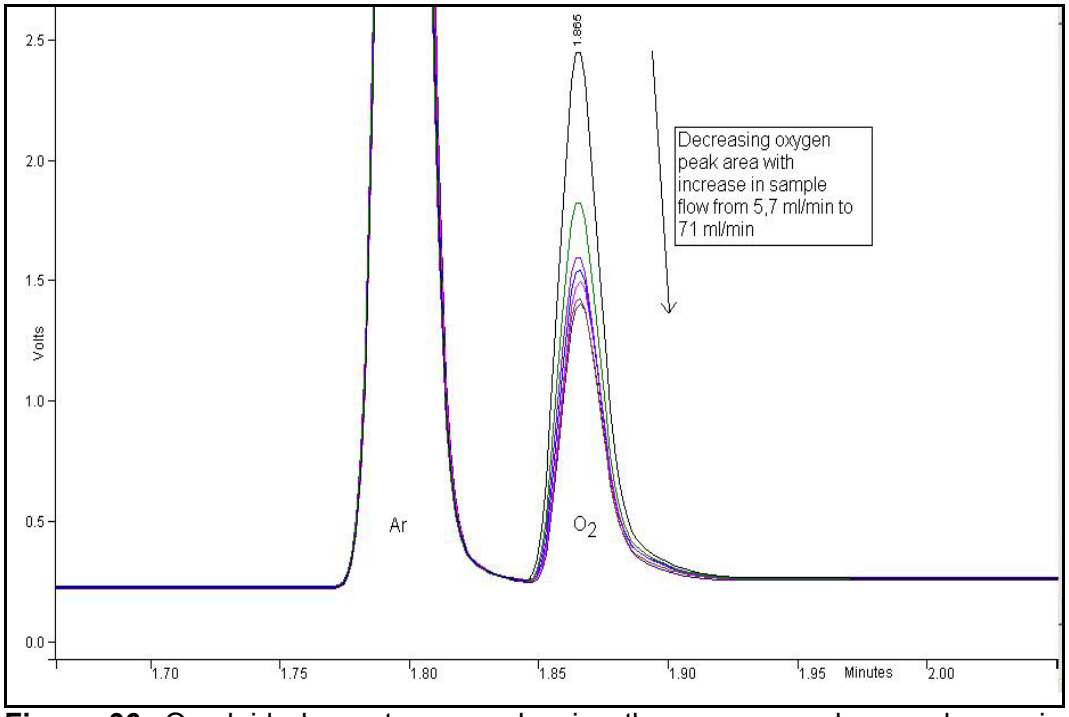

Figure 36: Overlaid chromatograms showing the oxygen peak area decreasing with increase in the sample flow rate for the 6.68 µmol·mol^{-1} oxygen sample.

From **Figure 36**, the oxygen peak height *increased* when the sample flow rate was *decreased*. The CO_2 and CO peak areas did not change with change in sample flow rate. The peak area of the oxygen peak was plotted against the sample flow rate in order to find the flow rate at which the oxygen contamination was minimised (**Figure 37**).

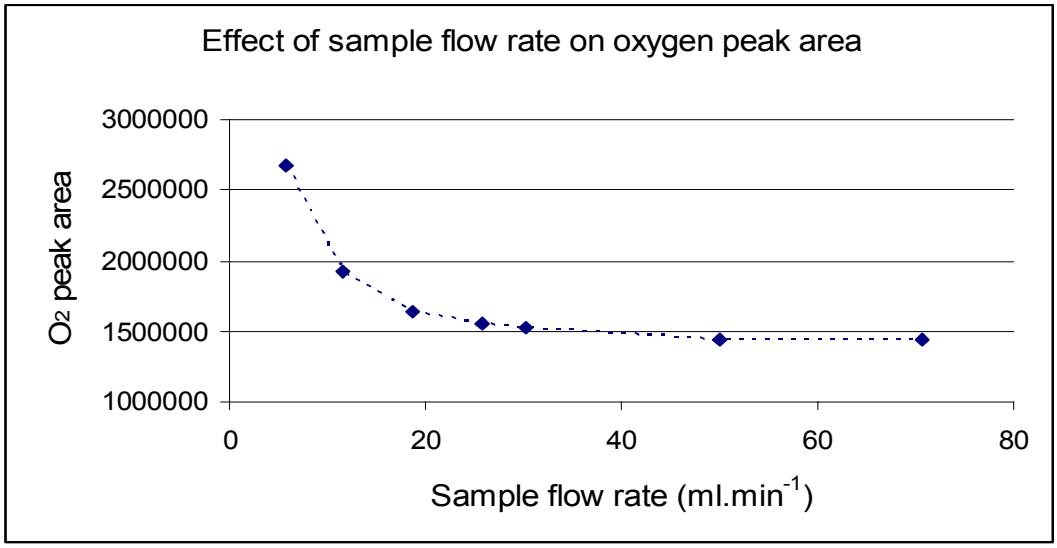

Figure 37: Plot of sample flow rate against the peak area of the O_2.

From **Figure 37**, a sample flow rate less than 50 mℓ·min^{-1} led to a large increase in the oxygen peak area. The only feasible source of oxygen contamination is from the atmosphere and it would seem that the diffusion of atmospheric oxygen into the system when the sample flow rate is lowered leads to increase in peak area. **Figure 38** shows how the oxygen leak is diminished with increase in the sample flow rate for the high purity nitrogen cylinder.

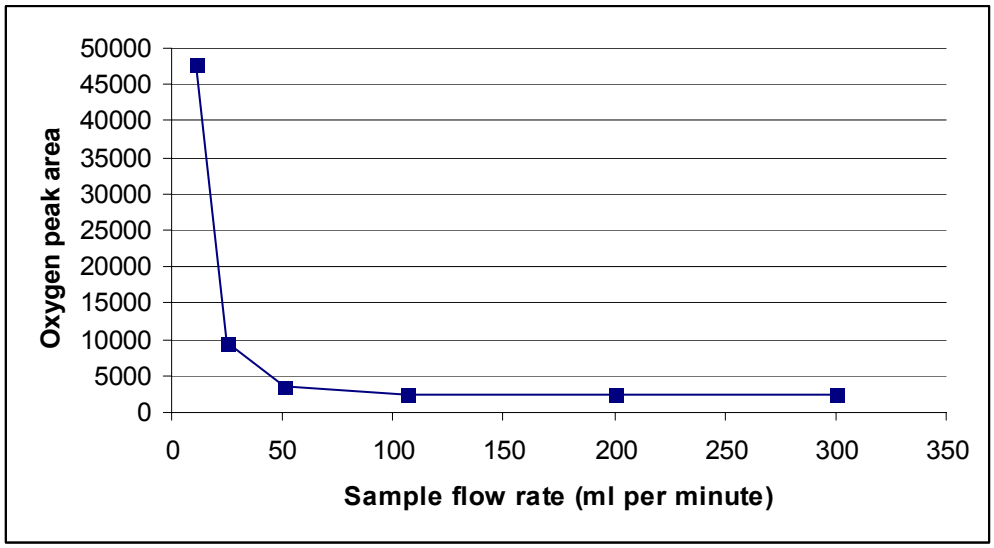

Figure 38: Graph showing the decrease in the amount of oxygen leaking into the high purity nitrogen sample stream with increase in sample flow rate.

The sample flow rate normally used was 25 mℓ·min^{-1} but **Figure 38** shows that the oxygen leaking into the system was only minimised at a flow rate >100 mℓ·min^{-1}. The high sample flow rate seems to minimize the effect of oxygen from the atmosphere diffusing into the sample stream through small leaks. Since the Valco valves have a maximum pressure of 1478 kPa (200 psi), and the pressure on the reducer corresponding to a sample flow of 100 mℓ·min^{-1} is only 45 kPa, the only detrimental effect of a high sample flow rate is that the sample would be diminished more quickly.

5.3.6 Optimization of the length of the column insert into the PDHID

The effect of varying the length to which the column is inserted into the PDHID (as measured from the bottom of the nut in the column oven to the tip of the column) was explored. The results are shown in **Figure 39**.

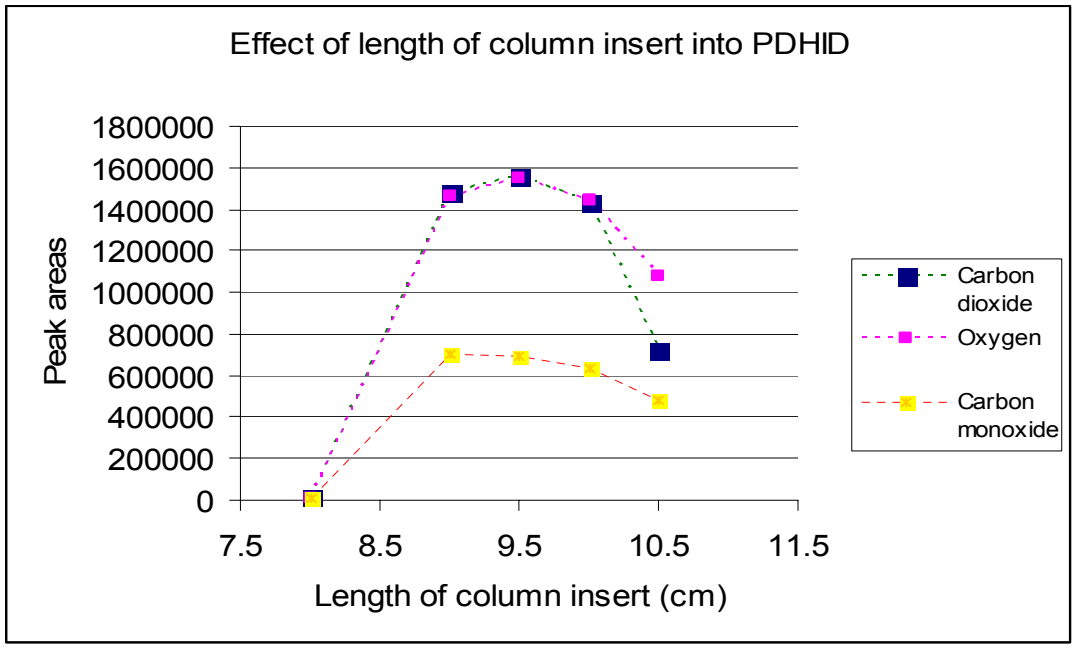

Figure 39: Plot of the length of the column insert into the PDHID against the peak areas of O_2; CO_2 and CO.

The length of the column insert using a knurled nut and capillary column adapter is recommended as 11.4 cm (VICI PDHID D-4-I-VA38-R Instruction manual, 2002). This length corresponds exactly to the experimentally derived optimum column insert length of 9.5 cm using a VICI Valco fused silica capillary column ferrule and liner set. Wentworth et al (1994) have said that the response for permanent gases may be improved if the column outlet were placed closer to the discharge region of the PDHID. From **Figure 39**, it is clear that this is not the case with the PDHID D4 model used in this investigation.

5.3.7 Effect of the adsorption of CO_2 onto the RT-Molesieve 5Å column

In order to test the effect of large amounts of CO_2 being absorbed onto the RT-Molesieve 5Å column, a 1% mixture of CO_2 in nitrogen was injected onto the dual column system. The lowest concentration standard (211 ppb CO) was injected before and after the 1% CO_2 in N_2 mixture was injected 9 consecutive times to test whether the adsorption of CO_2 had any effect on the peak areas or retention times of the small peaks. Thereafter, the oven temperature was increased to 150 ºC and held for 60 minutes to ascertain when the CO_2 absorbed onto the RT- Molesieve 5Å column would elute from the column. **Table 4** shows how peak areas and

retention times (minutes) of the 211 ppb CO peak before and after the injection of large amounts of CO_2.

Table 4: Comparison of CO peak areas before and after injection of 1% CO_2 in N_2 onto the dual column system

	CO peak areas and retention times before injection of 1% CO in N_2 mixture		**CO peak area and retention times after injection of 1% CO in N_2 mixture**	
1	12299	4.443 min	13629	4.444 min
2	11419	4.434 min	13819	4.448 min
3	12422	4.441 min	16125	4.448 min
4	15399	4.448 min	14558	4.454 min
5	12835	4.449 min	13551	4.446 min
6	13164	4.449 min	16368	4.449 min
7	13616	4.454 min	13878	4.452 min
Average peak area	13022		14561	
Standard deviation	1259.0		1198.4	
%CV	9.7		8.2	

There was no significant change in the repeatability, retention times or peak areas before and after the injection of large amounts of CO_2 onto the dual column system, except that there was some carryover of CO_2 when the low concentration standard was injected again. **Figure 40** shows the chromatogram obtained at a 150 ºC isothermal column temperature. The CO_2 adsorbed onto the column from the 9 consecutive injections had moved along the column slowly with temperature and pressure programming (conditions used for the method presented in this investigation) and eventually eluted at elevated temperature in a series of 9 peaks, with about 1.3 minutes between the maxima. The CO_2 adsorbed onto the RT-Molesieve 5Å column from the last injection eluted at 42.5 minutes. Since large amounts of CO_2 adsorbed onto the RT- Molesieve 5Å column had no effect on the column performance, the adsorption from mixtures containing below 5ppm CO_2 content used in this investigation was expected to make no difference to the results, except for an insignificant rise in the baseline when the CO_2 was eventually eluted.

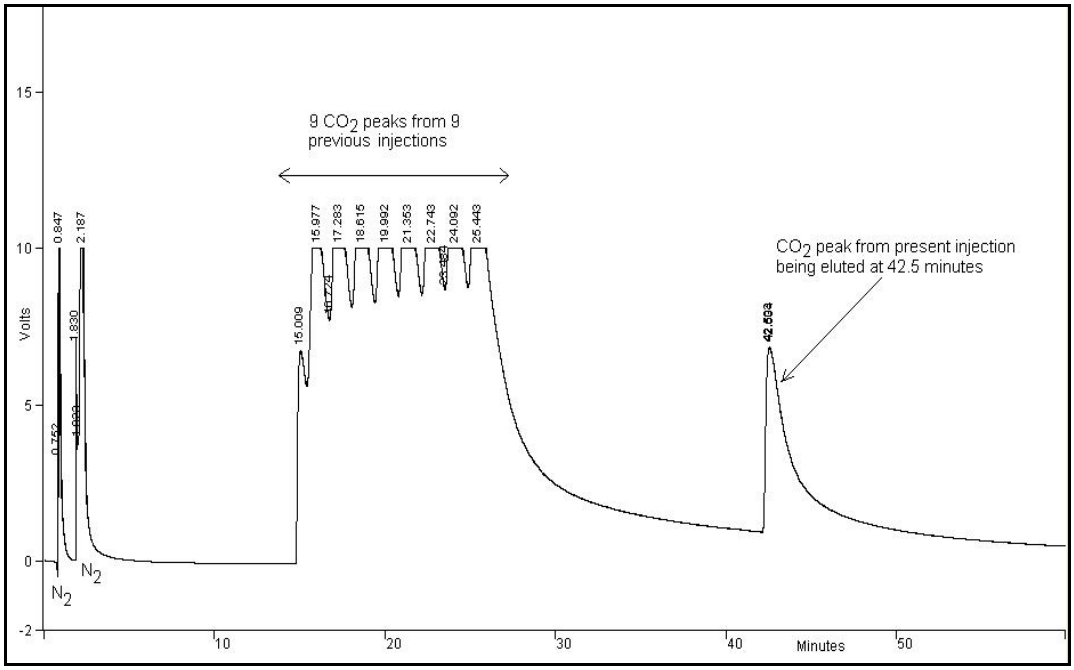

Figure 40: Chromatogram of 1% CO_2 in nitrogen standard at 150 ºC constant column temperature and 70 kPa (10 psi) constant pressure.

5.3.8 Treatment of the results

The peaks were integrated for peak area using the STAR 6.0 Chromatography software by enabling an integration inhibit function (a function on the chromatography software that disables peak recognition) just before and after the peak. The integration inhibit is used to avoid measurement of unwanted peaks or false triggering of integration by baseline disturbances (Dyson, 1990, pp 98). **Table 5** shows the results of a comparison with regard to the %CV value for results obtained with and without the integration inhibit function. The baseline is susceptible to upsets because the PDHID signal fluctuates with changes in column flow and the integration inhibit function isolates the peak or peaks of interest.

A forced peak event was used to integrate the peak of interest so that the start and end times of the peak for a particular concentration level remained the same. This improved the precision which in turn improved the detection limit for the analyte being measured (Brinkmann, 2003).

Table 5: Comparison of the results obtained with different integration modes for the CO peak.

Run number	Automated integration	Integration Inhibit only	Integration inhibit and forced peak event
1	146422	142824	147995
2	137965	149983	151641
3	144527	150019	152351
4	146834	146431	149752
5	141651	152851	151644
6	145612	154051	149720
7	137535	156872	157777
Average	142935.1	150433	151554.3
Std dev	3927.928	4737.864	3126.602
%CV	2.7	3.1	2.1

Figures 41 and 42 show how the integration differs when the integration inhibit function is used with STAR automated integration. Note that the O_2 peak is not even integrated with STAR automated integration in **Figure 41**.

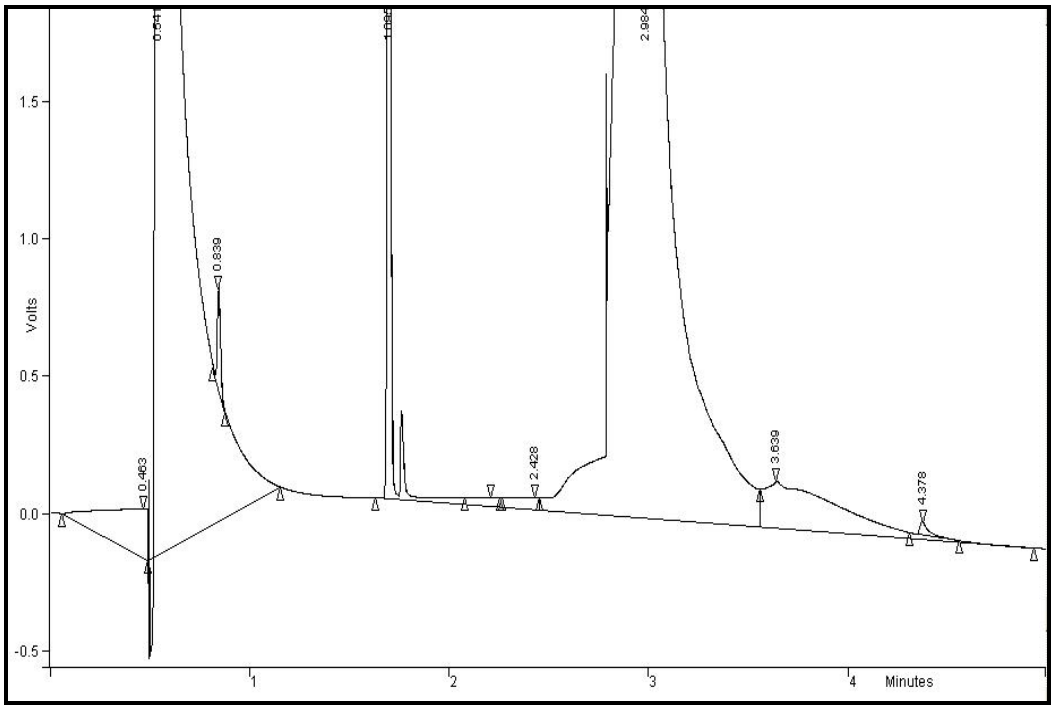

Figure 41: STAR Chromatography automated integration of the ~2µmol.mol^{-1} standard without "integration inhibit" or "forced peak" events.

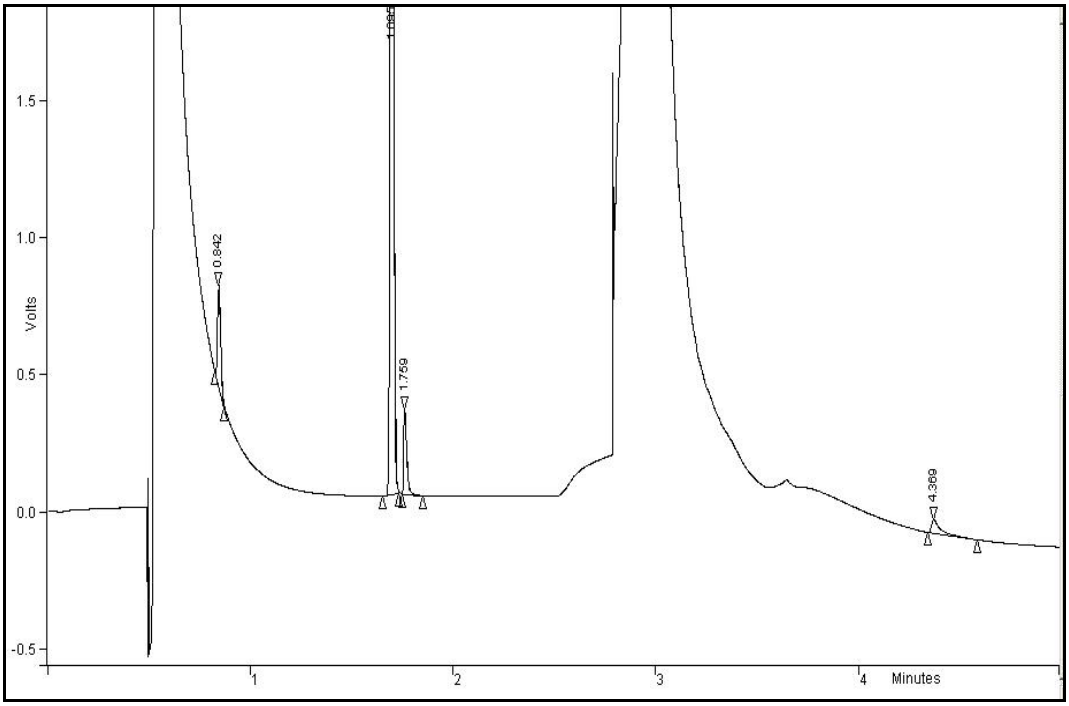

Figure 42: Integration of the ~2 µmol.mol^{-1} standard using "integration inhibit" and "forced peak" functions.

5.3.9 Optimum experimental parameters for the analysis of CO_2; O_2 and CO in nitrogen

Table 6: Optimum operating parameters for the PDHID and Varian CP3800 GC for the analysis of CO_2; O_2 and CO in nitrogen

Parameter	**Value**
Sample loop size	250µℓ
Column start temperature	28 °C
Column end temperature	100 °C
Column start pressure	90 kPa
Total initial column flow	28 mℓ·min^{-1} (Measured at outlet of dual capillary columns)
Column end pressure	170 kPa
Total final column flow	48 mℓ·min^{-1} (Measured at outlet of dual capillary columns)
PDHID temperature	100 °C
Helium inlet pressure	450 kPa
Column insert length to the PDHID	9,5 cm
Sample flow rate	> 100 mℓ·min^{-1}
Valve switching time for sequence reversal (column flow reversal)	3.5 minutes

5.3.10 Analysis of impurities in pure oxygen using the optimised method (without sequence reversal)

The optimised method was used to analyse for trace amounts of CO_2; N_2 and CO in oxygen and the chromatogram is shown in **Figure 43**. CO_2 and N_2 impurities were detected whereas CO was not detected

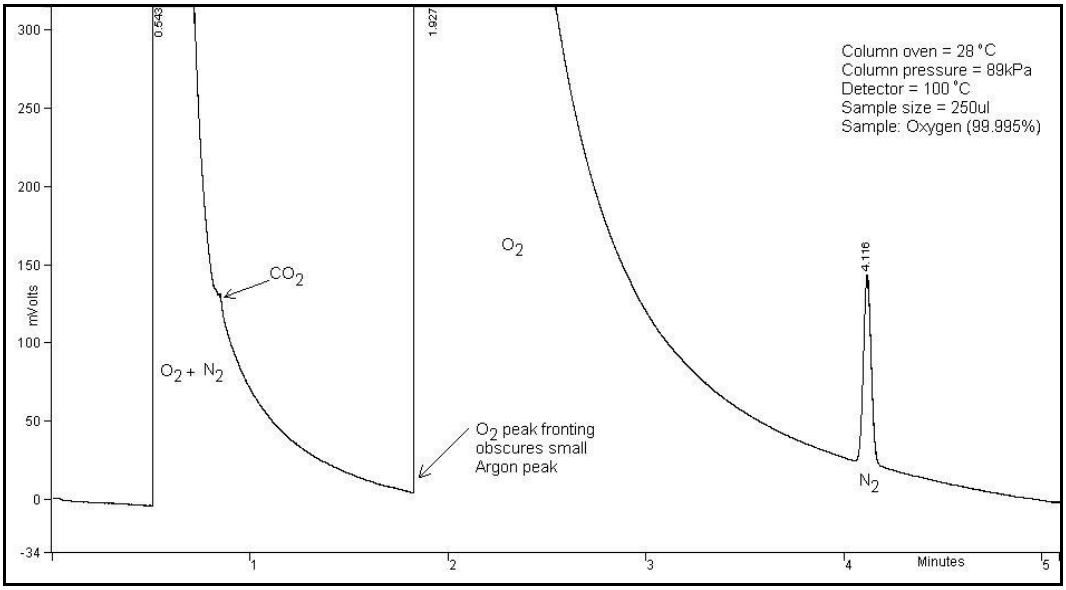

Figure 43: Chromatogram of 99,995% pure oxygen using the optimised method.

Chapter 6

Discussion and Conclusions

6.1 Comparison of the results obtained with sequence reversal and those obtained without sequence reversal

6.1.1 Results for O_2 in N_2

Table 7: Comparison of the results obtained for O_2 in N_2 with sequence reversal to the results obtained without sequence reversal

	No Sequence Reversal	Sequence Reversal
LOD ($x10^{-6}$ mol·mol^{-1})	0.007	0.036
LOQ ($x10^{-6}$ mol·mol^{-1})	0.030	0.118
Repeatability (%CV)	<1.0% (0.6 ppm)	<0.8% (0.6 ppm)
Linearity (Goodness of fit)	<2.7391	<1.4704
O_2 ($x10^{-6}$ mol·mol^{-1})	0.022	1.951
Expanded uncertainty ($x10^{-6}$ mol·mol^{-1})	0.006	0.187
UCL of Result ($x10^{-6}$ mol·mol^{-1})	0.028	2.138
LCL of Result ($x10^{-6}$ mol·mol^{-1})	0.016	1.764

The limit of detection (LOD) for O_2 with no sequence reversal is lower than the LOD obtained with sequence reversal. The repeatability is similar but the level of O_2 in the blank is much higher for the results obtained with sequence reversal. This difference is due to the greater number of leaks into the sample stream that were present when sequence reversal was used.

6.1.2 Results for CO_2 in N_2

Table 8: Comparison of the results obtained for CO_2 in N_2 with sequence reversal to the results obtained without sequence reversal

	No Sequence Reversal	Sequence Reversal
LOD ($x10^{-6}$ mol·mol^{-1})	0.009	0.026
LOQ ($x10^{-6}$ mol·mol^{-1})	0.030	0.088
Repeatability (%CV)	<1.1% (0.7 ppm)	<1.8% (0.7ppm)
Linearity (Goodness of fit)	<0.8265	<0.7406
CO_2 ($x10^{-6}$ mol·mol^{-1})	0.050	Not Detected
Expanded uncertainty ($x10^{-6}$ mol·mol^{-1})	0.019	
UCL of Result ($x10^{-6}$ mol·mol^{-1})	0.069	0.048
LCL of Result ($x10^{-6}$ mol·mol^{-1})	0.031	0.018

The LOD is lower and the repeatability better without sequence reversal. CO_2 is not detected when sequence reversal was used and this is consistent with the upper confidence limit of the detection limit calculated (0.048 x 10^{-6} mol.mol^{-1}) being less than the amount found using no sequence reversal (0.050 x 10^{-6} mol.mol^{-1}).

6.1.3 Results for CO in N_2

Table 9: Comparison of the results obtained for CO in N_2 with sequence reversal to the results obtained without sequence reversal

	No Sequence Reversal	Sequence Reversal
LOD ($x10^{-6}$ mol·mol^{-1})	0.037	0.043
LOQ ($x10^{-6}$ mol·mol^{-1})	0.123	0.143
Repeatability (%CV)	<6.7% (0.5 ppm)	<4.9% (0.5 ppm)
Linearity (Goodness of fit)	<1.2753	<2.2620
CO ($x10^{-6}$ mol·mol^{-1})	Not Detected	Not Detected
Expanded uncertainty ($x10^{-6}$ mol·mol^{-1})		
UCL of Result ($x10^{-6}$ mol·mol^{-1})	0.068	0.078
LCL of Result ($x10^{-6}$ mol·mol^{-1})	0.025	0.029

The LOD is better without sequence reversal although the repeatability is slightly worse without sequence reversal. CO in not detected in both methods although the LOD for CO (0.037 x 10^{-6} mol.mol^{-1}) is better than the LOD obtained using a packed column (0.7 x 10^{-6} mol.mol^{-1}), as stated in section 5.1.1.1.

6.1.4 Best experimental setup for the analysis of CO_2, O_2 and CO in N_2

From the results, the sequence reversal method offers no improvement on the limit of detection for CO_2, O_2 or CO. Since the purpose of sequence reversal was to improve the peak shape and therefore the limit of detection for CO, this has not been achieved. However, the dual capillary column method without sequence reversal offers a significant improvement on the results for CO obtained using a traditional packed column.

6.2 Conclusions on the analysis of O_2 in N_2 using the dual capillary column method without sequence reversal

The level of oxygen impurity in the BIP™ nitrogen used in the gas metrology laboratory at the CSIR NML has been found to have a concentration of 0.022 x 10^{-6} mol·mol^{-1} $\pm$ 0.006 x 10^{-6} mol.mol^{-1} at a level of confidence of 95.45%.

None of the valves were purged and the Stream Selection Valve (SSV) sampling system had at least ten possible leak sites per stream from the cylinder and reducer to the valve which had a further six possible leak sites. By increasing the sample flow to >100 mℓ·min^{-1}, it was shown that the majority of the leaks were from the sampling system and could therefore be circumvented. A purged valve would have little effect on minimising the leaks from the atmosphere if the sampling system (the pressure reducer, connecting lines, connections, needle valves, flow meters, pressure gauges) was the main source of leaks.

An automated sampling system is essential for method validation where calibration data is run preferably overnight when there are as few disturbances to the laboratory environment as possible. It is not possible to purge the entire sampling system as well as the valves as this would be expensive as well as impractical when cylinders and pressure reducers have to be changed. A high sample flow rate offers a temporary solution to the problem of leaks from the atmosphere when sampling for ultra-trace levels of oxygen and nitrogen. Increasing the sample flow rate can also help to identify leaks in the system, i.e.

when the oxygen peak decreases with increasing sample flow rate, it is a good indication that there are small leaks present in the flow path.

The manufacturer has certified an oxygen impurity of less than 0.010 x 10^{-6} mol·mol^{-1} but the oxygen measured was slightly higher than this at 0.022 x 10^{-6} mol·mol^{-1}. There are still very small leaks in the system, probably on the valves themselves, and a helium-purged valve compartment could be installed to get rid of these. The sampling system should also be rebuilt to minimise the number of connections from the pressure reducer on the sample cylinder to the six-port valve. A lower number of connections would probably require a lower sample flow rate to prevent influx of air into the sample flow path.

Oxygen cannot be analysed with the packed columns available in the laboratory because it can't be separated from argon on these columns. Oxygen also cannot be simultaneously analysed with CO_2 and CO using the GC-TCD-FID because O_2 quickly poisons the nickel catalyst used in the methaniser and renders it non-functional.

6.3 Conclusions on the analysis of CO_2 in N_2 using the dual capillary column method without sequence reversal

The level of carbon dioxide impurity in the BIP™ nitrogen used in the Gas Metrology laboratory at the CSIR NML has been found to have a concentration of 0.050 x 10^{-6} mol·mol^{-1} ± 0.019 x 10^{-6} mol·mol^{-1} at a level of confidence of 95.45% using the GC-PDHID with a 250 µℓ sample loop.

6.3.1 Comparison of the results obtained for the GC-PDHID method with the results from the GC-FID method (Janse van Rensburg, NML-06-0006, 2006)

Table 10 shows how the results from the GC-PDHID method compared with the results from the GC-FID

Table 10

Comparison of the results for CO_2 in BIP™ nitrogen by two different methods

	GC-PDHID	GC-FID
LOD (x10^{-6} mol·mol^{-1})	0.009	0.042
LOQ (x10^{-6} mol·mol^{-1})	0.030	0.141
Repeatability (%CV)	<1.1% (286 ppb)	<3.8% (496 ppb)
Linearity (Goodness of fit)	<0.8265	<0.0596
CO_2 (x10^{-6} mol·mol^{-1})	0.050	Not detected (<0.042)
Expanded uncertainty (x10^{-6} mol·mol^{-1})	0.019	
UCL of Result (x10^{-6} mol·mol^{-1})	0.069	0.077
LCL of Result (x10^{-6} mol·mol^{-1})	0.031	0.029

The detection limit for CO_2 using the GC-FID technique was obtained using a 2 mℓ sample loop and is significantly larger than that obtained for the GC-PDHID technique using a 250 µℓ sample loop. The range covered by the upper and lower confidence limits shows that the two methods agree on the level of CO_2 in BIP™ nitrogen, although the range is slightly broader for the GC-FID method due to fact that the precision on the present method is better than the GC-FID. The PDHID method, as validated in this report is therefore reliable for the analysis of CO_2 at trace levels in BIP™ nitrogen.

6.4 Conclusions on the analysis of CO in N_2 using the dual capillary column method without sequence reversal

The level of carbon monoxide impurity in the BIP™ nitrogen used in the gas metrology laboratory at the CSIR NML has been found to have a concentration between 0.025 x 10^{-6} mol·mol^{-1} and 0.068 x 10^{-6} mol·mol^{-1} at a level of confidence of 95% using the GC-PDHID with a 250µℓ sample loop.

6.3.1 Comparison of the results obtained for the GC-PDHID method with the results from the GC-FID method (Janse van Rensburg, NML-06-0010, 2006)

Table 11 shows how the results from the GC-PDHID method compare with the results from the GC-FID

Table 11

Comparison of the results for CO in BIP™ nitrogen by two different methods

	GC-PDHID	GC-FID
LOD ($x10^{-6}$ mol·mol^{-1})	0.037	0.038
LOQ ($x10^{-6}$ mol·mol^{-1})	0.123	0.125
Repeatability (%CV)	<10%(0.2ppm)	<1.4% (1.2ppm)
Linearity (goodness of fit)	<1.2753	<0.0949
CO ($x10^{-6}$ mol·mol^{-1})	Not detected (<0.037)	Not detected (<0.038)
UCL of Result ($x10^{-6}$ mol·mol^{-1})	0.068	0.069
LCL of Result ($x10^{-6}$ mol·mol^{-1})	0.025	0.026

The detection limit for CO using the GC-FID technique was obtained using a 2 mℓ sample loop and is almost the same as that obtained for the GC-PDHID technique using a 250µℓ sample loop. The range covered by the upper and lower confidence limits shows that the two methods agree on the level of CO in BIP™ nitrogen, although the CO peak was not detected in the blank by both methods. This indicates that the PDHID method, as validated in this report is reliable for the analysis of CO at ultra trace level (<1 x 10^{-6} mol.mol^{-1}) in BIP™ nitrogen.

Future work can include an investigation into the possibility of a dual column system using capillary columns other than the ones used in this investigation to improve the CO peak shape and thereby improve the detection limit for CO.

6.1 Conclusions on the analysis of N_2 in O_2 using the dual capillary column method without sequence reversal

Using the same system validated for CO_2, O_2 and CO in N_2, it has been shown that for the purity analysis of N_2 in O_2 4.5 (99,995% pure), the concentration of N_2 is in the range of 18.464 $x10^{-6}$ mol.mol^{-1} to 25.084 $x10^{-6}$ mol.mol^{-1} at a confidence level of 95,45%. The manufacturer's specification of N_2 in O_2 4.5 is < 40 x 10^{-6} mol.mol^{-1}.

CO_2 and CO in O_2 can also be analysed using slightly modified parameters from those used for the analysis of these impurities in N_2. The analysis of CO_2 and CO in O_2 cannot be accomplished using GC-FID with a methaniser because the oxygen quickly poisons the catalyst.

6.6 General conclusions on the analysis of permanent gases using the GC-PDHID

A simple, affordable alternative to the multi-column, multi-instrument methods used for the purity analysis of CO_2; O_2 and CO in nitrogen has been shown to be fit for purpose for the analysis of trace amounts of these impurities in high purity nitrogen. Trace components, according to the IUPAC definition, have concentrations less than 100 x 10^{-6} mol·mol^{-1}and quantities less than 1 x 10^{-6} mol·mol^{-1} are termed micro-trace components (Namiesnik, 2002). Therefore, the current method has been validated for the analysis of trace as well as micro-trace quantities of CO_2; O_2 and CO in high purity nitrogen. The same method may be used to analyse CO_2, N_2 and CO in high purity oxygen and has been validated for the analysis of N_2 in O_2.

The detection limits obtained for CO_2, O_2 and CO are lower and the precision better than the values published by Wurm *et al* (2003) for a dual capillary column method, where they analysed O_2, CO_2 and CO in helium and cited detection limits for the method (calculated using a 10 ppm mixture of O_2, CO_2 and CO) as being between 50 and 250 ppb, with precision being ±4.2% for O_2; ±7.8% for CO_2 and ±2.0% for CO. The detection limits in the present method for O_2, CO_2 and CO in nitrogen are calculated as being between 7 and 37 ppb with precision being ≤1.0% for O_2; ≤1.1% for CO_2 and ≤6.7% for CO for ~0.5ppm mixture. The analysis in the present investigation is also carried out in the matrix of interest (nitrogen) whereas Wurm *et al* used standards made up in helium where the matrix would be invisible to the PDHID and all the peaks of interest easily discernible.

Comparison of the method with a GC-FID method for analysing trace amounts of CO and CO_2 has shown that the present method is reliable for the trace analysis of CO and CO_2 in high purity nitrogen. Oxygen is analysed simultaneously with CO_2 and CO with the present method and this is not possible using the GC-FID method for the reasons stated in section 6.2.

The sample flow rate has a significant effect on the degree of contamination from the atmosphere entering the sample stream. It has been observed that the oxygen contamination increased when the sample flow rate from the sample cylinder was decreased. The sample flow rate of 100 mℓ·min^{-1} was found to be the minimum flow rate at which the effect of diffusion of oxygen from the atmosphere into the sample stream was minimised.

The molecular sieve columns have been said to retain CO_2 irreversibly at ambient temperature and change in retention characteristics over time as a result. It has been observed that there is no change in column performance even when large amounts of CO_2 are injected onto the dual column system. At sub-ppm level, the retention times; repeatability and the peak areas do not change significantly when a large amount of CO_2 is adsorbed onto the RT-Molesieve 5Å column. The adsorbed CO_2 is eluted in under an hour when the column temperature is increased to 150ºC.

Using the technique of sequence reversal, it is noted that the peak shape for CO may be improved but a comparison of the results obtained using sequence reversal with the results obtained without sequence reversal has shown there is no improvement in the limit of detection for CO.

References

1. ALINK, A., VAN DER VEEN, A., 2000, *Uncertainty calculations for the preparation of primary gas mixtures: Part 1: Gravimetry*, Metrologia, Volume 37, pages 641 to 650.
2. ANDRAWES, F., DENG, P., 1985, *Optimization of Helium Ionization Detector*, Journal of Chromatography, Volume 349, Pages 405 to 414.
3. ATKINS, P.W., 1990, *Physical Chemistry*, Fourth Edition, Oxford: Oxford University Press.
4. BOTHA, A., 2004, *Progress report on the Establishment of measurement traceability and measurement equivalence for ambient air monitoring for Southern Africa*, Proceedings of the 2004 Test and Measurement Conference, Muldersdrift, South Africa.
5. BREMSER, W., 1997, Bundesamsalt for Materialforschung und profung (BAM), Rundower Chausee 5, Geb.8.15, D-12489, Berlin.
6. BRINKMANN, F., VAN DER VEEN, A., 2003, *Analysis of greenhouse gases at atmospheric levels*, Poster presentation, Gas Analysis Symposium 2003, Amsterdam, Netherlands.
7. BROWN, A.S, MILTON, M.J.T., COWPER, C.J., SQUIRE, G.D., BREMSER, W., BRANCH, R.W., 2004, Journal of Chromatography A, Volume 1040, Pages 215 to 225.
8. CARLIN, C.F., 2004, Introduction to GC-FID, Course Notes, University of Northern Carolina Charlotte, Department of Chemistry, http://www.chem.uncc.edu/faculty/cooper/4111/GCIntroduction.PDF , Viewed 10 January 2004.
9. CORLEY, J., 2003, *Best practices in establishing detection and quantification limits for pesticide residues in foods*, Handbook of Residue Analytical Methods for Agrochemicals, http://media.wiley.com/product_data/excerpt/142/047/4919/0471491942-4.pdf
10. CURRIE, L.A., 1999, *Nomenclature in evaluation of analytical methods including detection and quantification capabilities*, Analitika Chimica Acta, Volume 391, Issue 2, Pages 105-126.
11. DE BEER, W., 1998, Statistical Quality Management Course Notes, Technical University of Tshwane.
12. DE CONING, P., 2005, personal communication via email.

13. DE NIJS, R.C.M., DE ZEEUW, J., 1983, *Aluminium Oxide-coated fused silica porous-layer open-tubular column for Gas-Solid Chromatography of C_1 to C_{10} hydrocarbons*, Journal of Chromatography, Volume 279, Pages 41 to 48.
14. DE VANSSAY, E., ZUBRZYCKI, S., STERNBERG, R., RAULIN, F., SERGENT, M., PHAN-TAN-LUU, R., 1994, *Gas Chromatography of Titan's Atmosphere V. Determination of Permanent gases in the presence of hydrocarbons and nitriles with a molecular sieve micopacked column and optimization of the GC parameters using a Doehlert experimental design*, Journal of Chromatography A, Volume 688, pages 161 to 170.
15. DE ZEEUW, J., DUVEKOT, C., PEENE, J., DIJKWEL, P., HEIJNSDIJK, P., 2003, *GC: A review of state-of-the-art column technologies for the determination of ppm to ppb levels of oxygenated sulfur and hydrocarbon impurities in C_1-C_5 hydrocarbon streams*, Journal of Chromatographic Science, Volume 41, Pages 535 to 544.
16. DOJAHN, J., WENTWORTH, W.E., DEMING, S.N., STEARNS, S.D., 2001, *Determination of percent composition of a mixture analysed by gas chromatography: Comparison of a helium pulsed-discharge photoionization detector with a flame ionization detector*, Journal of Chromatography A, Volume 917, Pages 187 to 204.
17. DYSON, N.A., 1990, *Chromatographic integration methods*, Royal Society of Chemistry, Great Britain.
18. ETIOPE, G., 1997, *Evaluation of a micro gas chromatographic technique for environmental analyses of CO_2 and C_1-C_6 alkanes*, Journal of Chromatography A, Volume 775, Pages 243 to 249.
19. EURACHEM GUIDE, 1998, *The Fitness for Purpose of Analytical Methods: A Laboratory Guide to Method Validation and Related Topics*, http://www.eurachem.ul.pt/guides/valid.pdf , Viewed 10 January 2005.
20. EURACHEM/CITAC GUIDE, 1995, *Quantifying Uncertainty in Analytical measurement*, Second Edition, http://www.measurementuncertainty.org/mu/guide/ , Viewed 10 January 2005.
21. FORSYTH, D.S., 2004, *Pulsed discharge detector: theory and applications*, Journal of Chromatography A, Volume 1050, Pages 63 to 68.
22. GIDDINGS, J.C., 1964, *Theory of Gas-Solid Chromatography*, Analytical Chemistry, Volume 36, Number 7, Pages 1170 to 1175.
23. GUM (Guide to the Expression of Uncertainty in measurement), 1993, International Standards Organization (ISO), Geneva.

24. HAESSELBARTH, W., BREMSER, W., 2004, *Correlation between repeated measurements: bane and boon of the GUM approach to the uncertainty of measurement*, Accreditation and Quality Assurance, Volume 9, Pages 597 to 600.
25. HAO YUN, LEE, M.L., 1995, *Charcoal porous layer open tubular column gas chromatography for permanent gas analysis*, Journal Microcolumn Separations, Volume 7, Issue 3, pages 207 to 212.
26. HAVENGA, W.J., ROHWER, E.R., 1992, *Rapid analysis of coke oven gas by capillary gas chromatography*, Journal of High Resolution Chromatography, Volume 15, Pages 381 to 386.
27. HINSHAW, J.V., 2004, Anatomy of a Peak, LC-GC Europe, Volume 17, Number 4, Pages 216 to 223, http://www.lcgceurope.com/lcgceurope/article/articleDetail.jsp?id=92337 , viewed on 24/05/2005.
28. HOGAN, J.D. Ed, 1997, *Speciality Gas Analysis: A Practical Guidebook*, New York: Wiley- VCH. Inc.
29. HUBER, W., 2003, *Basic calculations about the limit of detection and its optimal determination*, Accreditation and Quality Assurance, Volume 8, Pages 213 to 217.
30. HUE, W.A., SINGH, H., XUN-YUN SUN, 1994, *Fundamental noise in three chromatographic detectors*, Journal of Chromatography A, Volume 687, Pages 283 to 290.
31. ISO 6142, 1998, *Gas Analysis – Preparation of calibration gas mixtures - Gravimetric method*, International Organisation for Standardization.
32. ISO 6143, 1997, *Gas Analysis – Determination of composition and checking of calibration gas mixtures*, International Organisation for Standardization.
33. ISO 8186: 1989 (E), 1989, *Ambient Air – Determination of the mass concentration of carbon monoxide – Gas chromatographic method*, International Organization for Standardization, Geneva.
34. JANSE VAN RENSBURG, M., 2003, *Method development for the analysis of CO in nitrogen using the PDHID and GC-μTCD-FID*, NML-03-0154, NML Technical Output Database.
35. JANSE VAN RENSBURG, M., 2006, *Validation of GC-μTCD-FID Method for the Determination of CO_2 in BIP™ nitrogen*, NML-06-0006, CSIR NML Technical Output Database.

36. JANSE VAN RENSBURG, M., 2006, *Validation of GC-μTCD-FID method for Determination of CO in BIP™ Nitrogen*, NML-05-0010, NML Technical Output Database.
37. JEFFREY, P.G., KIPPING, P.J., 1964, *Gas Analysis by Gas Chromatography*, London: Pergamon Press.
38. KAARLS, R., QUINN, T.J., 1997, *The Comité Consultatif pour la Quantité de Matière: a brief review of its origin and present activities,* Metrologia, Volume 34, Pages 1 to 5
39. KAMINSKI, M., KARTANOWICZ, R., JASTRZEBSKI, D., KAMINSKI, M.M., 2003, *Determination of carbon monoxide and carbon dioxide in refinery hydrogen gases and air by gas chromatography*, Journal of Chromatography A, Volume 989, Issue 2, Pages 277 to 283.
40. LASA, J., MOCHALSKI, P., PUSZ, J., 2004, *Evaluation of a pulsed helium ionisation detector for determination of neon concentrations by gas chromatography*, Journal of Chromatography A, Volume 1035, Pages 261 to 264.
41. LAURENS, J.B., DE CONING, J.P., SWINLEY, J.N., 2001, *Gas chromatographic analysis of trace impurities in tungsten hexafluoride*, Journal of Chromatography A, Volume 911, Issue 1, pages 107 to 112.
42. LAURENS, J.B., SWINLEY, J.N., DE CONING, J.P., 2000, *Gas chromatographic analysis of trace impurities in chlorine trifluoride*, Journal of Chromatography A, Volume 873, Issue 2, pages 229 to 235.
43. LITTLEWOOD, A.B., 1962, *Gas Chromatography: Principles, Techniques and Applications*, London: Academic Press.
44. MILLER, J.N., MILLER, J.C., 2000, *Statistics and Chemometrics for Analytical Chemistry*, Fourth Edition, Harlow, England: Prentice Hall.
45. MILTON, M.J.T, QUINN, T.J., 2001, *Primary methods for the measurement of substance*, Metrologia, Volume 38, Pages 289 to 296.
46. NAMIESNIK, J., 2002, *Trace Analysis – Challenges and Problems*, Critical Reviews in Analytical Chemistry, Volume 32, Number 4, pages 271 to 300.
47. NAVALE, V., HARPOLD, D., VERTES, A., 1998, *Development and characterization of gas chromatographic columns for the analysis of prebiological molecules in Titan's atmosphere*, Analytical Chemistry, Volume 70, Number 4, Pages 689 to 697.
48. NEHRKORN, P.C., 2004, *Oxygen and argon content in high purity gases (nitrogen)*, Varian Application Note 767-GC, www.varianinc.com/image/vimage/docs/products/chrom/apps/gc767.pdf , viewed January 2004.

49. NOVELLI, P.C., 1999, *CO in the atmosphere: measurement techniques and related issues*, Chemosphere: Global Change Science 1, Pages 115 to 126.
50. OSHA (Occupational Safety and Health Administration), 1991, *Carbon Monoxide in Workplace atmospheres*, Method Number: ID-210, http://www.osha.gov/dts/sltc/methods/inorganic/id210/id210.html , Viewed 10 January 2005.
51. PERKIN ELMER, 2002, Trace H_2, O_2, Ar, N_2, CH_4 and CO in CO_2 and light hydrocarbons analyser Model 4083, http://www.arnelinc.com/pdf/149.pdf , Viewed 30 August 2006.
52. PETERS, D,G., HAYES, J, M., HIEFTJE, G.M., 1974, *Chemical Separations and Measurements: Theory and Practise of Analytical Chemistry*, Saunders Golden Series, W.B. Saunders Company, USA.
53. POLLOCK, G.E., O' HARA, D., 1984, *Gas Chromatographic separation of Nitrogen, Oxygen, Argon and Carbon Monoxide using custom-made Porous Polymers from High Purity Divinylbenzene*, Journal of Chromatographic Science, Volume 22, Pages 343 to 347.
54. PORTER, K., VOLMAN, D.H., 1962, *Flame ionization detection of carbon monoxide for gas chromatographic analysis*, Analytical Chemistry, Volume 34, Pages 748 to 749.
55. QINHAN JIN, WENJUN YANG, AIMIN YU, XIAODAN TIAN, FENDI WANG, 1997, *Helium direct current discharge ionization for gas chromatography*, Journal of Chromatography A, Volume 761, Pages 169 to 179.
56. RAMSEY, R.S., TODD, R.A., 1987, *Pulsed Modulated Helium Ionization Detection*, Journal of Chromatography, Volume 399, Pages 139 to 148.
57. REID,G.L., ARMSTRONG, D.W., 1994, *Cyclodextrin PLOT columns for gas-solid chromatographic separation of light hydrocarbons and inorganic gases*, Journal Microcolumn Separations, Volume 6, Issue 2, pages 151 to 157.
58. RESTEK , 2002, *Chromatography products catalogue*, RestekCorp.
59. ROBERGE, M.T., FINLEY, J.W., LUKASKI, H.C., BORGERDING, A.J., 2004, Evaluation of the pulsed discharge helium ionization detector for the analysis of hydrogen and methane in breath, Journal of Chromatography A, Volume 1027, Pages 19 to 23.
60. ROHWER, E.R., 2004, *Chromatography (Hons),* Course Notes, Pretoria: University of Pretoria.
61. SAINT-GOBAIN PERFORMANCE PLASTICS, 2005, FEP tubing from CHEMFLUOR, http://www.tygon.com/searching/fep-tubing.asp , viewed on 13 January 2005.

62. SANDRA, P., 1989, *Resolution – Column Efficiency*, Journal of High Resolution Chromatography, Volume 12, Pages 273 to 277.
63. SANDRA, P., 1989, *Resolution – Definition and Nomenclature*, Journal of High Resolution Chromatography, Volume 12, Pages 82 to 86.
64. SHERMAN, J.D., 1999, Synthetic zeolites and other microporous oxide molecular sieves, www.pnas.org/cgi/reprint/96/7/347, Proceedings of the National Academy of Sciences Colloqium, 1998, Volume 96, Issue 7, Pages 3471 to 3478, Viewed 8 December 2004.
65. SIGMA ALDRICH, Updated 2003, *Performance characteristic evaluations of PLOT Columns prepared with Carbons, Porous polymers, Alumina and other Adsorbents* http://www.sigmaaldrich.com/Brands/Supelco_Home/TheReporter/Gas_Chromatography/Reporter_21_9_main.html, Viewed 05/12/2004.
66. SKOOG, D.A., HOLLER, J.F., NIEMAN, T.A., 1998, *Principles of Instrumental Analysis*, Fifth Edition, Florida: Harcourt Brace and Company.
67. STEVENS, M., BELLOWS, H., Permanent Gas Contaminants in Beverage Grade Carbon Dioxide, www.varianinc.com/cgi-bin/scanweb/show_lists , Viewed December 2004.
68. SUNG HO KIM, SUNG MAN NAM, KWANG OH KOH, YONG WOOK CHOI, 1999, *Analysis of Natural Gas using a single capillary column and a Pulsed Discharge Helium Ionization Detector*, Bulletin of the Korean Chemical Society, Volume 20, Number 7, Pages 843 to 845.
69. Supelco, 1999, Capillary GC Troubleshooting guide: How to locate problems and solve them, http://www.sigmaaldrich.com/Graphics/Supelco/objects/6800/6725.pdf, Page 21, viewed on 24/01/2005.
70. SUPELCO, 2005, Bulletin 786E, *Column Selection for Gas and Light Hydrocarbon analysis by Packed column GC*, http://www.sigmaaldrich.com/Graphics/Supelco/objects/4500/4489.pdf, viewed 18/05/2005.
71. SUPELCO, 2005, *Packings*, http://www.sigmaaldrich.com/Brands/Supelco_Home/Datanodes.html?cat_path=976693,1004746&supelco_name=Gas%20Chromatography&id=1004746, viewed 18/05/2005.
72. SWINLEY, J., DE CONING P., 2004, *Gas Analysis*, Course Notes, Pretoria: Scientific Supply Services cc. Short Course.

73. TALASEK, R.T., DAUGHERTY, K.E., 1993, *Analysis of carbon monoxide by molecular sieve trapping, Journal of Chromatography*, Volume 639, Pages 221 to 226.
74. TALASEK, R.T., SCHOENKE, M.P., 1994, *Comparison of universal chromatographic detectors for trace gas analysis*, Journal of Chromatography A, Volume 667, Pages 205 to 211.
75. THOMPSON, B., 1977, *Fundamentals of Gas Analysis by Gas Chromatography*, Palo Alto, California: Varian Inc.
76. THOMPSON, B., 2006, *Determination of sub-ppm concentrations of CO and CO_2 in ethylene and propylene*, Varian Application Note Number 26 http://www.varianinc.com/media/sci/apps/gc26.pdf Viewed 30 August 2006.
77. VARIAN CUSTOM SOLUTIONS INC., 1999, *Test Gas Analyser*, Paolo Alto: California.
78. VASNIN, S.V., WENTWORTH, W.E., STEARNS, S.D., MEYER, C.J., 1992, *Pulsed Discharge Emission Detector – Application to Analytical Spectroscopy of Permanent Gases*, Chromatographia, Volume 34, Numbers 5 to 8, pages 226 to 234.
79. VICI Valco Cheminert Catalogue 50, 2002, Vici Valco Instruments.
80. VICI VALCO INSTRUMENTS CO. INC., Updated 2003, *Pulsed Discharge Detector Models D-4-I-TQ-R and D-4-I-TQI-R Instruction Manual*, http://www.vici.com/support/manuals/d4_therm.pdf , Page 1, Viewed 10 January 2004. Viewed 21 May 2005.
81. VIM (International Vocabulary of basic and general terms in Metrology), 1993, International Standards Organization (ISO), Geneva.
82. WENTWORTH, W.E., CAI, H., STEARNS, S., 1994, *Pulsed discharge helium ionization detector Universal Detector for inorganic and organic compounds at the low pictogram level*, Journal of Chromatography A, Volume 688, Pages 135 to 152.
83. WENTWORTH, W.E., NADEGE, H., ZLATKIS, A., CHEN, E.C.M., STEARNS, S., 1998, *Multiple detector responses for gas chromatographic peak identification*, Journal of Chromatography A, Volume 795, Pages 319 to 347.
84. WENTWORTH, W.E., VASNIN, S.V., STEARNS, S.D., MEYER, C.J., 1992, *Pulsed Discharge Helium Ionization detector,* Chromatographia, Volume 34, Numbers 5 to 8, Pages 219 to 225.
85. WESSEL, R., 2005, Personal communication via email.
86. WIKIPEDIA FREE ENCYCLOPEDIA, Updated 30/11/2004, *Earth's atmosphere*, http://en.wikipedia.org/wiki/Earth's_atmosphere, Viewed 01/12/2004.

87. WIKIPEDIA FREE ENCYLCOPEDIA, updated 30/11/2004, *Mikhail Tsvet*, http://en.wikipedia.org/wiki/Mikhail_Tsvet, viewed 01/12/2004.
88. WURM, D.B., SUN, K., WINNIFORD, W.L., 2003, *Analysis of low levels of Oxygen, Carbon Monoxide and Carbon Dioxide in Polyolefin feed streams using a pulsed discharge detector and two PLOT columns*, Journal of Chromatographic Science, Volume 41, Pages 545 to 549.
89. ZHENGHUA Ji, MAJORS, R.E., GUTHRIE, E.J., 1999, *Porous layer open-tubular capillary columns: preparations, applications and future directions*, Journal of Chromatography A, 842, pages 115 to 142.

Addendum: Results

1. Results obtained using sequence reversal

The method validation for sequence reversal was done using a different set of standards than those used for the method validation without sequence reversal because the gas pressures in the cylinders was not enough for the same standards to be used for both validation experiments as well as for method development.

1.1 Method validation results for O_2

1.1.1 Repeatability

Table 1: Results of repeatability tests for O_2 performed on the results from Day 1 (sequence reversal)

Concentration (µmol·mol^{-1})	13.36979	6.68474	4.40163	1.33961	0.67330	0
1	2434883	1391857	1041082	542888	434986	303781
2	2445264	1392600	1037193	540615	438054	303135
3	2430414	1399608	1042432	542439	438613	302493
4	2443255	1389459	1049984	543269	438546	303397
5	2442912	1395521	1046472	543037	438959	302859
6	2446549	1388431	1045088	540985	438291	301840
7	2445111	1386436	1044133	546568	435522	304644
8	2438636	1391712	1045949	544712	437858	299580
9	2442614	1389957	1044732	545453	435984	301069
10	2445821	1395175	1039314	545246	439512	299995
Average	2441546	1392076	1043638	543521.2	437632.5	302279.3
Standard deviation	5297.282	3874.308	3732.901	1948.111	1560.835	1645.606
%CV	0.22	0.28	0.36	0.36	0.36	0.54

Table 2: Results of repeatability tests for O_2 performed on the results from Day 2 (sequence reversal)

Concentration (µmol·mol^{-1})	13.36979	6.68474	4.40163	1.33961	0.67330	0
1	2460686	1411586	1065466	542998	446146	320120
2	2458779	1410985	1066658	544476	440644	319717
3	2455025	1413126	1060480	543608	444541	314452
4	2459656	1411245	1066490	547103	446835	316407
5	2448363	1407976	1081841	547797	442982	316504
6	2461377	1405642	1064680	549137	445706	316673
7	2460829	1409742	1064010	548721	446785	317548
8	2447800	1407044	1067278	542223	445709	319313
9	2463898	1410232	1064424	551790	444399	317451
10	2465827	1415062	1069261	543392	444219	318509
Average	2458224	1410264	1067059	546124.5	444796.6	317669.4
Standard deviation	6067.034	2822.164	5692.188	3217.714	1905.637	1762.674
%CV	0.25	0.20	0.53	0.59	0.43	0.55

Table 3: Results of repeatability tests for O_2 performed on the results from Day 3 (sequence reversal)

Concentration (µmol·mol^{-1})	13.36979	6.68474	4.40163	1.33961	0.67330	0
1	2458830	1405301	1050132	544780	423163	323068
2	2452302	1402399	1057070	544238	425124	322536
3	2454348	1399096	1053746	536909	421653	317779
4	2462734	1404164	1050409	536205	425986	319877
5	2453844	1406220	1056272	545264	433166	319196
6	2463754	1400285	1054409	540550	427525	317235
7	2463357	1406824	1050454	544110	429506	316613
8	2467329	1402032	1051899	541905	430208	316131
9	2451286	1409133	1054771	542954	426250	315845
10	2466728	1402292	1055455	537639	429974	317102
Average	2459451.2	1403774.6	1053461.7	541455.4	427255.5	318538.2
Standard deviation	6102.900	3121.012	2570.722	3438.624	3519.492	2578.076
%CV	0.25	0.22	0.24	0.64	0.82	0.81

1.1.2 Reproducibility

Table 4: Results from reproducibility limit test

	Day 1	**Day 2**	**Day 3**	**Range**	**Reproducibility Limit (R)**
Intercept	-2.0063	-1.9823	-1.8646	0.14170	0.21450
Slope (x10^{-6})	6.0918	5.9375	5.8321	0.25970	0.36944

From **Table 4**, the reproducibility limit is more than the absolute difference between the two results, showing that the difference is within a probability of 95%.

1.1.3 Limit of detection

The calculation of the limit of detection was done using the IUPAC method.

Table 5: Detection limit calculation

	Day 1	Day 2	Day 3
1	303781	320120	323068
2	303135	319717	322536
3	302493	314452	317779
4	303397	316407	319877
5	302859	316504	319196
6	301840	316673	317235
7	304644	317548	316613
8	299580	319313	316131
9	301069	317451	315845
10	299995	318509	317102
Standard Deviation	1645.606	1762.674	2578.076
Slope (mol.mol^{-1}) x 10^{-6}	6.0918	5.9375	5.8321
Slope (mol^{-1}.mol)	164155.0937	168421.0526	173716.6681
LOD_{IUPAC} (10^{-6} mol.mol^{-1})	0.030	0.031	0.045
Average LOD_{IUPAC} (10^{-6} mol.mol^{-1})			0.036
Lower confidence limit (10^{-6} mol.mol^{-1})			0.024
Upper confidence limit (10^{-6} mol.mol^{-1})			0.065

The manufacturer's specification for the oxygen impurity is less than 0.010 x 10^{-6} mol·mol^{-1} in BIP™ nitrogen. The LOD_{IUPAC} has been calculated to be around 0.036 x 10^{-6} mol·mol^{-1} (35 ppb) for oxygen impurity in nitrogen. The dual column method is therefore not capable of the detection of oxygen in BIP™ nitrogen at the manufacturer's specification of 10 ppb. The signal that is actually obtained is a result of the matrix being analysed together with all possible leaks and contamination from the atmosphere.

1.1.4 Limit of quantification

The value of the LOQ_{IUPAC} is 0.118 x 10^{-6} mol·mol^{-1}. The method is therefore not suitable for quantification of oxygen at the levels specified by the manufacturer for BIP™ nitrogen.

1.1.5 Selectivity or specificity

The method development for the analysis of O_2 in BIP™ nitrogen has proven that the method is specific for the analysis of oxygen if the optimum experimental parameters outlined in section 5.3.9 are used. However, the signal of the oxygen peak is enhanced by leaks from the atmosphere into the sampling lines.

1.1.6 Accuracy or bias

The CSIR NML's Gas Metrology section does not have oxygen-in–nitrogen CRMs at present, so the bias study will have to be completed when the required CRMs are obtained. For the moment, the bias will be assumed to be negligible.

1.1.7 Linearity

Figure 1 shows the Microsoft EXCEL plot of the results for Day 1 with a resultant calibration line of acceptable linearity (R^2 = 0.9999).

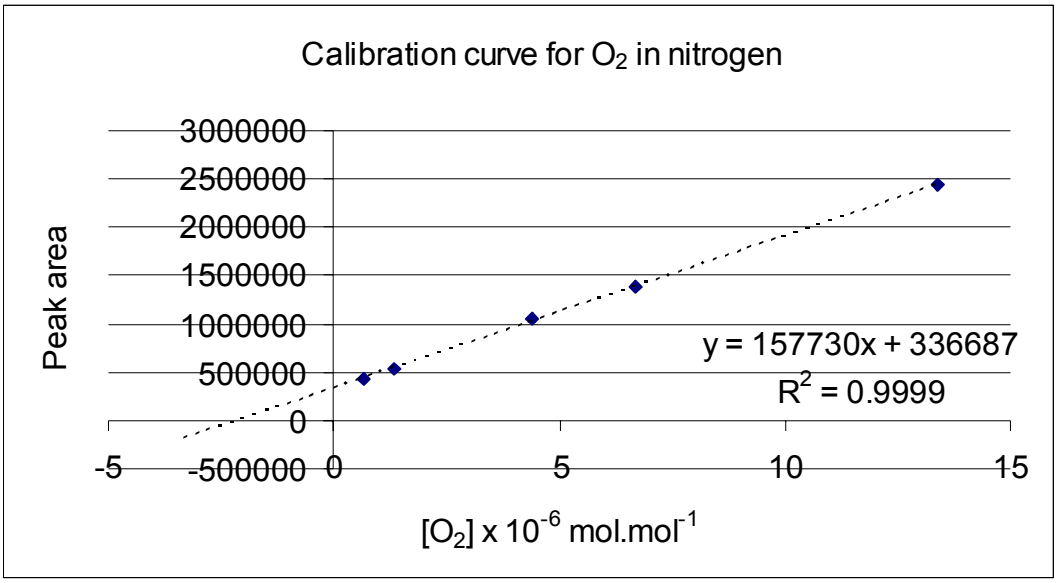

Figure 1: Plot of the oxygen concentration against the peak areas for Day 1 (sequence reversal)

Day 2 and Day 3 also showed acceptable linearity with R^2 values of 0.9997 and 0.9998 respectively. Using the regression analysis software, B_LEAST (Bremser,1997), the goodness of fit values met the acceptable criterion for linearity

(values ≤ 2) for the three days, with the linear/quadratic fit being the best fit for the results including uncertainties.

1.1.8 Influence of pressure, temperature and other possible sources of error

The temperature in the CSIR NML gas laboratory is controlled to 20 °C ±1 °C and the humidity to 50% RH ±10 %RH. This ensures that the GC temperature is not affected by the laboratory environment.

A source of error could be the inadequate conditioning of the columns that would cause the retention time of the O_2 peak to change. This can be avoided by always keeping the columns at 150 °C when samples are not being analysed, to avoid the saturation of the columns with moisture, and by conditioning the columns overnight at 170°C before a calibration set is run.

1.1.9 Measurement uncertainty and the uncertainty budget

1.1.9.1 Gravimetric preparation uncertainty

Table 6 shows the gravimetric uncertainties and the standard uncertainties for oxygen

Table 6

Uncertainties associated with the gravimetric preparation of the standards for oxygen

Cylinder Number	Concentration (µmol·mol^{-1})	Uncertainty (µmol·mol^{-1})
3884	13.36979	0.1337
3940	6.68474	0.0668
3886	4.40163	0.0440
3950	1.33961	0.0134
3895	0.67330	0.0067

The uncertainties used to calculate the slope and intercept were 1% of the value of the calculated concentration.

1.1.9.2 Uncertainty due to repeatability error

Table 7: Values and uncertainties for O_2 for Day 1

x_i	$u(x_i)$	y_i	$u(y_i)$
0.67330	0.0067	437632.5	1560.835
1.33961	0.0013	543521.2	1948.111
4.40163	0.0044	1043638	3732.901
6.68474	0.0067	1392076	3874.308
13.36979	0.1337	2441546	5297.282
0	0	302279.3	1645.606
m =6.0918 x 10^{-6}		$u(m)$ =1.514x 10^{-7}	
c =-2.0063		$u(c)$ =0.05910	
Goodness of fit value	0.7658		

Table 8: Values and uncertainties for O_2 for Day 2

x_i	$u(x_i)$	y_i	$u(y_i)$
0.67330	0.0067	444796.6	1905.637
1.33961	0.0013	546124.5	3217.714
4.40163	0.0044	1067059	5692.188
6.68474	0.0067	1410264	2822.164
13.36979	0.1337	2458224	6067.034
0	0	317669.4	1762.674
m =5.9375 x 10^{-6}		$u(m)$ =1.614 x 10^{-7}	
c =-1.9823		$u(c)$ =0.06383	
Goodness of fit value	1.4704		

Table 9: Values and uncertainties for O_2 for Day 3

x_i	$u(x_i)$	y_i	$u(y_i)$
0.67330	0.0067	427255.5	3519.492
1.33961	0.0013	541455.4	3438.624
4.40163	0.0044	1053461.7	2570.722
6.68474	0.0067	1403774.6	3121.012
13.36979	0.1337	2459451.2	6102.900
0	0	318538.2	2578.076
m =5.7565 x 10^{-6}		$u(m)$ =1.596 x 10^{-7}	
c =-1.8242		$u(c)$ =0.06725	
Goodness of fit value	1.0643		

1.1.9.3 Uncertainty due to Intermediate reproducibility error

According to the standard addition method, the amount of analyte in the matrix will be given by the intercept of the calibration curve with the x-axis (Miller and Miller, 2000). Therefore, the intercepts from **Tables 7**, **8** and **9** give the total amount of oxygen found in BIP™ nitrogen, along with an associated uncertainty. This

includes the small leaks from the atmosphere into the sample stream that enhances the oxygen signal.

Table 10: Calculation of reproducibility uncertainty

$[O_2]$ (Day 1)	2.0063 x 10^{-6} mol.mol^{-1}
$[O_2]$ (Day 2)	1.8646 x 10^{-6} mol.mol^{-1}
$[O_2]$ (Day 3)	1.9823 x 10^{-6} mol.mol^{-1}
Average $[O_2]$	1.9511 x 10^{-6} mol.mol^{-1}
Standard deviation	0.0758 x 10^{-6} mol.mol^{-1}
%CV	3.9%

1.1.9.4 Uncertainty due to the assumption of linearity

From **Figure 1**, the r^2 value of 0.9999 shows acceptable linearity without taking into consideration the uncertainties. The best fit was found to be a Linear/Quadratic fit when the uncertainties were included. From **Tables 7**, **8** and **9**, the goodness of fit values from the B_LEAST analysis for Linear/Quadratic fits were ≤ 2 for the three days, indicating that the error due to the assumption of linearity may be ignored.

1.1.9.5 Summary of uncertainty contributions

The uncertainty due to the assumption of linearity may be ignored in the uncertainty calculations because it has been shown to be negligible. The repeatability uncertainty can be obtained from **Tables 7, 8** and **9** from the uncertainty for the intercept and the intermediate reproducibility uncertainty from **Table 10**.

1.1.9.6 Calculation of combined uncertainty, effective degrees of freedom and the expanded uncertainty

The result for the combination of the uncertainties is shown in **Table 11**. The value of the sensitivity coefficient for each uncertainty contributor is 1 since they are all in the same units (x 10^{-6} mol.mol^{-1})

Table 11: Calculation of combined uncertainty for O_2 in N_2

	$u_i(y)$
$u_{DAY\,1}$	0.05910
$u_{DAY\,2}$	0.06383
$u_{DAY\,3}$	0.03769
S_{REPROD}	0.07584
$u_c(y)$	0.09353

The effective degrees of freedom (v_{eff}) can be evaluated by the Welch-Satterthwaite formula (**Equation 36**). The degrees of freedom for each day's calculation is ∞, since the degrees of freedom for the standard concentrations are ∞ and $n = 10$ measurements were made for each concentration standard. The degrees of freedom for the reproducibility uncertainty is also ∞ because this uncertainty was calculated using the measurements from three days where ($v = \infty$). Using the values calculated in **Table 11**, the effective degrees of freedom, v_{eff}, evaluates to ∞ and the corresponding value for k is 2 for a 95,45% confidence level. The result and the expanded uncertainty are shown in **Table 12**.

Table 12: Result and expanded uncertainty for O_2 in N_2

$u_c(y)$	0.09353
v_{eff}	∞
k	2
Expanded $u_c(y)$	0.187
Result [O_2]	1.951 x 10^{-6} mol.mol^{-1}
Relative expanded uncertainty (%)	9.6%
LOD	0.036 x 10^{-6} mol.mol^{-1}
LOQ	0.118 x 10^{-6} mol.mol^{-1}

1.2 Method Validation results for CO_2

1.1.1 Repeatability

Table 13: Results of repeatability tests performed on the results for CO_2 from Day 1 (sequence reversal)

Concentration ($\mu mol \cdot mol^{-1}$)	13.83701	6.926255	4.566069	1.400671	0.711862
1	1720581	873022	582712	168137	78734
2	1727773	881460	582779	168678	77222
3	1729109	880102	585529	164303	79854
4	1731158	880643	582071	169005	78936
5	1720677	877043	582028	169059	80454
6	1728674	875536	581804	168993	81299
7	1730547	879978	580953	163576	79813
8	1730542	879808	582392	170328	82231
9	1731248	881714	584936	169323	79364
10	1731487	878803	580397	170359	78603
Average	1728180	878810.9	582560.1	168176.1	79651
Standard deviation	4159.482	2792.598	1595.63	2339.522	1434.395
%CV	0.24	0.32	0.27	1.39	1.80

Table 14: Results of repeatability tests performed on the results for CO_2 from Day 2 (sequence reversal)

Concentration ($\mu mol \cdot mol^{-1}$)	13.83701	6.926255	4.566069	1.400671	0.711862
1	1777738	898269	593630	170469	81801
2	1775908	896714	593102	169253	81009
3	1786446	900566	593345	173094	79856
4	1786636	900591	595479	171300	82328
5	1774236	898364	594920	170648	82770
6	1777233	899638	597152	166876	81727
7	1788607	897750	592472	167054	81812
8	1785018	900943	595254	165951	80624
9	1778552	896418	596026	171142	79428
10	1785667	900143	593426	173359	82129
Average	1781604	898939.6	594480.6	169914.6	81348.4
Standard deviation	5334.057	1660.983	1504.547	2577.844	1090.777
%CV	0.30	0.18	0.25	1.52	1.34

Table 15: Results of repeatability tests performed on the results for CO_2 from Day 3 (sequence reversal)

Concentration (µmol·mol^{-1})	13.83701	6.92626	4.56607	1.40067	0.71186
1	1807158	918057	612458	180088	83370
2	1820089	918196	609733	176166	83895
3	1828961	921675	610679	177429	84720
4	1813779	917444	610587	175435	84802
5	1825260	918840	607021	173295	81724
6	1809122	920935	608100	178018	84447
7	1815531	920122	610117	175906	83636
8	1809391	920779	608716	176715	84803
9	1828298	919907	612426	176321	83194
10	1814223	921875	605678	177218	82544
Average	1817181.2	919783	609551.5	176659.1	83713.5
Standard deviation	8063.779	1572.802	2201.492	1771.767	1036.853
%CV	0.44	0.17	0.36	1.00	1.24

1.2.2 Reproducibility

Table 16: Results from reproducibility limit test

	Day 1	**Day 2**	**Day 3**	**Range**	**Reproducibility Limit (R)**
Intercept	-0.11295	-0.10776	-0.10778	0.005190	0.008459
Slope (x10^{-6})	7.5413	7.4576	7.2369	0.304400	0.444782

From **Table 16**, the reproducibility limit is more than the absolute difference between the two results, showing that the difference is within a probability of 95%.

1.2.3 Limit of detection

The limit of detection was calculated using the IUPAC method.

Table 17: Detection limit calculation

	Day 1	Day 2	Day 3
1	78734	81801	83370
2	77222	81009	83895
3	79854	79856	84720
4	78936	82328	84802
5	80454	82770	81724
6	81299	81727	84447
7	79813	81812	83636
8	82231	80624	84803
9	79364	79428	83194
10	78603	82129	82544
Standard Deviation	1434.394723	1090.777	1036.853
Slope (mol.mol^{-1}) x 10^{-6}	7.5413	7.4576	7.2369
Slope (mol^{-1}.mol)	132603.1321	134091.4	138180.7
LOD_{IUPAC} (10^{-6} mol.mol^{-1})	0.032	0.024	0.023
Average LOD_{IUPAC} (10^{-6} mol.mol^{-1})			0.026
Lower confidence limit (10^{-6} mol.mol^{-1})			0.018
Upper confidence limit (10^{-6} mol.mol^{-1})			0.048

1.2.4 Limit of quantification

The value of the LOQ_{IUPAC} is 0.088 x 10^{-6} mol·mol^{-1}. The method is therefore suitable for quantification of CO_2 at the levels specified (<0.25 x 10^{-6} mol·mol^{-1}) by the manufacturer for BIP™ nitrogen.

1.2.5 Selectivity or specificity

The conditions in section 5.3.9 were adhered to so that the CO_2 peak was separated from the other peaks and therefore no interferences were present.

1.2.6 Accuracy or bias

The bias could not be evaluated in this case because there was no CRM available for CO_2 in the range 0 to 10 x 10^{-6} mol·mol^{-1}.

1.2.7 Linearity

Figure 2 shows the plot of the calibration curve for the CO_2 analysis from Day 1.

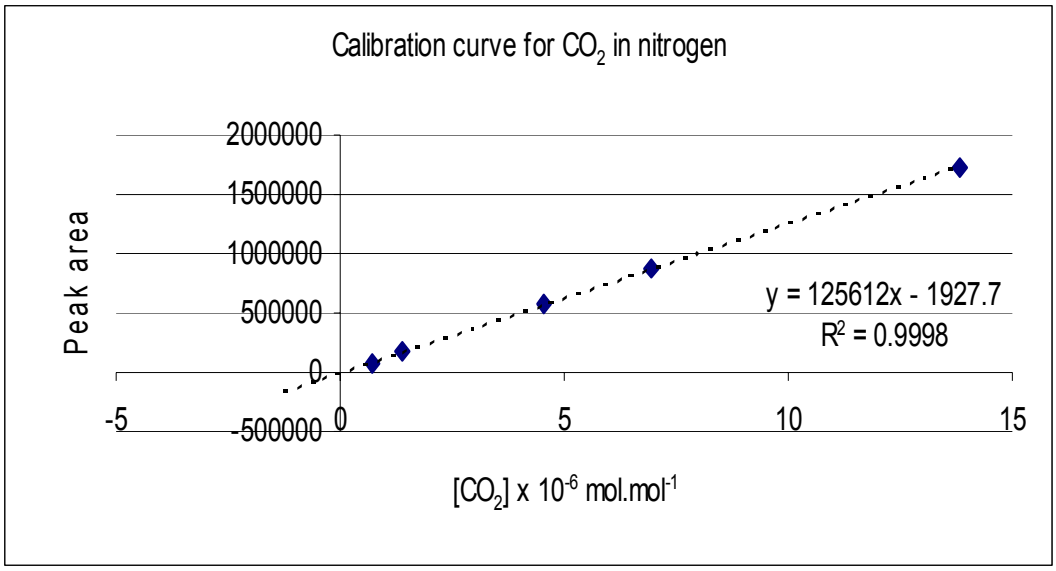

Figure 2: Calibration curve for the CO_2 results from Day 1 (sequence reversal).

Note that the regression coefficient value, r^2 was sufficiently close to 1 to assume linearity without taking into consideration the uncertainties. When the uncertainties were included, in the B_LEAST regression analysis, the Linear/Quadratic fit was found to be the best. From the B_LEAST analysis, the goodness-of-fit values were ≤2, showing acceptable linearity.

1.2.8 Influence of pressure, temperature and other possible sources of error

The temperature in the CSIR NML gas metrology laboratory is controlled to 20 °C ± 2 °C and the humidity to within 50% RH ± 10 %RH. This ensures that the GC temperature is not affected by the laboratory environment.

A source of error could be the inadequate conditioning of the gas chromatographic columns that would cause the retention time of the CO_2 peak to change. This is avoided by keeping the columns at 150 °C when samples are not being run, to avoid the saturation of the columns with moisture.

1.2.9 Measurement uncertainty and the uncertainty budget

1.2.9.1 Gravimetric preparation uncertainty

Table 18

Uncertainties associated with the gravimetric preparation of the standards for the carbon dioxide series

Cylinder Number	Component	Concentration (µmol·mol^{-1})	Uncertainty (µmol·mol^{-1})
3884	CO_2	13.8701	0.1387
3940	CO_2	6.9262	0.0693
3886	CO_2	4.5661	0.0457
3950	CO_2	1.4007	0.0140
3895	CO_2	0.7119	0.0071

1.2.9.2 Uncertainty due to repeatability error

Table 19: Values and uncertainties for CO_2 for Day 1

x_i	$u(x_i)$	y_i	$u(y_i)$
13.8701	0.1387	1728180	4159.482
6.9262	0.0693	878810.9	2792.598
4.5661	0.0457	582560.1	1595.63
1.4007	0.0140	16817601	2339.522
0.7119	0.0071	79651	1434.395
m =7.5413 x 10^{-6}		$u(m)$ =1.334 x 10^{-7}	
c =0.11295		$u(c)$ =0.018325	
Goodness of fit value	0.4494		

Table 20: Values and uncertainties for CO_2 for Day 2

x_i	$u(x_i)$	y_i	$u(y_i)$
13.8701	0.1387	1781604	5334.057
6.9262	0.0693	898939.6	1660.983
4.5661	0.0457	594480.6	1504.547
1.4007	0.0140	169914.6	2577.844
0.7119	0.0071	81348.4	1090.77
m =7.4576 x 10^{-6}		$u(m)$ =2.283 x 10^{-7}	
c = 0.10776		$u(c)$ =0.0016237	
Goodness of fit value	0.7406		

Table 21: Values and uncertainties for CO_2 for Day 3

x_i	$u(x_i)$	y_i	$u(y_i)$
13.8701	0.1387	1817181	8063.779
6.9262	0.0693	919783	1572.802
4.5661	0.0457	609551.5	2201.492
1.4007	0.0140	176659.1	1771.767
0.7119	0.0071	83713.5	1036.853
m =7.2369 x 10^{-6}		$u(m)$ =2.305 x 10^{-7}	
c = 0.10778		$u(c)$ =0.022507	
Goodness of fit value	0.5477		

1.2.9.3 Uncertainty due to intermediate reproducibility error

Since there was no signal for carbon dioxide in the blank, the detection limit of the system serves as the level of CO_2. From **Table 22**, the intermediate reproducibility uncertainty is calculated from the standard deviation of the calculated detection limits for three days.

Table 22: Calculation of reproducibility uncertainty

[CO_2] (Day 1)	0.0325 x 10^{-6} mol.mol^{-1}
[CO_2] (Day 2)	0.0244 x 10^{-6} mol.mol^{-1}
[CO_2] (Day 3)	0.0225 x 10^{-6} mol.mol^{-1}
Average [CO_2]	0.0264 x 10^{-6} mol.mol^{-1}
Standard deviation	0.005278 x 10^{-6} mol.mol^{-1}
%CV	20.0%

1.2.9.4 Uncertainty due to the assumption of linearity

The B_LEAST software has calculated the residuals as a “goodness of fit” value for the three different days as less than 2 signifying that the uncertainty arising from the assumption of linearity is negligible.

1.2.9.5 Summary of uncertainty contributions

The uncertainty due to the assumption of linearity may be ignored in the uncertainty calculations because it has been shown to be negligible. The repeatability uncertainty can be obtained from **Tables 19, 20 and 21** from the uncertainty for the intercept and the intermediate reproducibility uncertainty from **Table 22**.

1.2.9.6 Calculation of combined uncertainty, effective degrees of freedom and the expanded uncertainty

The upper and lower confidence limits of the LOD were used to calculate the uncertainty range as shown in **Table 23**.

Table 23: Calculation of expanded uncertainty for CO_2 in N_2

	$u_i(y)$
Upper confidence limit of LOD (x 10^{-6} mol.mol^{-1})	0.048
Average LOD (x 10^{-6} mol.mol^{-1})	0.026
Lower confidence limit of the LOD (x 10^{-6} mol.mol^{-1})	0.018
Range of CO_2 in BIP™ nitrogen at 95% level of confidence	0 < CO < 0.048

Since there was no CO_2 peak in the BIP™ nitrogen, the detection limit of CO_2 was taken as the amount of CO_2. The upper and lower confidence limits of the detection limits have been calculated as discussed and are shown in **Table 23** for a 95% level of confidence for $n = 10$. This result is already an expanded uncertainty and there is no need to expand it any further.

1.3 Method validation results for CO

1.3.1 Repeatability

Table 24: Results of repeatability tests performed on the results for CO from Day 1 (sequence reversal)

Concentration (µmol·mol^{-1})	9.151163	4.76993	3.150526	0.978639	0.506024
1	1467910	698270	444752	117523	59434
2	1484232	700791	436262	113948	60756
3	1478617	692086	452325	114727	57017
4	1479763	700503	447627	115829	58066
5	1471039	699632	452178	111798	60923
6	1476467	702918	452942	113688	59821
7	1475667	700054	452099	115216	64796
8	1477577	697397	447861	110353	59989
9	1485554	690877	445080	117958	60921
10	1480967	706456	450068	118800	64417
Average	1477779	698898.4	448119.4	114984	60614
Standard deviation	5435.901	4651.23	5148.199	2688.176	2449.59
%CV	0.37	0.67	1.15	2.34	4.04

Table 25: Results of repeatability tests performed on the results for CO from Day 2 (sequence reversal)

Concentration (µmol·mol^{-1})	9.151163	4.76993	3.150526	0.978639	0.506024
1	1519826	714907	465051	121669	50361
2	1522371	717347	460405	118832	53357
3	1523093	710163	465719	122112	50423
4	1507368	716182	468112	119287	51278
5	1516838	714400	467225	120103	50800
6	1523054	705768	461172	121639	51211
7	1518294	725577	464186	123004	49243
8	1518726	711888	466426	118413	50264
9	1523736	719759	465678	120546	53291
10	1521148	724256	463430	121053	53276
Average	1519445	716024.7	464740.4	120665.8	51350.4
Standard deviation	4840.161	6103.547	2491.521	1503.043	1463.948
%CV	0.32	0.85	0.54	1.25	2.85

Table 26: Results of repeatability tests performed on the results for CO from Day 3 (sequence reversal)

Concentration (µmol·mol^{-1})	9.15116	4.76993	3.15053	0.97864	0.50602
1	1553951	750462	469021	123011	47729
2	1552888	736150	471891	126400	46818
3	1547901	740323	473869	126909	44387
4	1554260	736723	471342	124713	44853
5	1552139	743254	475295	123268	47768
6	1556141	737344	475892	124162	49216
7	1552689	738144	480234	123507	48805
8	1556237	739114	477352	122185	49546
9	1544313	732831	470757	121170	51064
10	1557354	735959	476465	126289	51382
Average	1552787.3	739030.4	474211.8	124161.4	48156.8
Standard deviation	3995.210	4891.201	3461.221	1908.927	2347.072
%CV	0.26	0.66	0.73	1.54	4.87

1.3.2 Reproducibility

Table 27: Results from reproducibility limit test

	Day 1	**Day 2**	**Day 3**	**Range**	**Reproducibility Limit (R)**
Intercept	0.10247	0.16405	0.18271	0.04199	0.118764
Slope (x10^{-6})	7.2351	6.7516	6.5229	0.363617	1.028465

From **Table 27**, the reproducibility limit is more than the absolute difference between the two results, showing that the difference is within a probability of 95%.

1.3.3 Limit of detection

The limit of detection was calculated using the IUPAC method.

Table 28: Detection limit calculation

	Day 1	Day 2	Day 3
1	59434	50361	47729
2	60756	53357	46818
3	57017	50423	44387
4	58066	51278	44853
5	60923	50800	47768
6	59821	51211	49216
7	64796	49243	48805
8	59989	50264	49546
9	60921	53291	51064
10	64417	53276	51382
Standard Deviation	2449.590	1463.948	2347.072
Slope ($mol.mol^{-1}$) x 10^{-6}	7.2351	6.7516	6.5229
Slope ($mol^{-1}.mol$)	138215.090	148113.040	153306.045
LOD_{IUPAC} (10^{-6} $mol.mol^{-1}$)	0.0532	0.0297	0.0459
Average LOD_{IUPAC} (10^{-6} $mol.mol^{-1}$)			0.043
Lower confidence limit (10^{-6} $mol.mol^{-1}$)			0.029
Upper confidence limit (10^{-6} $mol.mol^{-1}$)			0.078

The limit of detection (0.043 x 10^{-6} $mol.mol^{-1}$) is less than the amount of CO expected in BIP™ nitrogen (0.25 x 10^{-6} $mol.mol^{-1}$) and this indicates that the method is fit for purpose for the analysis of CO in BIP™ nitrogen.

1.3.4 Limit of quantification

The LOQ_{IUPAC} is calculated as 0.143 x 10^{-6} $mol.mol^{-1}$. The limit of quantification is lower than the level of CO specified by the manufacturer in BIP™ nitrogen (0.25 x 10^{-6} $mol.mol^{-1}$) indicating that the method is fit for purpose for quantifying these low levels of CO in BIP™ nitrogen.

1.3.5 Selectivity or specificity

The conditions in section 5.3.9 were adhered to so that the CO peak was separated from the other peaks therefore, no interferences were present.

1.3.6 Accuracy or bias

The bias could not be evaluated in this case because there was no CRM for CO available in the range 0 to 10 x 10^{-6} mol·mol^{-1}.

1.3.7 Linearity

Figure 3 shows the plot of the calibration curve for the CO analysis from Day 1.

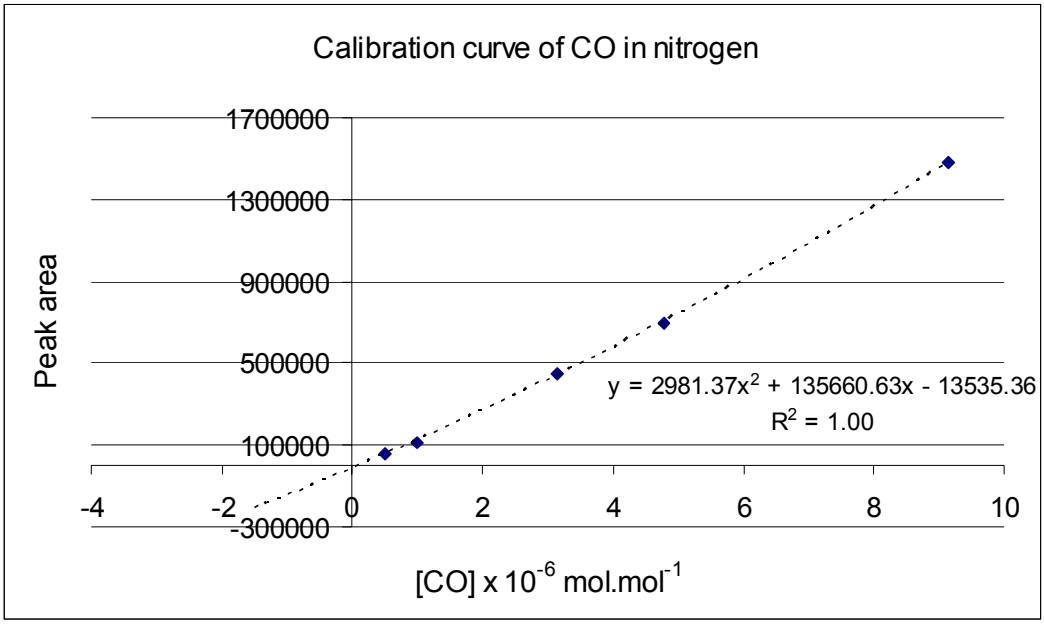

Figure 3: Calibration curve for the CO results from Day 1 (sequence reversal).

Note that the best fit was a polynomial and not a straight line, with the r^2 for a linear fit being 0.9974 but the r^2 for a polynomial fit being 0.9999 as shown in **Figure 3** above. The fact that the curve is not linear could be as a result of using temperature and pressure programming in the method or some other effect at low CO concentrations. Using the B_LEAST regression analysis, the results showed acceptable goodness of fit values (≤2) i.e. the goodness-of-fit value for all three days with linear/quadratic fits.

1.3.8 Influence of pressure, temperature and other possible sources of error

The temperature in the CSIR NML gas metrology laboratory is controlled to 20 °C ± 2 °C and the humidity to within 50% RH ± 10 %RH. This ensures that the GC temperature is not affected by the laboratory environment.

A source of error could be the inadequate conditioning of the gas chromatographic columns that would cause the retention time of the CO peak to change. This is avoided by keeping the columns at 150 °C when samples are not being run, to avoid the saturation of the columns with moisture.

1.3.9 Measurement uncertainty and the uncertainty budget

1.3.9.1 Gravimetric preparation uncertainty

Table 29: Uncertainties associated with the gravimetric preparation of the standards for carbon monoxide

Cylinder Number	Component	Concentration (µmol·mol^{-1})	Uncertainty (µmol·mol^{-1})
3884	CO	9.1512	0.0915
3940	CO	4.7699	0.0477
3886	CO	3.1505	0.0315
3950	CO	0.9786	0.0098
3895	CO	0.5060	0.0051

1.3.9.2 Uncertainty due to repeatability error

Table 30: Values and uncertainties for CO for Day 1

x_i	$u(x_i)$	y_i	$u(y_i)$
9.1512	0.0915	1477779	5435.901
4.7699	0.0477	698898.4	4651.23
3.1505	0.0315	448119.4	5148.199
0.9786	0.0098	114984	2688.176
0.5060	0.0051	60614	2449.59
m =7.2351 x 10^{-6}		$u(m)$ =7.426 x 10^{-7}	
c =0.10247		$u(c)$ =0.019773	
Goodness of fit value	2.2620		

Table 31: Values and uncertainties for CO for Day 2

x_i	$u(x_i)$	y_i	$u(y_i)$
9.1512	0.0915	1519445	4840.161
4.7699	0.0477	716024.7	6103.547
3.1505	0.0315	464740.4	2491.521
0.9786	0.0098	120665.8	1503.043
0.5060	0.0051	51350.4	1463.948
m =6.7516 x 10^{-6}		$u(m)$ =5.776 x 10^{-7}	
c =0.16405		$u(c)$ =0.013054	
Goodness of fit value	0.8453		

Table 32: Values and uncertainties for CO for Day 3

x_i	$u(x_i)$	y_i	$u(y_i)$
9.1512	0.0915	1552787	3995.21
4.7699	0.0477	739030.4	4891.201
3.1505	0.0315	474211.8	3461.221
0.9786	0.0098	124161.4	1908.927
0.5060	0.0051	48156.8	2347.072
m =6.5229 x 10^{-6}		$u(m)$ =7.017 x 10^{-7}	
c =0.18271		$u(c)$ =0.015480	
Goodness of fit value	0.8876		

1.3.9.3 Uncertainty due to intermediate reproducibility error

Since there was no signal for carbon monoxide in the blank, the detection limit of the system serves as the level of CO. From **Table 33**, the intermediate reproducibility uncertainty is calculated from the standard deviation of the calculated detection limits for three days.

Table 33: Calculation of reproducibility uncertainty

[CO] (Day 1)	0.0532 x 10^{-6} mol.mol^{-1}
[CO] (Day 2)	0.0297 x 10^{-6} mol.mol^{-1}
[CO] (Day 3)	0.0459 x 10^{-6} mol.mol^{-1}
Average [CO]	0.043 x 10^{-6} mol.mol^{-1}
Standard deviation	0.01204 x 10^{-6} mol.mol^{-1}
%CV	28.1%

The reproducibility uncertainty is smaller than the upper and lower confidence limits that have been calculated for the LOD in **Table 28**. Therefore, the confidence limits for the LOD from **Table 28** were used in the calculation of the final uncertainty.

1.3.9.4 Uncertainty due to the assumption of linearity

The B_LEAST software has calculated the residuals as a "goodness of fit" value for the two different days as ≤2 signifying that the uncertainty arising from the assumption of linearity is negligible.

1.3.9.5 Summary of uncertainty contributions

The uncertainty due to the assumption of linearity may be ignored in the uncertainty calculations because it has been shown to be negligible. The intermediate reproducibility uncertainty from **Table 33** is smaller than the confidence limits calculated for the LOD in **Table 28**, and therefore it was ignored in the uncertainty calculation.

1.3.9.6 Calculation of the expanded uncertainty

The upper and lower confidence limits of the LOD were used to calculate the uncertainty range as shown in **Table 34**.

Table 34: Calculation of expanded uncertainty for CO in N_2

	$u_i(y)$
Upper confidence limit of LOD (x 10^{-6} mol.mol^{-1})	0.078
Average LOD (x 10^{-6} mol.mol^{-1})	0.043
Lower confidence limit of the LOD (x 10^{-6} mol.mol^{-1})	0.029
Range of CO in BIP™ nitrogen at 95% level of confidence	0 < CO < 0.078

Since there was no CO peak in the BIP™ nitrogen, the detection limit of CO was taken as the amount of CO. The upper and lower confidence limits of the detection limits have been calculated as discussed and are shown in **Table 34** for a 95% level of confidence for $n = 10$. This result is already an expanded uncertainty and there is no need to expand it any further.

2. Results obtained without sequence reversal

2.1 Method validation results for O_2

2.1.1 Repeatability

Table 35: Results of repeatability tests for O_2 performed on the results from Day 1

Concentration (µmol·mol^{-1})	4.4016	2.6854	1.3396	0.6733	0.2674	**Blank**
1	499006	308876	146016	72048	27494	2466
2	500495	310758	146293	71876	27922	2140
3	498940	310629	147173	71840	28381	2172
4	498019	307199	147989	73097	28257	2017
5	501332	310511	146682	73560	28595	2031
6	503924	312039	147531	73184	28563	2066
7	503507	312381	148544	73407	28736	2207
8	503698	313651	148068	73262	28240	1934
9	503235	312658	147266	73360	28571	2207
10	505432	313262	148149	73833	28586	2091
Average	501758.8	311196.4	147371.1	72946.7	28334.5	2133.1
Standard deviation	2548.755	2024.535	843.116	737.979	379.203	146.487
%CV	0.51	0.65	0.57	1.01	1.34	6.87

Table 36: Results of repeatability tests for O_2 performed on the results from Day 2

Concentration (µmol·mol^{-1})	4.4016	2.6854	1.3396	0.6733	0.2674	**Blank**
1	519594	326303	152033	74358	28761	2407
2	521091	324632	152037	75020	29270	2553
3	517463	327439	153440	75314	29135	2605
4	515672	328730	153328	74833	30146	2458
5	520798	327796	154210	75625	29065	3053
6	523564	327316	153617	74542	28777	2971
7	518445	326090	154899	75062	29464	3114
8	523053	329514	152820	75328	29661	2659
9	516034	329670	153917	75370	28922	2586
10	525158	328757	154423	75525	29449	2549
Average	520087.2	327624.7	153472.4	75097.7	29265	2695.5
Standard deviation	3229.360	1615.002	959.238	417.391	431.170	254.246
%CV	0.62	0.49	0.63	0.56	1.47	9.43

Table 37: Results of repeatability tests for O_2 performed on the results from Day 3

Concentration (µmol·mol^{-1})	4.4016	2.6854	1.3396	0.6733	0.2674	**Blank**
1	505243	314961	154930	71126	28690	2512
2	506141	315934	154887	72084	28566	2244
3	506783	315335	155332	70102	27883	2391
4	505125	316791	155085	70506	28961	2842
5	503647	317841	155229	71337	28108	2291
6	506997	316428	155891	69751	28943	2673
7	507025	317323	155940	70056	28574	2417
8	507331	318161	155881	69501	28651	2926
9	508239	318224	154931	70106	28647	1753
10	507697	318658	155467	70116	28601	2764
Average	506422.8	316965.6	155357.3	70468.5	28562.4	2481.3
Standard deviation	1391.633	1283.736	419.976	803.385	334.120	346.524
%CV	0.27	0.41	0.27	1.14	1.17	13.97

2.1.2 Reproducibility

Table 38: Results from reproducibility limit test

	Day 1	**Day 2**	**Day 3**	**Range**	**Reproducibility Limit (R)**
Intercept	-0.02167	-0.02391	-0.01978	0.00413	0.00585
Slope (x10^{-6})	9.2752	8.8739	8.7352	0.5400	0.7932

From **Table 38**, the reproducibility limit is more than the absolute difference between the two results, showing that the difference is within a probability of 95%.

2.1.3 Limit of detection

The calculation of the limit of detection was done using the IUPAC method.

Table 39: Detection limit calculation

	Day 1	Day 2	Day 3
1	2466	2407	2512
2	2140	2553	2244
3	2172	2605	2391
4	2017	2458	2842
5	2031	3053	2291
6	2066	2971	2673
7	2207	3114	2417
8	1934	2659	2926
9	2207	2586	1753
10	2091	2549	2764
Standard Deviation	146.487	254.246	346.524
Slope (mol.mol^{-1}) x 10^{-6}	9.2752	8.8739	8.7352
Slope (mol^{-1}.mol)	107814.387	112690.024	114479.348
LOD_{IUPAC} (10^{-6} mol.mol^{-1})	0.0041	0.0068	0.0091
Average LOD_{IUPAC} (10^{-6} mol.mol^{-1})			0.007
Lower confidence limit (10^{-6} mol.mol^{-1})			0.004
Upper confidence limit (10^{-6} mol.mol^{-1})			0.012

The manufacturer's specification for the oxygen impurity is less than 0.010 x 10^{-6} mol·mol^{-1} in BIP™ nitrogen. The LOD_{IUPAC} has been calculated to be around 0.007 x 10^{-6} mol·mol^{-1} (7 ppb) for oxygen impurity in nitrogen. The dual column method is therefore capable of the detection of oxygen in BIP™ nitrogen at the manufacturer's specification of 10 ppb. The signal that is actually obtained is a result of the matrix being analysed together with all possible leaks and contamination from the atmosphere.

2.1.4 Limit of quantification

The value of the LOQ_{IUPAC} is 0.030 x 10^{-6} mol·mol^{-1}. The method is therefore not suitable for quantification of oxygen at the levels specified by the manufacturer for BIP™ nitrogen.

2.1.5 Selectivity or specificity

The method development for the analysis of O_2 in BIP™ nitrogen (Chapter 5) has proven that the method is specific for the analysis of oxygen if the optimum experimental parameters outlined in section 5.3.9 are used. However, the signal of

the oxygen peak is enhanced by leaks from the atmosphere into the sampling lines. Sample flow must be greater than 100 mℓ·min^{-1} in order to minimise the interference from the oxygen in the atmosphere.

2.1.6 Accuracy or bias

The CSIR NML's Gas Metrology section does not have oxygen-in–nitrogen CRMs at present, so the bias study will have to be completed when the required CRMs are obtained. For the moment, the bias will be assumed to be negligible.

2.1.7 Linearity

Figure 4 shows the Microsoft EXCEL plot of the results for Day 1 with a resultant calibration line of acceptable linearity (R^2 = 0.9997).

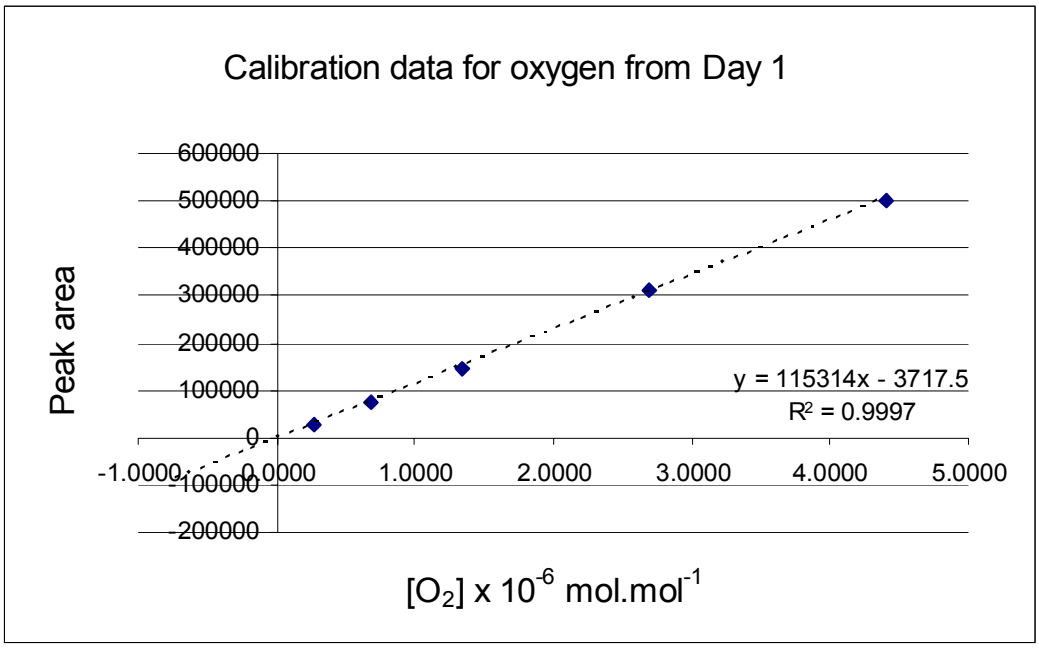

Figure 4: Calibration curve for the O_2 results from Day 1 (no sequence reversal).

Day 2 and Day 3 also showed acceptable linearity with R^2 values of 0.9993 and 0.9994 respectively. Using the regression analysis software, B_LEAST (Bremser, 1997), the goodness of fit values met the acceptable criterion for linearity (values ≤ 2) for the three days, with the linear/quadratic fit being the best fit for the results including uncertainties.

2.1.8 Influence of pressure, temperature and other possible sources of error

The temperature in the CSIR NML gas laboratory is controlled to 20 °C ±1 °C and the humidity to 50% RH ±10 %RH. This ensures that the GC temperature is not affected by the laboratory environment.

A source of error could be the inadequate conditioning of the column that would cause the retention time of the O_2 peak to change. This can be avoided by always keeping the column at 150 °C when samples are not being analysed, to avoid the saturation of the column with moisture.

2.1.9 Measurement uncertainty and the uncertainty budget

2.1.9.1 Gravimetric preparation uncertainty

Table 40: Uncertainties associated with the gravimetric preparation of the standards for oxygen

Cylinder Number	Concentration (µmol·mol^{-1})	Uncertainty (µmol·mol^{-1})
3886	4.402	0.010
3940	2.685	0.008
3950	1.340	0.006
3895	0.673	0.005
3884	0.267	0.006

2.1.9.2 Uncertainty due to repeatability error

Table 41: Values and uncertainties for O_2 for Day 1

x_i	$u(x_i)$	y_i	$u(y_i)$
4.402	0.010	501758.8	2548.755
2.685	0.008	311196.4	2024.535
1.340	0.006	147371.1	843.116
0.673	0.005	72946.7	737.979
0.267	0.006	28334.5	379.203
0	0	2133.1	146.487
m =8.7352 x 10^{-6}		$u(m)$ =1.315x 10^{-7}	
c =-0.021674		$u(c)$ =0.003087	
Goodness of fit value	1.5023		

Table 42: Values and uncertainties for O_2 for Day 2

x_i	$u(x_i)$	y_i	$u(y_i)$
4.402	0.010	520087.2	3229.360
2.685	0.008	327624.7	1615.000
1.340	0.006	153472.4	959.238
0.673	0.005	75097.7	417.391
0.267	0.006	29265	431.170
0	0	2695.5	254.246
m =8.8739 x 10^{-6}		$u(m)$ =1.407 x 10^{-7}	
c =-0.023912		$u(c)$ =0.002327	
Goodness of fit value	2.7391		

Table 43: Values and uncertainties for O_2 for Day 3

x_i	$u(x_i)$	y_i	$u(y_i)$
4.402	0.010	506422.8	1391.633
2.685	0.008	316965.6	1283.736
1.340	0.006	155357.3	419.976
0.673	0.005	70468.5	803.385
0.267	0.006	28562.4	334.120
0	0	2481.3	346.524
m =9.2752 x 10^{-6}		$u(m)$ =1.428 x 10^{-7}	
c =-0.01978		$u(c)$ =0.001414	
Goodness of fit value	1.9170		

2.1.9.3 Uncertainty due to intermediate reproducibility error

According to the standard addition method, the amount of analyte in the matrix will be given by the intercept of the calibration curve with the x-axis (Miller and Miller, 2000). Therefore, the intercepts from **Tables 41**, **42** and **43** give the total amount of oxygen found in BIP™ nitrogen, along with an associated uncertainty. This includes the small leaks from the atmosphere into the sample stream that enhances the oxygen signal. The uncertainty due to reproducibility is calculated from the standard deviation of the results from the three days (**Table 44**).

Table 44: Calculation of reproducibility uncertainty

[O_2] (Day 1)	0.02167 x 10^{-6} mol.mol^{-1}
[O_2] (Day 2)	0.02391 x 10^{-6} mol.mol^{-1}
[O_2] (Day 3)	0.01978 x 10^{-6} mol.mol^{-1}
Average [O_2]	0.02179 x 10^{-6} mol.mol^{-1}
Standard deviation	0.00207 x 10^{-6} mol.mol^{-1}
%CV	9.5%

2.1.9.4 Uncertainty due to the assumption of linearity

From **Figure 4**, the r^2 value of 0.9997 shows acceptable linearity without taking into consideration the uncertainties. The best fit was found to be a Linear/Quadratic fit when the uncertainties were included. From **Tables 41**, **42** and **43**, the goodness of fit values from the B_LEAST analysis for Linear/Quadratic fits were ≤ 2 for the three days, indicating that the error due to the assumption of linearity may be ignored.

2.1.9.5 Summary of uncertainty contributions

The uncertainty due to the assumption of linearity may be ignored in the uncertainty calculations because it has been shown to be negligible. The repeatability uncertainty can be obtained from **Tables 41, 42** and **43** from the uncertainty for the intercept and the intermediate reproducibility uncertainty from **Table 44**.

2.1.9.6 Calculation of combined uncertainty, effective degrees of freedom and the expanded uncertainty

The result for the combination of the uncertainties using **Equation 34** is shown in **Table 45**. The value of the sensitivity coefficient for each uncertainty contributor is 1 since they are all in the same units (x 10^{-6} mol.mol^{-1})

Table 45: Calculation of combined uncertainty for O_2 in N_2

	$u_i(y)$
$u_{DAY\,1}$	0.003087
$u_{DAY\,2}$	0.002327
$u_{DAY\,3}$	0.001414
S_{REPROD}	0.002068
$u_c(y)$	0.003151

The effective degrees of freedom (v_{eff}) can be evaluated by the Welch-Satterthwaite formula (**Equation 36**). The degrees of freedom for each day's calculation is ∞, since the degrees of freedom for the standard concentrations are

∞ and $n = 10$ measurements were made for each concentration standard. The degrees of freedom for the reproducibility uncertainty is also ∞ because this uncertainty was calculated using the measurements from three days where ($v = \infty$). Using the values calculated in **Table 45**, the effective degrees of freedom, v_{eff} , evaluates to ∞ and the corresponding value for k is 2 for a 95,45% confidence level. The result and the expanded uncertainty are shown in **Table 46**.

Table 46: Result and expanded uncertainty for O_2 in N_2

$u_c(y)$	0.00315
v_{eff}	∞
k	2
Expanded $u_c(y)$	0.006
Result [O_2]	0.022 x 10^{-6} mol.mol^{-1}
Relative expanded uncertainty (%)	28.9%

2.2 Method validation results for CO_2

2.2.1 Repeatability

Table 47

Results of repeatability tests performed on the results for CO_2 from Day 1

Concentration (µmol·mol^{-1})	**4.5661**	**2.7860**	**1.4007**	**0.7119**	**0.2863**	**Blank**
1	623297	399991	205920	110325	50482	8214
2	625173	400448	207274	110649	51207	8284
3	626079	397916	207706	111498	51678	8687
4	626766	401146	208181	110871	51646	8792
5	625400	399991	208887	110944	51517	9248
6	628156	401216	207763	111060	52582	8612
7	625339	401191	207980	111917	52120	9165
8	623482	401799	207814	111773	51322	9362
9	623956	403003	207144	112993	51772	9484
10	629506	402638	209690	112490	51203	8550
Average	625715.4	400933.9	207835.9	111452	51552.9	8839.8
Standard deviation	2000.798	1462.34731	1009.409	845.756	567.301	449.953
%CV	0.32	0.36	0.49	0.76	1.10	5.09

Table 48: Results of repeatability tests performed on the results for CO_2 from Day 2

Concentration ($\mu mol \cdot mol^{-1}$)	**4.5661**	**2.7860**	**1.4007**	**0.7119**	**0.2863**	**Blank**
1	615377	392395	199621	102001	44799	5677
2	619170	394536	199234	101481	45198	5966
3	622988	395574	200490	102138	44783	6427
4	619504	396427	200870	101666	45035	6327
5	622829	397039	198603	102765	45681	6803
6	620641	397912	201557	102480	44253	6598
7	621731	397729	202758	102120	45634	5981
8	622575	398355	201258	101962	45276	6624
9	623595	397476	200202	102449	45626	6181
10	624484	396901	200870	101505	45164	6109
Average	621289.4	396434.4	200546.3	102056.7	45144.9	6269.3
Standard deviation	2701.462	1822.001354	1206.724	427.643	451.741	350.604
%CV	0.43	0.46	0.60	0.42	1.00	5.59

Table 49: Results of repeatability tests performed on the results for CO_2 from Day 3

Concentration ($\mu mol \cdot mol^{-1}$)	**4.5661**	**2.7860**	**1.4007**	**0.7119**	**0.2863**	**Blank**
1	606063	386870	198463	102748	44163	5885
2	602982	387317	199842	103286	43397	5715
3	607858	386296	199640	102949	44857	6610
4	608105	388482	199066	104160	43745	6388
5	606419	387941	198847	102913	44484	7329
6	608826	387341	199709	103383	44863	6706
7	607509	387850	200098	102762	44186	6909
8	608677	389623	198983	101000	44486	6478
9	605316	388666	199966	102612	44796	6103
10	608857	390098	200750	101972	44092	5843
Average	607061.2	388048.4	199536.4	102778.5	44306.9	6396.6
Standard deviation	1884.722	1192.358	688.128	844.664	487.587	516.277
%CV	0.31	0.31	0.34	0.82	1.10	8.07

2.2.2 Reproducibility

Table 50: Results from reproducibility limit test

	Day 1	**Day 2**	**Day 3**	**Range**	**Reproducibility Limit (R)**
Intercept	-0.059660	-0.043953	-0.044979	0.01571	0.02485
Slope ($x10^{-6}$)	6.7401	7.0071	7.0261	0.2860	0.4523

From **Table 50**, the reproducibility limit is more than the absolute difference between the two results, showing that the difference is within a probability of 95%.

2.2.3 Limit of detection

The limit of detection was calculated using the IUPAC method.

Table 51: Detection limit calculation for CO_2

	Day 1	Day 2	Day 3
1	8214	5677	5885
2	8284	5966	5715
3	8687	6427	6610
4	8792	6327	6388
5	9248	6803	7329
6	8612	6598	6706
7	9165	5981	6909
8	9362	6624	6478
9	9484	6181	6103
10	8550	6109	5843
Standard Deviation	449.953	350.604	516.277
Slope (mol.mol^{-1}) x 10^{-6}	6.7401	7.0071	7.0261
Slope (mol^{-1}.mol)	148365.751	142712.392	142326.468
LOD_{IUPAC} (10^{-6} mol.mol^{-1})	0.0091	0.0074	0.0109
Average LOD_{IUPAC} (10^{-6} mol.mol^{-1})			0.009
Lower confidence limit (10^{-6} mol.mol^{-1})			0.006
Upper confidence limit (10^{-6} mol.mol^{-1})			0.016

2.2.4 Limit of quantification for CO_2

The value of the LOQ_{IUPAC} is 0.022 x 10^{-6} mol·mol^{-1}. The method is therefore suitable for quantification of CO_2 at the levels specified (<0.25 x 10^{-6} mol·mol^{-1}) by the manufacturer for BIP™ nitrogen.

2.2.5 Selectivity or specificity

The conditions in section 5.3.9 were adhered to so that the CO_2 peak was adequately separated from the other peaks and therefore no interferences were present.

2.2.6 Accuracy or bias

The bias could not be evaluated in this case because there was no CRM available for CO_2 in the range 0 to 10 x 10^{-6} mol·mol^{-1}. However, the results obtained by the

present method were compared to results obtained by a previously validated method and the results are presented in Chapter 6.

2.2.7 Linearity

Figure 5 shows the plot of the calibration curve for the CO_2 analysis from Day 1.

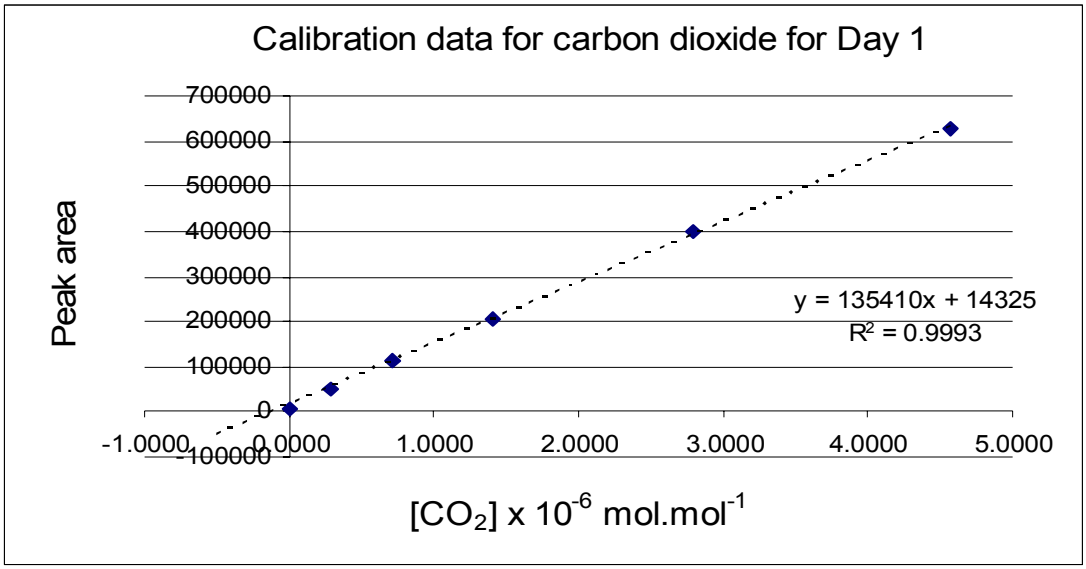

Figure 5: Calibration curve for the CO_2 results from Day 1(no sequence reversal).

Note that the regression coefficient value, r^2 was sufficiently close to 1 to assume linearity without taking into consideration the uncertainties. When the uncertainties were included, in the B_LEAST regression analysis, the Linear/Quadratic fit was found to be the best. From the B_LEAST analysis, the goodness-of-fit values were ≤2, showing acceptable linearity.

2.2.8 Influence of pressure, temperature and other possible sources of error

The temperature in the CSIR NML gas metrology laboratory is controlled to 20 °C ± 2 °C and the humidity to within 50% RH ± 10 %RH. This ensures that the GC temperature is not affected by the laboratory environment.

A source of error could be the inadequate conditioning of the gas chromatographic columns that would cause the retention time of the CO_2 peak to change. This is avoided by keeping the columns at 150 °C when samples are not being run, to avoid the saturation of the columns with moisture.

2.2.9 Measurement uncertainty and the uncertainty budget

2.2.9.1 Gravimetric preparation uncertainty

Table 52: Uncertainties associated with the gravimetric preparation of the standards for the carbon dioxide series

Cylinder Number	Component	Concentration (µmol·mol^{-1})	Uncertainty (µmol·mol^{-1})
3886	CO_2	4.566	0.046
3940	CO_2	2.786	0.046
3950	CO_2	1.401	0.043
3895	CO_2	0.712	0.042
3884	CO_2	0.286	0.042

2.2.9.2 Uncertainty due to repeatability error

Table 53: Values and uncertainties for CO_2 for Day 1

x_i	$u(x_i)$	y_i	$u(y_i)$
4.566	0.046	8839.8	449.953
2.786	0.046	51552.9	567.301
1.401	0.043	111452	845.756
0.712	0.042	207835.9	1009.409
0.286	0.042	400933.9	1462.347
0	0	625715.4	2000.798
m =6.7401 x 10^{-6}		$u(m)$ =2.252 x 10^{-7}	
c =-0.059660		$u(c)$ =0.003787	
Goodness of fit value	0.4388		

Table 54: Values and uncertainties for CO_2 for Day 2

x_i	$u(x_i)$	y_i	$u(y_i)$
4.566	0.046	6269.3	350.604
2.786	0.046	45144.9	451.741
1.401	0.043	102056.7	427.643
0.712	0.042	200546.3	1206.724
0.286	0.042	396434.4	1822.001
0	0	621289.4	2701.462
m =7.0071 x 10^{-6}		$u(m)$ =2.283 x 10^{-7}	
c =-0.043953		$u(c)$ =0.002940	
Goodness of fit value	0.9028		

Table 55: Values and uncertainties for CO_2 for Day 3

x_i	$u(x_i)$	y_i	$u(y_i)$
4.566	0.046	6396.6	516.277
2.786	0.046	44306.9	487.587
1.401	0.043	102778.5	844.664
0.712	0.042	199536.4	688.128
0.286	0.042	388048.4	1192.358
0	0	607061.2	1884.722
m =7.0261 x 10^{-6}		$u(m)$ =2.305 x 10^{-7}	
c =-0.044979		$u(c)$ =0.004076	
Goodness of fit value	0.6635		

2.2.9.3 Uncertainty due to intermediate reproducibility error

In **Table 56**, the intermediate reproducibility uncertainty is calculated from the standard deviation of the CO_2 concentrations found in the blank for three different days.

Table 56: Calculation of reproducibility uncertainty

[CO_2] (Day 1)	0.059660 x 10^{-6} mol.mol^{-1}
[CO_2] (Day 2)	0.043953 x 10^{-6} mol.mol^{-1}
[CO_2] (Day 3)	0.044979 x 10^{-6} mol.mol^{-1}
Average [CO_2]	0.0495 x 10^{-6} mol.mol^{-1}
Standard deviation	0.008787 x 10^{-6} mol.mol^{-1}
%CV	17.7%

2.2.9.4 Uncertainty due to the assumption of linearity

The B_LEAST software has calculated the residuals as a “goodness of fit” value for the three different days as less than 2 signifying that the uncertainty arising from the assumption of linearity is negligible.

2.2.9.5 Summary of uncertainty contributions

The uncertainty due to the assumption of linearity may be ignored in the uncertainty calculations because it has been shown to be negligible. The repeatability uncertainty can be obtained from **Tables 53, 54 and 55** from the uncertainty for the intercept and the intermediate reproducibility uncertainty from **Table 56**.

2.2.9.6 Calculation of combined uncertainty, effective degrees of freedom and the expanded uncertainty

The result for the combination of the uncertainties using **Equation 34** is shown in **Table 57**. The value of the sensitivity coefficient for each uncertainty contributor is 1 since they are all in the same units (x 10^{-6} mol.mol^{-1})

Table 57: Calculation of combined uncertainty for CO_2 in N_2

	$u_i(y)$
$u_{DAY\,1}$	0.003787
$u_{DAY\,2}$	0.002940
$u_{DAY\,3}$	0.004076
S_{REPROD}	0.008787
$u_c(y)$	0.009509

The effective degrees of freedom (v_{eff}) can be evaluated by the Welch-Satterthwaite formula (**Equation 36**). The degrees of freedom for each day's calculation is ∞, since the degrees of freedom for the standard concentrations are ∞ and $n = 10$ measurements were made for each concentration standard. The degrees of freedom for the reproducibility uncertainty is also ∞ because this uncertainty was calculated using the measurements from three days where ($v = \infty$). Using the values calculated in **Table 57**, the effective degrees of freedom, v_{eff} , evaluates to ∞ and the corresponding value for k is 2 for a 95,45% confidence level. The result and the expanded uncertainty are shown in **Table 58**.

Table 58: Result and expanded uncertainty for CO_2 in N_2

$u_c(y)$	0.009509
v_{eff}	∞
k	2
Expanded $u_c(y)$	0.0190
Result [CO_2]	0.050 x 10^{-6} mol.mol^{-1}
Relative expanded uncertainty (%)	38.4%

2.3 Method validation results for CO

2.3.1 Repeatability

Table 59: Results of repeatability tests performed on the results for CO from Day 1

Concentration ($\mu mol \cdot mol^{-1}$)	3.1505	1.9259	0.9786	0.5060	0.2112
1	258194	143926	71460	31511	14613
2	262428	143024	67066	32688	14170
3	255039	144487	69669	32629	15272
4	261652	142769	69425	33419	14405
5	260250	146004	74365	32113	15200
6	262287	148561	70459	32658	13615
7	264572	150355	70632	35135	14622
8	262333	148675	71740	31734	14641
9	268392	147753	73360	33148	14212
10	261898	154922	71912	35004	14148
Average	261704.5	147047.6	71008.8	33003.9	14489.8
Standard deviation	3545.126	3804.492	2072.026	1235.141	498.941
%CV	1.35	2.59	2.92	3.74	3.44

Table 60: Results of repeatability tests performed on the results for CO from Day 2

Concentration ($\mu mol \cdot mol^{-1}$)	3.1505	1.9259	0.9786	0.5060	0.2112
1	271811	159364	69851	34939	10766
2	273402	153744	70332	31102	11729
3	275271	157996	69632	31070	12778
4	280109	158289	68689	34142	12580
5	277227	157115	72139	30724	12021
6	275670	158377	73261	31050	15269
7	272669	157679	72257	31049	11290
8	271238	163783	70711	29064	12842
9	274738	159461	71842	30086	13800
10	273003	161210	71688	32572	13354
Average	274513.8	158701.8	71040.2	31579.8	12642.9
Standard deviation	2699.507	2625.567	1422.741	1800.533	1307.154
%CV	0.98	1.65	2.00	5.70	10.34

Table 61: Results of repeatability tests performed on the results for CO from Day 3

Concentration (µmol·mol^{-1})	3.1505	1.9259	0.9786	0.5060	0.2112
1	254137	144770	60228	24780	11571
2	251307	146346	61248	26169	11304
3	256214	150433	62342	30180	13043
4	254500	152060	66234	28567	11590
5	250456	148489	59913	29292	11225
6	254869	152599	61072	26433	10575
7	254303	151480	66011	27648	11942
8	254913	150852	63425	29417	12768
9	249778	152675	67360	29646	13640
10	250003	150749	68023	30180	11607
Average	253048	150045.3	63585.6	28231.2	11926.5
Standard deviation	2389.829	2682.992	3072.270	1884.987	939.200
%CV	0.94	1.79	4.83	6.68	7.87

2.3.2 Reproducibility

Table 62: Results from reproducibility limit test

	Day 1	**Day 2**	**Day 3**	**Range**	**Reproducibility Limit (R)**
Intercept	0.13908	0.083202	0.074491	0.06459	0.09913
Slope (x10^{-6})	14.448	12.7937	13.739	0.16543	0.23475

From **Table 62**, the reproducibility limit is more than the absolute difference between the two results, showing that the difference is within a probability of 95%.

2.3.3 Limit of detection

The limit of detection was calculated using the IUPAC method.

Table 63: Detection limit calculation for CO

	Day 1	Day 2	Day 3
1	14613	10766	11571
2	14170	11729	11304
3	15272	12778	13043
4	14405	12580	11590
5	15200	12021	11225
6	13615	15269	10575
7	14622	11290	11942
8	14641	12842	12768
9	14212	13800	13640
10	14148	13354	11607
Standard Deviation	498.941	1307.154	939.200
Slope (mol.mol^{-1}) x 10^{-6}	14.448	12.937	13.739
Slope (mol^{-1}.mol)	69213.732	77297.673	72785.501
LOD_{IUPAC} (10^{-6} mol.mol^{-1})	0.0387	0.0507	0.0216
Average LOD_{IUPAC} (10^{-6} mol.mol^{-1})			0.037
Lower confidence limit (10^{-6} mol.mol^{-1})			0.025
Upper confidence limit (10^{-6} mol.mol^{-1})			0.068

The limit of detection (0.037 x 10^{-6} mol.mol^{-1}) is less than the amount of CO expected in BIP™ nitrogen (0.25 x 10^{-6} mol.mol^{-1}) and this indicates that the method is fit for purpose for the analysis of CO in BIP™ nitrogen.

2.3.4 Limit of quantification

The LOQ_{IUPAC} is calculated as 0.123 x 10^{-6} mol.mol^{-1}. The limit of quantification is lower than the level of CO specified by the manufacturer in BIP™ nitrogen (0.25 x 10^{-6} mol.mol^{-1}) indicating that the method is fit for purpose for quantifying these low levels of CO in BIP™ nitrogen.

2.3.5 Selectivity or specificity

The conditions in section 5.3.9 were adhered to so that the CO peak was separated from the other peaks therefore, no interferences were present.

2.3.6 Accuracy or bias

The bias could not be evaluated in this case because there was no CRM for CO available in the range 0 to 10 x 10^{-6} mol.mol^{-1}. In Chapter 6, the results obtained were compared with the results obtained from a previously validated method.

2.3.7 Linearity

Figure 6 shows the plot of the calibration curve for the CO analysis from Day 1.

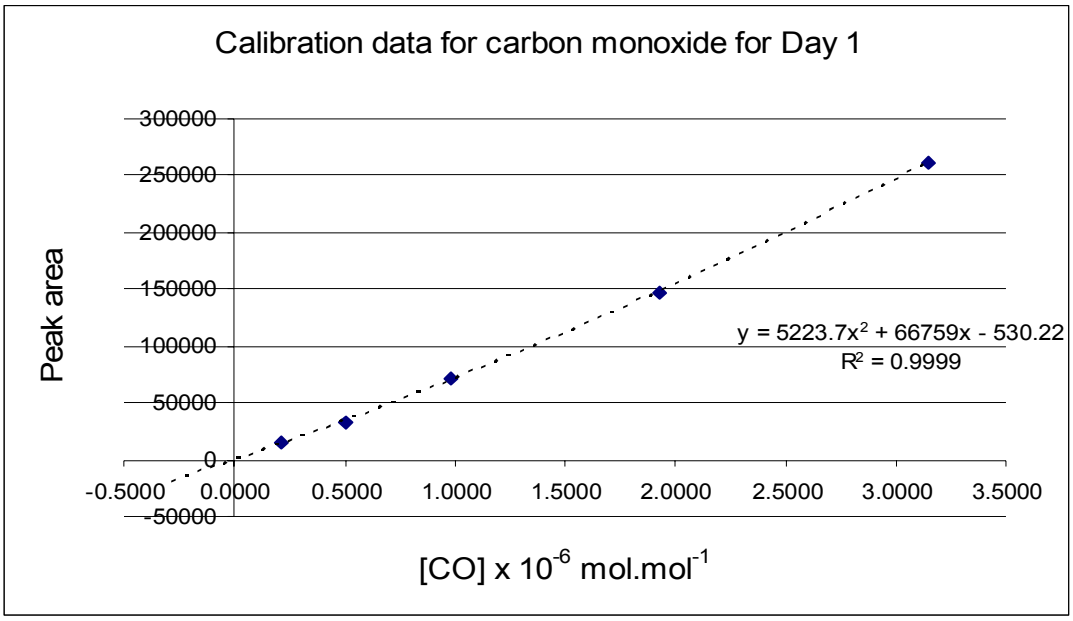

Figure 6: Calibration curve for the CO results from Day 1(no sequence reversal).

Note that the best fit was a polynomial and not a straight line, with the r^2 for a linear fit being 0.9974 but the r^2 for a polynomial fit being 0.9999 as shown in **Figure 6** above. The fact that the curve is not linear could be as a result of using temperature and pressure programming in the method or some other effect at low CO concentrations. Using the B_LEAST regression analysis, the results showed acceptable goodness of fit values (≤2) i.e. the goodness-of-fit value for all three days with linear/quadratic fits.

2.3.8 Influence of pressure, temperature and other possible sources of error

The temperature in the CSIR NML gas metrology laboratory is controlled to 20 °C ± 2 °C and the humidity to within 50% RH ± 10 %RH. This ensures that the GC temperature is not affected by the laboratory environment. A source of error could be the inadequate conditioning of the gas chromatographic columns that would cause the retention time of the CO peak to change. This is avoided by keeping the columns at 150 °C when samples are not being run, to avoid the saturation of the columns with moisture.

2.3.9 Measurement uncertainty and the uncertainty budget

2.3.9.1 Gravimetric preparation uncertainty

Table 64: Uncertainties associated with the gravimetric preparation of the standards for carbon monoxide

Cylinder Number	Component	Concentration (µmol·mol^{-1})	Uncertainty (µmol·mol^{-1})
3886	CO	3.150	0.020
3940	CO	1.926	0.028
3950	CO	0.979	0.018
3895	CO	0.506	0.018
3884	CO	0.211	0.018

2.3.9.2 Uncertainty due to repeatability error

Table 65: Values and uncertainties for CO for Day 1

x_i	$u(x_i)$	y_i	$u(y_i)$
3.150	0.020	261704.5	3545.126
1.926	0.028	147047.6	3804.492
0.979	0.018	71008.8	2072.026
0.506	0.018	33003.9	1235.141
0.211	0.018	14489.8	498.941
m =14.448 x 10^{-6}		$u(m)$ =7.426 x 10^{-7}	
c =0.013908		$u(c)$ =0.02484	
Goodness of fit value	0.7475		

Table 66: Values and uncertainties for CO for Day 2

x_i	$u(x_i)$	y_i	$u(y_i)$
3.150	0.020	274513.8	2699.507
1.926	0.028	158701.8	2625.567
0.979	0.018	71040.2	1422.741
0.506	0.018	31579.8	1800.533
0.211	0.018	12642.9	1307.154
m =12.937 x 10^{-6}		$u(m)$ =5.776 x 10^{-7}	
c =0.083202		$u(c)$ =0.02265	
Goodness of fit value	1.1412		

Table 67: Values and uncertainties for CO for Day 3

x_i	$u(x_i)$	y_i	$u(y_i)$
3.150	0.020	253048	2389.829
1.926	0.028	150045.3	2682.992
0.979	0.018	63585.6	3072.270
0.506	0.018	28231.2	1884.987
0.211	0.018	11926.5	939.200
m =13.739 x 10^{-6}		$u(m)$ =7.017 x 10^{-7}	
c =0.074491		$u(c)$ =0.02483	
Goodness of fit value	1.2753		

2.3.9.3 Uncertainty due to intermediate reproducibility error

Since there was no signal for carbon monoxide in the blank, the detection limit of the system serves as the level of CO. In **Table 68**, the intermediate reproducibility uncertainty is calculated from the standard deviation of the calculated detection limits for three days.

Table 68: Calculation of reproducibility uncertainty

[CO] (Day 1)	0.0216 x 10^{-6} mol.mol^{-1}
[CO] (Day 2)	0.0507 x 10^{-6} mol.mol^{-1}
[CO] (Day 3)	0.0387 x 10^{-6} mol.mol^{-1}
Average [CO]	0.037 x 10^{-6} mol.mol^{-1}
Standard deviation	0.0146 x 10^{-6} mol.mol^{-1}
%CV	39.4%

The reproducibility uncertainty is smaller than the upper and lower confidence limits that have been calculated for the LOD in **Table 63**. Therefore, the confidence limits for the LOD from **Table 63** were used in the calculation of the final uncertainty.

2.3.9.4 Uncertainty due to the assumption of linearity

The B_LEAST software has calculated the residuals as a “goodness of fit” value for the two different days as less than 2 signifying that the uncertainty arising from the assumption of linearity is negligible.

2.3.9.5 Summary of uncertainty contributions

The uncertainty due to the assumption of linearity may be ignored in the uncertainty calculations because it has been shown to be negligible. The intermediate reproducibility uncertainty from **Table 68** is smaller than the

confidence limits calculated for the LOD in **Table 63**, and therefore it was ignored in the uncertainty calculation.

2.3.9.6 Calculation of the expanded uncertainty

The upper and lower confidence limits of the LOD were used to calculate the uncertainty range as shown in **Table 69**.

Table 69: Calculation of expanded uncertainty for CO in N_2

	$u_i(y)$
Upper confidence limit of LOD (x 10^{-6} mol.mol^{-1})	0.068
Average LOD (x 10^{-6} mol.mol^{-1})	0.037
Lower confidence limit of the LOD (x 10^{-6} mol.mol^{-1})	0.025
Range of CO in BIP™ nitrogen at 95% level of confidence	0 < CO < 0.068

Since there was no CO peak in the BIP™ nitrogen, the detection limit of CO was taken as the amount of CO. The upper and lower confidence limits of the detection limits have been calculated and are shown in **Table 41** for a 95% level of confidence for $n = 10$. This result is already an expanded uncertainty and there is no need to expand it any further.

2.4 Method validation results for N_2 in O_2

2.4.1 Repeatability

Table 70: Repeatability tests performed on Day 1 for N_2 in O_2

[N_2] x 10^{-6} mol.mol^{-1}	**Pure O_2**	**3.9167**	**10.3935**	**16.6344**	**30.2724**
1	160710	24049	70227	124951	240804
2	160285	24060	68774	124896	241526
3	159832	22708	69476	125465	241340
4	160797	23145	69580	125067	240654
5	160486	22310	69618	125289	240647
6	161163	23244	70025	125132	241526
7	161074	23436	70135	125551	242138
8	160481	22441	70686	125207	240839
9	161033	23559	70899	125278	242854
10	161079	22780	70179	125321	243009
Average	160694	23173.2	69959.9	125215.7	241533.7
Standard deviation	426.527	617.288	620.494	209.864	875.449
%CV	0.26	2.66	0.89	0.17	0.36

Table 71: Repeatability tests performed on Day 2 for N_2 in O_2

[N_2] x 10^{-6} mol.mol^{-1}	**Pure O_2**	**3.9167**	**10.3935**	**16.6344**	**30.2724**
1	191196	27209	78477	138605	256970
2	191597	27773	76353	137978	257058
3	191410	26874	79401	139702	260976
4	189646	28136	80545	139043	259799
5	191425	23919	77779	135834	258092
6	193910	24358	79043	135675	258663
7	191002	28225	79136	138950	261062
8	190964	24971	79711	137280	258417
9	194661	26198	76693	136638	257501
10	193397	27644	77265	139818	258488
Average	191920.8	26530.7	78440.3	137952.3	258702.6
Standard deviation	1553.35	1594.898	1376.166	1527.767	1475.341
%CV	0.81	6.01	1.75	1.11	0.57

2.4.2 Reproducibility

Table 72: Results from reproducibility limit test

	Day 1	**Day 2**	**Range**	R
Intercept	1.5473	1.1647	0.3826	0.7652
Slope (x10^{-4})	1.1953	1.1269	0.0684	0.1368

From **Table 72**, the reproducibility limit is more than the absolute difference between the two results, showing that the difference is within a probability of 95,45%.

2.4.3 Accuracy or Bias

The bias could not be evaluated in this case because there was no CRM available in the range required.

2.4.4 Limit of detection

The limit of detection (LOD) was calculated using the IUPAC method.

Table 73: Detection limit calculation for N_2 in O_2

	Day 1	Day 2
1	24049	27209
2	24060	27773
3	22708	26874
4	23145	28136
5	22310	23919
6	23244	24358
7	23436	28225
8	22441	24971
9	23559	26198
10	22780	27644
Standard Deviation	617.288	1594.898
Slope ($mol^{-1}.mol$)	8366.101	8878.629
LOD (10^{-6} $mol.mol^{-1}$)	0.221	0.539
Average LOD (10^{-6} $mol.mol^{-1}$)		0.380
Lower confidence limit (10^{-6} $mol.mol^{-1}$)		0.262
Upper confidence limit (10^{-6} $mol.mol^{-1}$)		0.694

2.4.5 Limit of quantification

Table 74: Calculation of LOQ for N_2 in O_2

Average LOD (10^{-6} $mol.mol^{-1}$)	0.380
LOQ (10^{-6} $mol.mol^{-1}$)	1.267

The limit of quantitation is within the manufacturer's specifications for N_2 in O_2 (less than 40 x 10^{-6} $mol.mol^{-1}$).

2.4.6 Selectivity or specificity

The conditions in section 5.3.9 were adhered to so that the N_2 peak was separated from the other peaks therefore, no interferences were present.

2.4.7 Linearity

Figure 7 shows the plot of the calibration curve for the N_2 analysis from Day 2.

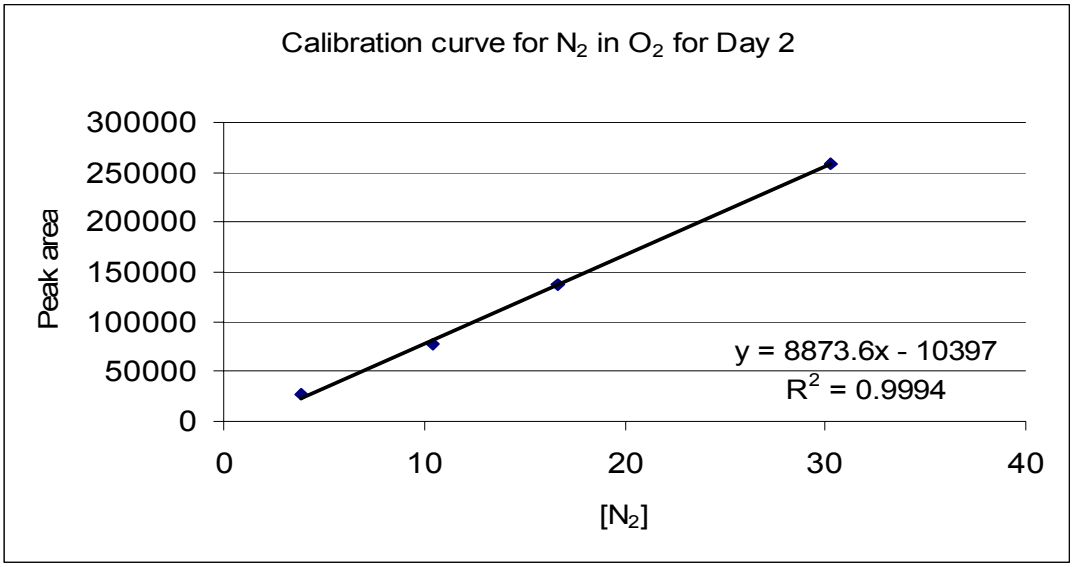

Figure 7: Calibration curve for the N_2 results from Day 2 (no sequence reversal).

Note that the regression coefficient value, r^2 was close to 1 for acceptable linearity. Also, from the B_LEAST analyses, the goodness-of-fit value for Day 1 was 0.3506 and for Day 2 was 0.2794. These goodness-of-fit values were both less than 2, showing acceptable linearity.

2.4.8 Influence of pressure, temperature and other possible sources of error

The temperature in the CSIR NML gas laboratory is controlled to 20 °C ±1 °C and the humidity to within 50% RH ±10 %RH. This ensures that the GC temperature is not affected by the laboratory environment.

A source of error could be the inadequate conditioning of the gas chromatographic column that would cause the retention time of the N_2 peak to change. This is avoided by keeping the columns at 150 °C when samples are not being run, to avoid the saturation of the column with moisture.

2.4.9 Measurement uncertainty and the uncertainty budget

2.4.9.1 Gravimetric preparation uncertainty

Table 75

Uncertainties associated with the gravimetric preparation of the standards for the N_2 in Helium series

Gravimetric concentration (µmol·mol^{-1})	Weighing Uncertainty (µmol·mol^{-1})	Standard Uncertainty (µmol·mol^{-1})
113763.973	17.545	8.773
5655.753	7.057	3.528
285.012	2.807	1.403
30.272	2.618	1.309
16.634	2.746	1.373
10.394	2.752	1.376
3.917	2.612	1.306

The uncertainties for the gravimetrically prepared standards for N_2 in He are high because of the amount of uncertainty of the N_2 present in the helium 5.0 that was used to make up the standards.

2.4.9.2 Uncertainty due to repeatability error

This uncertainty is evaluated from 10 consecutive runs done on each calibration standard and is reflected as $u(y_i)$. **Tables 76** and **77** show the results from Day 1 and Day 2 with the repeatability uncertainty, $u(y_i)$ of the response (y_i) and the standard uncertainty, $u(x_i)$, of the N_2 standard concentration (x_i) in units of 10^{-6} mol.mol^{-1}. These results were used to calculate the slope and intercept for each day.

Table 76: Values and uncertainties for Day 1

x_i	$u(x_i)$	y_i	$u(y_i)$
3.917	1.306	23173.2	617.288
10.394	1.376	69959.9	620.494
16.634	1.373	125215.7	209.864
30.272	1.309	241533.7	875.449
N_2 in O_2		160694	426.527
m =1.1953 x10^{-4}		$u(m)$ =8.0753 x10^{-6}	
c =1.5473		$u(c)$ =1.1498	
Goodness-of-fit		0.3506	
[N_2] in O_2		20.755 x 10^{-6} mol.mol^{-1}	
Standard uncertainty of result		0.765 x 10^{-6} mol.mol^{-1}	

Table 77: Values and uncertainties for Day 2

x_i	$u(x_i)$	y_i	$u(y_i)$
3.917	1.306	26530.7	1594.898
10.394	1.376	78440.3	1376.166
16.634	1.373	137952.3	1527.767
30.272	1.309	258702.6	1475.341
N_2 in O_2		191920.8	1553.35
m =1.1269 x10^{-4}		$u(m)$ =7.6548x10^{-6}	
c =1.1647		$u(c)$ =1.1785	
Goodness-of-fit		0.2794	
[N_2] in O_2		22.793 x 10^{-6} mol.mol^{-1}	
Standard uncertainty of result		0.860 x 10^{-6} mol.mol^{-1}	

The degrees of freedom for the uncertainties for the standards, $u(x_i)$, are ∞ and the degrees of freedom for uncertainties for the responses are 9 (since $n=10$ for each response point on the calibration curve). Therefore, the total degrees of freedom for the results from the calibration curve are ∞. The uncertainties for the slope (m) and the intercept (c) are calculated by the B_LEAST software from the input uncertainties $u(x_i)$ and $u(y_i)$.

2.4.9.3 Uncertainty due to intermediate reproducibility error

This uncertainty is evaluated from the results for two different days, in the form of the standard deviation of the results obtained for the different levels over these days.

The reproducibility uncertainty is taken as the standard deviation of the results from the two different days as shown in **Table 78**.

Table 78: Calculation of reproducibility uncertainty

[N_2] (Day 1)	20.755 x 10^{-6} mol.mol^{-1}
[N_2] (Day 2)	22.793 x 10^{-6} mol.mol^{-1}
Average [N_2]	21.774 x 10^{-6} mol.mol^{-1}
Standard deviation	1.4411 x 10^{-6} mol.mol^{-1}

2.4.9.4 Uncertainty due to the assumption of linearity

The uncertainty arising from the assumption of a linear relationship between x and y is not normally large enough to require an additional estimate. The B_LEAST software has calculated the residuals as a "goodness of fit" value for the two different days as less than 2 signifying that the uncertainty arising from the assumption of linearity is negligible.

2.4.9.5 Summary of uncertainty contributions

The uncertainty due to the assumption of linearity may be ignored in the uncertainty calculations if it has been shown to be negligible. The repeatability uncertainty can be obtained from **Tables 76 and 77** and the intermediate reproducibility uncertainty from **Table 78**. The gravimetric uncertainties of the calibration standards have been included in the repeatability uncertainty when the B_LEAST software used these uncertainties in the calculation of the uncertainty for the slope and the intercept of the calibration curve.

2.4.9.6 Calculation of the expanded uncertainty

The result for the combination of the uncertainties is shown in **Table 79**.

Table 79: Calculation of combined uncertainty for N_2 in O_2

	$u_i(y)$
$u_{DAY\,1}$	0.765
$u_{DAY\,2}$	0.860
S_{REPROD}	1.4411
$u_c(y)$	1.655

The CSIR NML has chosen a level of confidence of 95,45% for all measurements made. From *t*-distribution tables, the appropriate value of k (the factor by which the uncertainty is multiplied to ensure a 95,45% degree of certainty in the final result) for v_{eff} (**Equation 36**) is chosen and the standard uncertainty converted to an expanded uncertainty for a 95,45% level of confidence.

The degrees of freedom for each day's calculation is ∞, since the degrees of freedom for the standard concentrations are ∞ and $n = 10$ measurements were made for each concentration standard. The degrees of freedom for the reproducibility uncertainty is also ∞ because this uncertainty was calculated using the measurements from two days where ($v = \infty$). Using the values calculated in **Table 79**, the effective degrees of freedom, v_{eff}, evaluates to ∞ and the corresponding value for k is 2 for a 95,45% confidence level. The result and the expanded uncertainty are shown in **Table 80**.

Table 80: Result and expanded uncertainty for N_2 in O_2

N_2 result (y)	21.774
$u_c(y)$	1.655
v_{eff}	∞
k	2
Expanded $u_c(y)$	3.310
[N_2] at a 95,45% confidence level	18.464 < [N_2] < 25.084 x 10^{-6} mol·mol^{-1}
Relative expanded uncertainty (%)	15.2%